



UNIVERSIDADE FEDERAL DO PARÁ  
INSTITUTO DE GEOCIÊNCIAS  
PROGRAMA DE PÓS-GRADUAÇÃO EM CIÊNCIAS AMBIENTAIS

VITOR HUGO FREITAS GOMES

IMPACTOS DAS MUDANÇAS CLIMÁTICAS E DO  
DESFLORESTAMENTO SOBRE A FLORA ARBÓREA DA AMAZÔNIA

BELÉM-PA  
2018

VITOR HUGO FREITAS GOMES

IMPACTOS DAS MUDANÇAS CLIMÁTICAS E DO DESFLORESTAMENTO  
SOBRE A FLORA ARBÓREA DA AMAZÔNIA

Tese apresentada ao Programa de Pós-Graduação em Ciências Ambientais do Instituto de Geociências, da Universidade Federal do Pará em parceria com a Empresa Brasileira de Pesquisa Agropecuária/Amazônia Oriental e Museu Paraense Emílio Goeldi, como requisito parcial para a obtenção do título de Doutor em Ciências Ambientais.

Área de concentração: Clima e Dinâmica Socioambiental na Amazônia

Orientadora: Ima Célia Guimarães Vieira  
Coorientador: Hans ter Steege

BELÉM-PA  
2018

**Dados Internacionais de Catalogação na Publicação (CIP) de acordo com ISBD  
Sistema de Bibliotecas da Universidade Federal do Pará  
Gerada automaticamente pelo módulo Ficat, mediante os dados fornecidos pelo(a) autor(a)**

---

Gomes, Vitor Hugo Freitas.

Impactos das mudanças climáticas e do desflorestamento sobre a flora arbórea da  
Amazônia / Vitor Hugo Freitas Gomes. — 2018.

155 f. : il. color.

Orientador(a): Profa. Dra. Ima Célia Guimarães Vieira

Coorientador(a): Prof. Dr. Hans ter Steege

Tese (Doutorado) - Programa de Pós-Graduação em Ciências Ambientais, Instituto de  
Geociências, Universidade Federal do Pará, Belém, 2018.

1. Mudanças climáticas. 2. Desflorestamento. 3. Flora arbóreas. 4. Amazônia. I. Título.

CDD 574.522209811

---

**VITOR HUGO FREITAS GOMES**

**IMPACTOS DAS MUDANÇAS CLIMÁTICAS E DO DESFLORESTAMENTO  
SOBRE A FLORA ARBÓREA DA AMAZÔNIA**

Tese apresentada para obtenção do grau de Doutorado pelo Programa de Pós-Graduação em Ciências Ambientais, Instituto de Geociências, Universidade Federal do Pará em convênio com o Museu Paraense Emílio Goeldi e EMBRAPA – Amazônia Oriental. Área de concentração em Clima e Dinâmica Socioambiental na Amazônia.

Data de aprovação: 30 / 11 / 2018

Banca Examinadora:



Ima Célia Guimarães Vieira - Orientadora  
Doutora em Ecologia  
Museu Paraense Emílio Goeldi



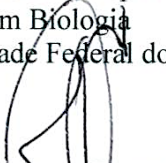
José Henrique Cattaneo - Membro  
Doutor em Agronomia  
Universidade Federal do Pará



Everaldo Barreiros de Souza - Membro  
Doutor em Meteorologia  
Universidade Federal do Pará



Maria Aparecida Lopes - Membro  
Doutora em Biologia  
Universidade Federal do Pará



Silvio Brienza Junior - Membro  
Doutor em Agricultura Tropical  
Empresa Brasileira de Pesquisa Agropecuária



Joice Nunes Ferreira - Membro  
Doutora em Ecologia  
Empresa Brasileira de Pesquisa Agropecuária

## AGRADECIMENTOS

Um doutorado é resultado de esforço conjunto. De certo, muitas pessoas contribuíram para que este trabalho fosse possível. Cronologicamente, a jornada se iniciou com o árduo apoio de meus pais, José e Myriam, que se comprometeram com a educação de minha família, sobretudo minha mãe, que muito lutou, e ainda luta para sempre seguirmos em frente. O amor, carinho e confiança de minha família foram fundamentais, e por estes três pilares, agradeço também meus irmãos Gabriel e Amanda, e minha avó Estela. Ainda sobre estes pilares, tive a sorte de encontrar minha amada Letícia, que com uma dedicação inabalável, seguiu comigo para todos os lados, companheira de muitas madrugadas em claro, e finais de semana sacrificados para construção deste trabalho. Além disso meus amigos/irmãos Dinda Dete, Will, Vilson, Luger, Rajiv, Carlinhos, Tri, Leandro, Peteca, Biel, Danilo e Paca.

Tive também ao menos quatro grandes referências acadêmicas, pelos quais guardo afeto especial. O Rafael me apresentou à pesquisa e ao trabalho árduo. Me viu crescer, praticamente um segundo pai, e como filho, o segui na pesquisa. Sem entender muito bem o que fazia à época, acabei dando muito trabalho pra ele. Obrigado Rafael. Deixo aqui também meu agradecimento a Nelson de Araújo Rosa, que mesmo sem um título acadêmico, é um dos maiores pesquisadores que tive a honra de conhecer. Obrigado Nelson. Também faço referência a minha orientadora Ima, que confiou que eu conseguiria conduzir uma tese de doutorado, e topou todos os desafios que nos apareceram. Obrigado Ima. Por fim, tive o privilégio de conhecer uma pessoa muito especial, de paciência infinita, que mesmo sendo filho de cultura e idioma diferentes dos meus, me mostrou como é a pesquisa por dentro. Meu amigo Hans, você abriu as portas de seu país e de sua casa para mim, o convívio com você me faz uma falta enorme. Dank u Hans.

Claro que muitos outros parceiros trocaram conhecimentos e experiências comigo ao longo desta jornada. Agradeço a toda equipe do PPGCA, nas pessoas da Professora. Aline Meiguins, que me ajudou em diversas etapas deste projeto, e também a Elisane Gabriel e Professores Everaldo Barros e Edson Rocha. Agradeço ao Museu Goeldi, nas pessoas do Leandro Ferreira, Mário Jardim, Regina Noronha e Ana Albernaz, à Embrapa na pessoa do amigo e Professor Silvio Brienza, e ao Naturalis, nas pessoas da Sylvia Oliveira, Jesús Aguirres, Niels Raes, Edwin Pos, Sofia Gomes, Larissa Dória e Saroj Ruchisansakun e Leon Marshall. Obrigado a todos!

## RESUMO

A Amazônia detém uma incrível biodiversidade, moldada ao longo de milhões de anos. Nos últimos milênios o clima na região se tornou mais úmido, aumentando a disponibilidade de habitat adequado para espécies florestais e influenciando suas distribuições e a expansão da floresta neste período. Todavia, as influências humanas sobre o clima e o uso da terra têm promovido a redução do habitat de muitas espécies na região, e projeções apresentam uma intensificação no futuro, com impactos potencialmente negativos para a riqueza e distribuição da biodiversidade amazônica. Além disso, existem diversas lacunas de conhecimento sobre como o clima e o uso da terra tem moldado e moldarão a floresta Amazônica, e a ampla variedade de métodos disponíveis para tal análise abrem espaços para questionamentos sobre as melhores práticas metodológicas para estudar uma área tão grande e diversa como a Amazônia. Entender a origem, manutenção e perda da biodiversidade tem uma profunda importância para vida humana futura. Esta tese aborda algumas das lacunas de conhecimento sobre estes tópicos, comparando métodos de estimativa de riqueza e distribuição de espécies na floresta Amazônica em diferentes escalas temporais. Este estudo é uma pesquisa interdisciplinar que relaciona aspectos de diferentes áreas científicas para o entendimento das consequências das duas principais ameaças à biodiversidade amazônica, atribuídas às mudanças climáticas e ao desflorestamento. O estudo contou com uma cooperação entre o Naturalis Biodiversity Center – Holanda e o Museu Paraense Emílio Goeldi – MPEG, por meio de uma bolsa de Doutorado Sanduíche no Exterior – SWE (Processo CNPq 203102/2015-0). Além disso, o estudo se insere no projeto INCT Biodiversidade e Uso da Terra na Amazônia (Processo CNPq 574008/2008-0), coordenado pelo MPEG, dedicado ao estudo da biodiversidade e da paisagem amazônica, visando o entendimento das consequências ambientais e sociais de diferentes usos da terra, fornecendo bases científicas para práticas econômicas sustentáveis e apoio a políticas públicas para a Amazônia.

Palavras-chave: Biodiversidade. Desflorestamento. Mudanças climáticas. Amazônia.

## ABSTRACT

Amazonia has an incredible biodiversity, shaped over millions of years. In recent millennia the climate in the region has become more humid, increasing the availability of suitable habitat for forest species and influencing its distributions and the expansion of the forest in this period. However, human influences on climate and land use have led to a reduction in the habitat of many species in the region, and projections show an intensification in the future with impacts potentially negative on the richness and distribution of Amazonian biodiversity. In addition, there are several knowledge gaps on how climate and land use has shaped and will shape the Amazonian rainforest, and the wide variety of methods available for such analysis also raises questions on the best methodological practices for studying an area as large and diverse as Amazonia. Understanding the origin, maintenance and loss of biodiversity has a profound importance for future human life. This thesis addresses some of the knowledge gaps on these topics, comparing methods of estimating richness and distribution of species of the Amazonian rainforest at different time scales. This study is an interdisciplinary research that relates aspects of different scientific areas to understanding the consequences of the two main threats to Amazonian biodiversity attributed to climate change and deforestation. The study was supported by a cooperation between the Naturalis Biodiversity Center – The Netherlands and Museu Paraense Emílio Goeldi – MPEG on a Sandwich Doctorate Scholarship – SWE (CNPq Proccess 203102/2015-0). Furthermore, the study is part of the INCT project Biodiversidade e Uso da Terra na Amazônia (Biodiversity and Land Use in Amazonia) (CNPq Proccess 574008/2008-0), coordinated by MPEG, which is dedicated to the study of biodiversity and Amazonian landscape, aiming to understand environmental and social consequences of different land uses, providing scientific bases for sustainable economic practices and support for public policies for Amazonia.

Keywords: Biodiversity. Climate change. Deforestation. Amazonia.

## LISTA DE ILUSTRAÇÕES

- Figure 2.1- Simulation of a 10,000-ha virtual forest with mean dispersal distance of 20 m. Parameters used are  $m_{plot} = 0.78688$ ;  $m_{adjacent} = 0.192$ ;  $m_{forest} = 0.0192$ ;  $m_{mc} = 0.00192$ ;  $v = 10^{-4}$ . (a) rank abundance distribution (rad) of the total virtual (black) with logseries fit (red) and lognormal fit (blue). (b) species area (spar) curve for the total virtual forest and estimated richness (sestimated) based on chao1 (blue). (c) fisher's  $\alpha$  area curve for the virtual forest. (d) species richness estimated with fisher's  $\alpha$  (black), chao1 (blue), each with 95% ci (red), and actual species richness of the simulated community (horizontal line).  $M_{plot}$  = local recruitment;  $m_{adjacent}$  = recruitment from adjacent plots;  $m_{forest}$  = recruitment from total forest;  $m_{mc}$  = recruitment from metacommunity;  $v$  = speciation..... 35
- Figure 2.2- Barro Colorado island field data (BCI). A. Rank abundance distribution (RAD) of BCI with logseries fit (red) and lognormal fit (blue). B. Species area curve for BCI and estimated richness (Sestimated) based on chao1 (blue). C. Fisher's  $\alpha$  area curve for bci. D. Species richness estimated for a 50 ha area on bci with fisher's  $\alpha$  (black) and chao1 (blue), each with 95% ci (red)..... 37
- Figure 2.3- Reserva Ducke field data (RD). A. Rank abundance distribution (RAD) of rd with logseries fit (red) and lognormal fit (blue). B. Species area curve for rd and estimated richness (Sestimated) based on chao1 (blue). C. Fisher's  $\alpha$  area curve for RD. D. Species richness estimated for the total 100km<sup>2</sup> rd area with fisher's  $\alpha$  (black) and chao1 (blue), each with 95% ci (red). ..... 38
- Figure 2.4- Piste de Saint Elie field data (PSE). A. Rank abundance distribution (RAD) of rd with logseries fit (red) and lognormal fit (blue). B. Species area curve for rd and estimated richness (Sestimated) based on chao1 (blue). C. Fisher's  $\alpha$  area curve for rd. D. Species richness estimated for the total 15km<sup>2</sup> area surrounding the plots with fisher's  $\alpha$  (black) and chao1 (blue), each with 95% ci (red). ..... 39
- Figure 2.5- Monte Branco plateau field data (MBP). A. Rank abundance distribution (RAD) of MBP with logseries fit (red) and lognormal fit (blue). B. Species area curve for MBP and estimated richness (Estimated) based on Chao1 (blue). C. Fisher's  $\alpha$  area curve for mbp. D. Species richness estimated for the total 37.5 km<sup>2</sup> MBP area with Fisher's  $\alpha$  (black) and Chao1 (blue), each with 95% ci (red)..... 40
- Figure 3.1- Frequency distributions for 189 significant hyperdominant amazonian treespecies of (a) the spearman's correlation index rho between Maxent's predicted environmental suitability and relative local abundance of the plots; (b) the slopes of the linear 90th percentile quantile regression between maxent's predicted environmental suitability and the relative local abundance of the plots; (c) the true presence (sensitivity) of the distribution predicted by the idw maps compared to the collection localities; and (d) the true presence (sensitivity) of the distribution predicted by the maxent maps compared to the plot presence. .... 59

- Figure 3.2- The predicted area of occupancy by Maxent (green) and the idw map (grey) of (a) *Triplaris weigeltiana* (Rchb.) Kuntze; and (b) *Macrolobium acaciifolium* (Benth.) Benth. The localities of the collections, presence and absence plots are also indicated. Maps created with custom R script. Base map source (country.shp, rivers.shp): ESRI..... 60
- Figure 3.3- Maxent environmental suitability maps for (a) *Eperua falcata* Aubl.; (b) *Licania alba* (Bernoulli) Cuatrec.. Maxent maps constructed using GBIF records, cleaned GBIF records, kernel-density estimate GBIF records, and kernel- density estimate gbif records plus the buffer clip. Black dots: GBIF records. Red dots: GBIF records after the use of the cleaning pipeline. Dashed blue line: buffer based on a convex hull around species cleaned collections. Light blue: predicted environmental suitability using GBIF records. Light green: predicted environmental suitability using cleaned GBIF records. Medium green: predicted environmental suitability using kernel density estimate GBIF records. Dark green: predicted environmental suitability using kernel density estimate GBIF records and the buffer clip, resulting in the final predicted area of occupancy. Maps created with custom R script. Base map source (country.shp, rivers.shp): ESRI..... 63
- Figure 4.2- Current mean environmental suitability and current mean species richness for moraceae and urticaceae. A, map for current mean environmental suitability. B, map for current mean species richness. Circles in blue, numbers of species collections by 0.5-degree cell (a); number of single species collected by 0.5-degree cell (b). Gray line, amazonian rainforest. Maps created with custom R script. Base map source (country.shp, rivers.shp): ESRI. .... 78
- Figure 4.1- Relative abundance for moraceae and urticaceae families. Circles in blue, number of plots with presence of the families. Circles in red, percentage of modern pollen assemblages in the core's sediment of the paleoecological sites corresponding to the values in appendix S4.4. Gray line, amazonian rainforest. Maps created with custom R script. Base map source (country.shp, rivers.shp): ESRI. .... 79
- Figure 4.4- Relationship between the tree relative abundance of moraceae and urticaceae species in modern vegetation versus their modern pollen assemblages. Graph created with custom R script. .... 80
- Figure 4.3- Increment in mean environmental suitability and increment in mean species richness during the mid-late holocene (% , between current and middle holocene, last 6,000 yr bp. A, increment in mean environmental suitability during late holocene. B, increment in mean species richness. Gray line, amazonian rainforest and amazonian sub-regions . Maps created with custom R script. Base map source (country.shp, rivers.shp): ESRI. .... 81

Figure 5.1- Loss by global change for *eschweiler coriacea* (d.c.) s.a. *mori*, the most common species in amazonia15. Beige, loss in aoo (area of occupancy). A, original AOO. B, original aoo and deforestation by 2013. C, original AOO and 2050 IGS (improved governance deforestation scenario). D, original AOO and 2050 BAU (business as usual deforestation scenario). E, 2050 RCP 2.6 AOO. F, 2050 RCP 2.6 AOO and 2050 IGS (improved governance deforestation scenario). (g) 2050 RCP 2.6 AOO and 2050 BAU deforestation. H, 2050 RCP 8.5 AOO. I, 2050 RCP 8.5 AOO and 2050 IGS deforestation. J, 2050 RCP 8.5 AOO and 2050 BAU deforestation. Maps created with custom R script. Base map source (country.shp, rivers.shp): ESRI. .... 95

Figure 5.2- Amazonian species richness (number of species per grid cell) impacted by global change and deforestation. A, original AOO only. B, original AOO and 2050 IGS (improved governance deforestation scenario). C, original AOO and 2050 BAU (business as usual deforestation scenario). D, 2050 RCP 2.6 AOO only. E, 2050 RCP 2.6 AOO combined with 2050 IGS deforestation. F, 2050 RCP 2.6 AOO combined with 2050 BAU deforestation, g, 2050 RCP 8.5 AOO only. H, 2050 RCP 8.5 AOO combined with 2050 igs deforestation. I, 2050 RCP 8.5 AOO combined with 2050 BAU deforestation. Maps created with custom R script. Base map source (country.shp, rivers.shp): ESRI. .... 97

Figure 5.3- Only half of the amazonian forest may remain in 2050 (2050 RCP 8.5 AOO combined with 2050 BAU deforestation). Green, a relatively intact amazonian forest block, composed of north-western and central amazonia, the guiana shield and smaller part of southwestern amazonia (max number of species per grid cell of 1393, with mean 578). Red, a largely degraded amazonian forest block composed of eastern, southern and a major part of southwestern amazonia (max number of species per grid cell of 898, with mean 142). Light grey, forest loss. Map created with custom R script. Base map source (country.shp, rivers.shp): ESRI. .... 100

Figure S4.1- Current mean environmental suitability for the families moraceae and urticaceae (%). A, moraceae. B, urticaceae. Gray polygon, amazonian rainforest. Circles in blue, numbers of collections found in gbif database, and checked for inconsistencies. Maps created with custom R script. Base map source (country.shp, rivers.shp): ESRI..... 142

Figure S4.2- Species richness. A, modelled species richness for moraceae. B, modelled species richness for urticaceae. Both maps are the result of stacking individual thresholded species distribution models. Circles in blue, numbers of species collected by 0.5 degree cell. Maps created with custom R script. Gray line, amazonian rainforest. Circles in blue, numbers of species collected by 0.5-degree cell. Base map source (country.shp, rivers.shp): ESRI. .... 142

- Figure S4.3- Relative abundance for moraceae and urticaceae families. A, relative abundance map for moraceae based on tree inventory plot data. B, relative abundance map for urticaceae based on tree inventory plot data. Circles in blue, number of plots with presence of the families. Circles in pink, percentage of modern pollen assemblage of moraceae/urticaceae obtained from pollen diagrams of the paleoecological sites. Gray polygon, amazonian rainforest. Maps created with custom R script. Base map source (country.shp, rivers.shp): ESRI. .... 143
- Figure S4.4- Increment in environmental suitability between the middle and late holocene (% , between current and last 6 ka years). A, increment for moraceae family. B, increment for urticaceae family. Maps created with custom R script. Gray line, amazonian rainforest and amazonian sub-regions. Base map source (country.shp, rivers.shp): ESRI..... 143
- Figure S4.5- Increment in species richness between the middle and late holocene (% , between current and last 6 ka years). A, increment for moraceae family. B, increment for urticaceae family. Gray polygon, amazonian rainforest and amazonian sub-regions. Maps created with custom R script. Maps created with custom r script. Base map source (country.shp, rivers.shp): ESRI..... 144
- Figure S4.6- Relationship between relative abundance. A, all moraceae species, and b, all urticaceae species in the vegetation and the percent abundance of their pollen in lake/bog surface sediment pollen assemblages. .... 144
- Figure S4.7- Map of original amazonian lowland forest. The green area represents lowland forest area. Amazonia sub-regions: CA, central amazonia; EA, eastern amazonia; GS, guiana shield; SA, southern amazonia; WAN, northwestern amazonia; WAS, southwestern. Map created with custom R script. Base map source (country.shp, rivers.shp): ESRI. .... 145
- Figure S4.8- Locations for 45 paleoecological sites. Amazonian paleoecological sites locations in green and numeric id in red corresponding to appendix S4.4. Maps created with custom R script. Base map source (country.shp, rivers.shp): ESRI. 146
- Figure S5.1- Modelling the estimated area of occupancy (AOO). The representation of the area of occupancy (AOO) according to IUCN. A, spatial distribution of all know collections of a species. B, extent of occurrence (EOO) estimated as the boundary (convex hull) of all collections. C, known area of occupancy (AOO), defined as the number of grid cells occupied by the species. D, modelled aoo the result of modelling the suitable habitat for the species but constraining this by the known eoo plus a small buffer..... 147
- Figure S5.2- Deforestation scenarios by 2013 and projected forest loss by 2050. Green, forested area. Red, deforested area. A, historical deforestation by 2013. B, improved governance scenario (IGS) deforestation by 2050. C, business as usual scenario (BAU) deforestation by 2050. Maps created with custom R script. Base map source (country.shp, rivers.shp): ESRI. .... 148

- Figure S5.3- Amazonian protected areas network. Green, original amazonian lowland forest. Blue, amazonian protected areas network. Map created with custom R script. Base map source (country.shp, rivers.shp): ESRI. .... 149
- Figure S5.4- Map of original amazonian lowland forest. The green area represents lowland forest area. Amazonia sub-regions: CA, central amazonia; EA, eastern amazonia; GS, guiana shield; SA, southern amazonia; WAN, northwestern amazonia; WAS, southwestern. Map created with custom R script. Base map source (country.shp, rivers.shp): ESRI. .... 150
- Figure S5.5- Estimated AOO loss x population size loss. Loss in relative trees population size shows low but significant relationship with loss in trees AOO size in a, 2013 deforestation. B, 2050 IGS deforestation. C, 2050 BAU deforestation scenarios. 151
- Figure S5.6- Contrasting the estimated aoo loss for three hyperdominant amazonian tree species. Green, forested area. Red, deforested area. Salmon, loss in AOO. A, *Tetragastris altissima* (Aubl.) Swart, eastern/southern species. B, *Eperua falcata* aubl., northern/central species. C, *Iriartea deltoidea* Ruiz & Pav., western species. Maps created with custom R script. Base map source (country.shp, rivers.shp): ESRI. .... 152
- Figure S5.7- Tree species richness loss (fraction) by grid cell. A, original AOO only. B, original AOO and 2050 IGS deforestation. C, original AOO and 2050 BAU deforestation. D, 2050 RCP 2.6 AOO scenario only. E, 2050 RCP 2.6 AOO scenario combined with 2050 IGS deforestation. F, 2050 RCP 2.6 AOO scenario combined with 2050 BAU deforestation. G, 2050 RCP 8.5 AOO scenario only. H, 2050 RCP 8.5 AOO scenario combined with 2050 IGS deforestation. I, 2050 RCP 8.5 AOO scenario combined with 2050 BAU deforestation. Maps created with custom R script. Base map source (country.shp, rivers.shp): ESRI. .... 153
- Figure S5.8- Tree species richness of the forest fragments inside the protected area network. A, species richness by 2013. B, species richness by 2050 for the best-case scenario (RCP 2.6 AOO scenario and IGS deforestation). C, species richness by 2050 for the worst-case scenario (RCP 8.5 AOO scenario and BAU deforestation). Maps created with custom R script. Base map source (country.shp, rivers.shp): ESRI. 154
- Figure S5.9- Tree species richness of the forest fragments outside amazonian protected area network. A, species richness by 2013. B, species richness by 2050 for the best-case scenario (RCP 2.6 AOO scenario and IGS deforestation). C, species richness by 2050 for the worst-case scenario (RCP 8.5 AOO scenario and BAU deforestation). Maps created with custom R script. Base map source (country.shp, rivers.shp): ESRI. .... 155

## LISTA DE TABELAS

Table 2.1- Botanical inventories used for the analysis, with locality (Barro Colorado Island (BCI), Reserva Ducke (RD), Piste de St Elie (PSE), monte branco plateau (MBP), number of plots sampled, plot area (ha), number of individuals sampled (n), number of species recorded (s), the target area for which estimates were made, number of individuals in the target area based on average density, and reference to the data source: 1) BCI; 2) RD; 3) PSE; 4) MBP. ....	33
Table 2.2- Species estimates based on plot samples in BCI, RD, PSE, and PMB. ....	41
Table 5.1- Results for all ten scenarios, estimating the losses of AOO, mean species richness, number of species listed in IUCN A2, A4, B1 and D2 criteria, total number of threatened species and percentage of threatened species.....	102

## SUMÁRIO

<b>CAPÍTULO 1 INTRODUÇÃO GERAL</b> .....	17
<b>1.1 Referencial teórico</b> .....	17
1.1.1 Diversidade de espécies arbóreas amazônicas.....	17
1.1.2 Estimando a riqueza e a distribuição de espécies .....	18
1.1.3 As mudanças globais e a floresta amazônica.....	15
<b>1.2 A questão da pesquisa</b> .....	24
<b>1.3 Objetivos</b> .....	24
<b>1.4 Estrutura da tese</b> .....	25
<b>CAPÍTULO 2 ESTIMATING SPECIES RICHNESS IN HYPER-DIVERSE LARGE TREE COMMUNITIES</b> .....	27
<b>2.1 Introduction</b> .....	27
<b>2.2 Methods</b> .....	28
2.2.1 Simulations .....	28
2.2.2 Field data .....	29
<b>2.3 Results</b> .....	34
2.3.1 Simulations .....	34
2.3.2 Simulations of 49 ha of bci.....	36
2.3.3 Field data .....	36
<b>2.4 Discussion</b> .....	39
2.4.1 Is estimating species richness still a long way off? .....	46
2.4.2 Fisher’s paradox.....	47
<b>2.5 Conclusion</b> .....	48
<b>CAPÍTULO 3 SPECIES DISTRIBUTION MODELLING: CONTRASTING PRESENCE-ONLY MODELS WITH PLOT ABUNDANCE DATA</b> .....	49
<b>3.1 Introduction</b> .....	50
<b>3.2 Methods</b> .....	52
3.2.1 Species.....	49
3.2.2 Collections.....	49
3.2.3 Collections cleaning pipeline.....	49
3.2.4 Plot abundance data .....	50
3.2.5 Constructing abundance maps .....	51

3.2.6 Constructing presence-only sdms using maxent.....	52
3.2.7 Data analysis.....	56
<b>3.3 Results</b> .....	58
3.3.1 NHCs data distribution and relative abundance analysis .....	58
3.3.2 Predicted environmental suitability compared to species relative abundances.....	58
3.3.3 NHCs data cleaning treatment and MaxEnt map building.....	59
<b>3.4 Discussion</b> .....	61
3.4.1 Using nhcs for presence-only SDMs .....	61
3.4.2 MaxEnt maps vs. IDW maps.....	62
3.4.3 Collections versus abundance plot data .....	67
3.4.4 Environmental suitability versus dispersal limitation.....	67
3.4.5 Collection data and cleaning pipeline .....	68
<b>3.5 Conclusion</b> .....	69
<b>CAPÍTULO 4 MODELING THE DISTRIBUTION OF TREE SPECIES OF THE AMAZONIAN RAINFOREST TO LONG-TERM CLIMATE CHANGE DURING THE MID-LATE HOLOCENE</b> .....	70
<b>4.1 Introduction</b> .....	71
<b>4.2 Aims and approach</b> .....	72
<b>4.3 Methods</b> .....	73
4.3.1 Amazonian base map .....	73
4.3.2 Tree families .....	73
4.3.3 Collections.....	73
4.3.4 Environmental suitability .....	74
4.3.5 Species relative abundance.....	75
4.3.6 Constructing abundance maps .....	75
4.3.7 Pollen data .....	76
4.3.8 Data analysis.....	76
<b>4.4 Results</b> .....	77
<b>4.5 Discussion</b> .....	82
<b>4.6 Conclusion</b> .....	86
<b>CAPÍTULO 5 AMAZONIAN TREE SPECIES THREATENED BY DEFORESTATION AND CLIMATE CHANGE</b> .....	87
<b>5.1 Introduction</b> .....	87

<b>5.2 Methods</b> .....	89
5.2.1 Species and collections.....	89
5.2.2 Deforestation, protected areas and indigenous territories.....	90
5.2.3 Amazonian base map.....	90
5.2.4 Species area of occupancy.....	91
5.2.5 Data analysis.....	93
5.2.6 Data availability.....	94
<b>5.3 Results</b> .....	94
5.3.1 Original area of occupancy.....	94
5.3.2 Impact of historical forest loss.....	96
5.3.3 Impact of projected forest loss.....	96
5.3.4 Impacts of climate change.....	98
5.3.5 Impacts of combined projected deforestation and climate change.....	98
5.3.6 Impacts on species richness.....	99
5.3.7 Protected areas and indigenous territories.....	101
<b>5.4 Discussion</b> .....	103
<b>5.5 Conclusion</b> .....	107
<b>CAPÍTULO 6 SÍNTESE</b> .....	108
<b>6.1 Principais conclusões</b> .....	109
<b>6.2 Discussão geral</b> .....	111
6.2.1 Estimativa da distribuição e da riqueza de espécies arbóreas na amazônia.....	111
6.2.2 A influência do clima sobre a riqueza e a distribuição de espécies durante o holoceno.....	113
6.2.3 Os impactos das mudanças globais sobre a floresta amazônica.....	115
<b>6.3 Perspectiva futura</b> .....	118
<b>REFERÊNCIAS</b> .....	119
<b>APÊNDICES</b> .....	141
<b>APÊNDICE A</b> .....	142

## CAPÍTULO 1 INTRODUÇÃO GERAL

### 1.1 Referencial teórico

#### 1.1.1 Diversidade de espécies arbóreas amazônicas

A Amazônia é a maior e mais biodiversa floresta tropical no planeta, e abriga a maior riqueza de espécies arbóreas (CARDOSO et al., 2017; HANSEN et al., 2013; TER STEEGE et al., 2016). Ela é compartilhada por nove países do neotrópico (MORRONE, 2014), e estima-se que a região tenha aproximadamente 390 bilhões de árvores, para um total de aproximadamente 16.000 espécies, das quais, 227 são consideradas hiperdominantes, ocorrendo com grande abundância, sendo tão comuns que elas representam metade de todas as árvores acima de 10 cm de diâmetro à altura do peito (DAP) de todas as tipologia de florestas Amazônicas (TER STEEGE et al., 2013). Em contraste, as 5.800 espécies mais raras (36% das espécies) têm uma população estimadas em menos de 1.000 indivíduos (0.0003%). Este baixo número de indivíduos é suficiente para classificá-las como globalmente ameaçadas segundo os critérios da União Internacional para Conservação da Natureza (*Union for Conservation of Nature – IUCN*) (TER STEEGE et al., 2013, 2015).

Recentemente, um número substancial de registros de ocorrência de espécies tornou-se disponível por meio de plataformas on-line, em uma acentuada acumulação de dados, contendo muitos conjuntos de dados, coleções e informações de herbários (CRIA, 2018; GBIF, 2018). Esta acumulação foi possível graças ao rápido desenvolvimento de plataformas computacionais e ferramentas de bioinformática (NEWBOLD, 2010). Um estudo de ter Steege et al. (2016) encontrou 503.025 coletas arbóreas na Amazônia, datando de 1707 a 2015, em um total de 11,676 espécies, total este, que suporta o número estimado de 16.000 espécies possíveis para a região como um todo. Estas espécies estão distribuídas em 1.225 gêneros e 140 famílias. Todavia, a diversidade Amazônica é ainda um tema de grande debate.

Uma lista taxonômica recente proposta por Cardoso et al. (2017), baseada no estudo de Steege et al. (2016), sugeriu um número bem menor de 6.727 espécies. Uma nova lista proposta por Steege et al. (submetido) motivada pela grande redução do número de espécies proposta pela lista de Cardoso (2017), reavaliou o grande número de taxa excluídos, e com base em considerações ecológicas, sugeriu um novo total de 10.067 espécies arbóreas já coletadas na Amazônia.

Apesar do grande número de espécies registradas, a floresta amazônica ainda é amplamente inexplorada. Florestas tropicais ao redor do mundo apresentam um “grande vazio de dados” (*gapping data void*), com mais de 90% de espécies tão mal amostradas que chegam a ser invisíveis para as ferramentas modernas de modelagem e conservação (FEELEY; SILMAN, 2010). Na floresta Amazônica, ao longo de mais de 300 anos de coletas botânicas, a densidade de coletas atingiu apenas um total aproximado de 10 coletas/100km<sup>2</sup> (TER STEEGE et al., 2016). Além do “grande vazio de dados”, os registros de ocorrência de espécies destas coletas botânicas carregam um elevado número de inconsistências, por conta da rápida acumulação destes registros nas plataformas *on-line*, e dentre estas inconsistências podem ser citados os erros taxonômicos e incertezas geográficas dos registro de ocorrência das espécies (MALDONADO et al., 2015).

### 1.1.2 Estimando a riqueza e a distribuição de espécies

A riqueza de espécies representa, de forma simples, o número total de espécies em um espaço definido (MAGURRAN, 2004). Em geral, a riqueza de espécies é incrementada com o aumento da área (GOTELLI; COLWELL, 2001). Para uma área tão grande e tão subamostrada quanto a Amazônia, a riqueza pode apenas ser estimada. A estimativa de riqueza é uma análise amplamente utilizada na Ecologia, e é um meio comum utilizado para examinar padrões de diversidade baseados em amostras da riqueza observada de uma área ou comunidade (COLWELL, 1988; GASTON; SPICER, 2004).

Estimar a riqueza pode não ser tão direto quanto o seu conceito, pois ela não se encontra igualmente distribuída, admitindo ser também examinada pela uniformidade entre as populações das espécies, se referindo ao quão comum ou raras as espécies são, utilizando-se dados de abundância (HUBBELL, 2001). Na Amazônia, a estimativa do número de espécies varia amplamente de acordo com a técnica utilizada, variando entre 6.000-7.000 até 16.000 (TER STEEGE et al., 2013). Na Amazônia Ocidental, a riqueza e a diversidade de espécies são mais altas, e também são fortemente correlacionadas com a precipitação anual (GENTRY, 1988<sup>a</sup>, 1988b; TER STEEGE et al., 2003).

A riqueza de espécies é intimamente relacionada com a forma na qual as espécies estão espacialmente distribuída (ELITH; LEATHWICK, 2009). A distribuição espacial de espécies representa a presença de indivíduos ou populações em um espaço geográfico (PETERSON et al., 2011). A tipo particular de modelagem estatística permite estimar a distribuição de um espécie utilizando sua abundância e um índice para a agregação de seus indivíduos no espaço (HE; GASTON, 2000; VANDERWAL et al., 2009). A distribuição das espécies pode também ser estimada combinando os locais de ocorrências conhecidos das espécies e a dimensões ambientais nestes locais, definindo assim a distribuição potencial das espécies (ANDERSON; MARTÍNEZ-MEYER, 2004; ARAÚJO; PETERSON, 2012; PHILLIPS; ANDERSON; SCHAPIRE, 2006; PHILLIPS; DUDÍK; SCHAPIRE, 2004).

A associação das ocorrências conhecidas com os fatores ambientais está diretamente relacionada com a definição de nicho ecológico de Hutchinson, ou o espaço multidimensional onde as coordenadas representam as condições para a existência das espécies (HUTCHINSON, 1957). O conceito de nicho ecológico tem sido utilizado para estimar a distribuição potencial das espécies baseado nos registros de ocorrência observados, por meio da utilização da “modelagem de distribuição de espécies”, afim de prever áreas potenciais de distribuição além da ocorrência conhecida das espécies (ASPINALL; LEES, 1994; GUISAN; ZIMMERMANN, 2000; HIRZEL et al., 2002). Modelar a distribuição das espécies utilizando dados de abundância é uma prática mais conservadora quando comparada a técnicas que utilizam fatores ambientais, pois a modelagem baseada na abundância utiliza apenas a latitude e a longitude como variáveis preditivas, modelando a distribuição das espécies próxima de suas presenças confirmadas, não permitindo a predição de espécies longe dos locais onde sua ocorrência é conhecida (TER STEEGE et al., 2013).

A modelagem de distribuição de espécies tem sido uma área de conhecimento em crescimento, com a finalidade de endereçar perguntas relacionadas à Ecologia e Biogeografia, na qual os modelos preditivos das espécies permitem o desenvolvimento de análises de padrões de diversidade, incluindo a estimativa da riqueza de espécies (ELITH et al., 2011; IKNAYAN et al., 2014; MATEO et al., 2012; ORTEGA-HUERTA; PETERSON, 2008; PINEDA; LOBO, 2009). Predizer mudanças induzidas pelo clima e pelo uso da terra sobre a distribuição de espécies tem também sido um objeto da modelagem de distribuição (ARAÚJO; NEW, 2007). Medir os impactos das mudanças climáticas e de uso da terra sobre a riqueza e distribuição de espécies é fundamental para o estabelecimento de estratégias efetivas para conservação (GRENYER et al., 2006; MITTERMEIER et al., 2003; PERES et al., 2010; TUCKER et al., 2016). A maioria das espécies na natureza é rara, e podem sofrer grandes ameaças de extinção em resposta às referidas mudanças (TER STEEGE et al., 2013, 2015). Além disso, estas mudanças podem afetar diretamente o habitat das espécies e mudar seus padrões de distribuição (DUAN et al., 2016; PEARSON, 2010; PECL et al., 2017; SKOV; SVENNING, 2004; SLIK et al., 2009). As espécies podem perder adaptação à novos conjuntos de condições ambientais em seus habitats, devido a mudanças climáticas e de uso da terra, acabando fora de seus nichos ecológicos (BELLARD et al., 2012).

### 1.1.3 As mudanças globais e a floresta Amazônica

As mudanças globais podem ser vistas erroneamente como sinônimos de mudanças apenas no clima, mas elas também estão relacionadas a qualquer impacto de larga escala na natureza, incluindo mudanças de uso da terra, poluição ou superexploração de recursos naturais (HUBBELL et al., 2008; TER STEEGE, 2010). A floresta Amazônica foi moldada e influenciada por mudanças climáticas ao longo de milhões de anos durante sua história geológica (HOORN et al., 2010; JARAMILLO et al., 2010). Nos últimos milênios, durante o médio Holoceno, entre 8.000 e 4.000 anos atrás, as condições climáticas na Amazônia eram significativamente mais secas, o que contribuiu para uma maior presença de florestas secas e savanas (MAYLE et al., 2004).

Registros paleoecológicos presos em sedimentos de lagos ao sul da região Amazônica sugerem que estes limites da floresta expandiram em direção ao sul nos últimos 3.000 anos, em área de ecótono entre a floresta Amazônica e as savanas do Cerrado, representando a maior expansão ao sul já registrada nos últimos 50.000 (BURBRIDGE; MAYLE; KILLEEN, 2004; MAYLE; BURBRIDGE; KILLEEN, 2000). Esta expansão é atribuída ao aumento da precipitação e mudanças em sua sazonalidade, que podem ter facilitado o estabelecimento de novas populações de espécies amazônicas nesta região de ecótono. Estas mudanças nos padrões de precipitação também causaram a redução na frequência de incêndios, contribuindo para a expansão da floresta (MAYLE; POWER, 2008).

No presente, a floresta Amazônica tem sido influenciada por mudanças induzidas pela humanidade, as quais promovem a degradação de grandes áreas de florestas tropicais. A Amazônia já perdeu aproximadamente 12% de sua cobertura original (HANSEN et al., 2013). Muitos estudos têm apresentado preocupações com as pressões humanas na região, as quais levam ao desflorestamento, para a abertura de estradas, construção de hidroelétricas, mineração, criação de gado e expansão das fronteiras agrícolas (DAVIDSON et al., 2012; FEARNSIDE, 2003; HUBBELL et al., 2008; LAURANCE et al., 2001; SOARES-FILHO; ASSUNÇÃO; PANTUZZO, 2001).

O desflorestamento é uma ameaça direta à biodiversidade, com impactos ecológicos negativos, tal como, a criação de barreiras, restringindo a dispersão e o movimento de espécies (FEELEY; REHM, 2012). Praticamente todos os serviços ecossistêmicos podem ser afetados pelo desflorestamento, sendo os mais impactados são aqueles relacionados à ciclagem da água e armazenamento do carbono (FEARNSIDE, 2006; STRAND et al., 2018). Ele pode também aumentar as diferenças entre o clima atual e futuro, tendo influências em escalas local, regional e global, alterando as correntes convectivas de umidade e, conseqüentemente, também o microclima (FEELEY; SILMAN, 2009; SHUKLA; NOBRE; SELLERS, 1990).

Análises baseadas em cenários futuros sugerem que as mudanças climáticas podem ultrapassar os impactos provocados pelo desflorestamento na Amazônia, com base nas mudanças induzidas pelo clima em todo o planeta durante o século 20 (BELLARD et al., 2012; NEPSTAD et al., 2008; PEREIRA; NAVARRO; MARTINS, 2012). Um aumento médio de 3° C na temperatura ao longo do século 21, combinado com redução da humidade e a fragmentação de florestas, pode ser o suficiente para causar um maior aumento no estresse hídrico e vulnerabilidade florestal (MALHI; WRIGHT, 2004; MAYLE; POWER, 2008). O estresse hídrico provocado pelos períodos secos podem aumentar ao longo do século 21, criando um clima típico de florestas sazonais, associado com altas temperaturas, vulnerabilidade à incêndios e desflorestamento, os quais podem levar à diminuição da biomassa florestal suscetível ao fogo (MALHI et al., 2009). Projeções baseadas em cenários de emissão de gases de efeito estufa estimam que aproximadamente 40% de todas as ecoregiões amazônicas serão impactadas pelas mudanças climáticas até 2050 (FEELEY; REHM, 2012).

As mudanças induzidas pelo clima, combinadas com o desflorestamento, podem criar ameaças ainda mais sérias para o meio ambiente, e a perda de habitat está entre as maiores ameaças (FEARNSSIDE, 2006; TRAVIS, 2003). A perda de habitat é uma das principais causas de extinção de espécies, reduzindo suas áreas de ocupação (BROOKS et al., 2002; FEELEY; SILMAN, 2009; IUCN, 2012; TILMAN et al., 1994). Por meio da mensuração da redução da área de ocupação das espécies é possível avaliar impactos sobre a biodiversidade e risco de extinção (GASTON; SPICER, 2004; IUCN, 2012). A perda de habitat pode colocar entre 5-9% de todas as espécies de plantas na Amazônia em categorias de risco de extinção, e para espécies arbóreas este percentual pode ser ainda maior, variando entre 40-64% (FEELEY; REHM, 2012; STEEGE et al., 2015).

A extinção de espécies é um dos mais debatidos impactos sobre a biodiversidade. Ela pode ser classificada por categorias, variando de acordo com a intensidade do risco de extinção de espécies, e elencadas em Listas Vermelhas (IUCN, 2012). As listas vermelhas constituem uma metodologia adotada no mundo todo para avaliar a probabilidade de extinção de espécies. Elas são um primeiro passo em direção à conservação de espécies, e representam a base de muitas iniciativas para proteção de espécies ameaçadas, seja em escala local, regional ou global (e.g. TABARELLI et al., 2005). Apesar de as Listas Vermelhas terem muitas limitações, elas têm se tornado uma ferramenta importante para o planejamento, gestão e monitoramento da conservação da biodiversidade (RODRIGUES et al., 2006).

Uma outra ferramenta importante para a conservação da biodiversidade são as áreas protegidas. Estas áreas são originalmente delimitadas para conservar paisagens peculiares e a vida selvagem, mas o aumento das preocupações sobre a degradação ambiental nas últimas décadas do século 20 influenciou a emergência de sistemas de áreas protegidas, que apresentam um grande número de objetivos (WATSON et al., 2014). A efetividade destas áreas em conservar a biodiversidade tem sido questionada, por conta da alta governabilidade demandada, todavia, estudos mostram que elas têm contribuído para a manutenção e conservação da biodiversidade (BARNES et al., 2018; FERREIRA; VENTICINQUE; ALMEIDA, 2005; GRAY et al., 2016; NAUGHTON-TREVES; HOLLAND; BRANDON, 2005; THOMAS et al., 2012; WALKER et al., 2009). Projeções mostram que elas podem também contribuir para a conservação em cenários futuros, apesar de que as mudanças globais podem também ameaçar os objetivos destas áreas (FEELEY; SILMAN, 2016; KILLEEN; SOLÓRZANO, 2008; SOARES-FILHO et al., 2010; TER STEEGE et al., 2015).

## 1.2 A questão da pesquisa

A riqueza e a distribuição das espécies arbóreas na Amazônia têm sido influenciadas por mudanças climáticas. Nos últimos milênios, em um processo natural, tais mudanças se desenvolveram de maneira gradual. Já nas últimas décadas, as alterações climáticas promovidas pela humanidade, associadas a perda de habitat produzida pelo desflorestamento, impactaram significativamente as espécies arbóreas Amazônicas, e podem ser ainda mais intensas até o ano de 2050, alterando a floresta Amazônica de maneira irreversível. No entanto, estas alterações podem ser mitigadas, considerando cenários de melhoria de governança, que projetam a redução das mudanças climáticas, e um maior controle sobre o desflorestamento.

## 1.3 Objetivos

Avaliar os impactos das mudanças climáticas e do desflorestamento sobre a biodiversidade Amazônia no passado, presente e futuro, por meio da avaliação da riqueza e da distribuição das espécies arbóreas da flora arbórea amazônica.

Os objetivos específicos são:

1. Testar e comparar as premissas e resultados de estimadores de riqueza baseados em métodos paramétricos e não-paramétricos para uma floresta tropical simulada e cinco diferentes bases de dados florestais obtidas em levantamento de campo na Amazônia.
2. Estimar a distribuição atual das espécies arbóreas hiperdominantes da Amazônia, e comparar modelos de distribuição baseados na abundância e aptidão ambiental das espécies.
3. Estimar a distribuição de espécies arbóreas amazônicas durante os períodos Holoceno médio e Holoceno tardio, e avaliar a correlação entre a abundância das espécies arbóreas e seus registros paleoecológicos de pólen na Amazônia.
4. Estimar a riqueza e distribuição atual de todas as espécies arbóreas amazônicas conhecidas, e em dois cenários de emissões para o ano de 2050, e avaliar os impactos do desflorestamento histórico e futuro para o ano de 2050.

## 1.4 Estrutura da tese

Esta tese investiga os impactos das globais na riqueza e distribuição de espécies da flora arbórea da Amazônia, utilizando estimativa de riqueza e distribuição de espécies para condições do presente, e também projetando cenários para o passado e o futuro. Além disso, a tese foca nas duas principais fontes modernas de mudanças globais que ameaçam as florestas tropicais, as mudanças climáticas e o desflorestamento. As mudanças globais impactam o habitat natural, que está consistentemente relacionado com a forma pela qual as espécies se distribuem espacialmente, e desta forma, está também relacionado com a riqueza de espécies. Mensurar as respostas da riqueza e da distribuição de espécies em função das mudanças globais é vital para o estabelecimento de estratégias de conservação eficazes.

O capítulo 2 investiga as proposições e resultados de estimadores de riqueza de espécies baseados em métodos paramétricos e não-paramétricos, comparando a capacidade de extrapolação de cada um destes estimadores para grandes áreas de floresta tropical. Foram realizadas estimativas de riqueza de espécies para uma floresta tropical simulada e para cinco base de dados de levantamentos de campo diferentes.

O capítulo 3 foca na modelagem de distribuição para as espécies de árvores amazônicas hiperdominantes. Este grupo conta com 227 espécies, que representam metade do número total de indivíduos arbóreos na floresta Amazônica. É conduzida uma comparação entre os modelos de distribuição de espécies e modelos baseados em um conjunto independente de dados de abundância, para avaliar as semelhanças e diferenças entre predições baseadas na aptidão ambiental das espécies, que utilizam dados de coleções e variáveis climáticas, e predições baseadas em dados de abundância, que utilizam dados de parcelas de inventários florestais.

O capítulo 4 investiga as respostas da floresta Amazônica às mudanças climáticas de longa duração ao longo do Holoceno médio e do Holoceno tardio (últimos 6.000 anos). A floresta expandiu ao sul através dos limites da floresta e da savana nos últimos três mil anos, e este processo é evidenciado por registros fósseis de pólen obtidos em núcleos de sedimentos de lagos amazônicos. Estes limites ao sul representam uma região de ecótono, muito sensível a mudanças climáticas. Esta expansão é atribuída a variações nos padrões de precipitação, especialmente em relação à sua sazonalidade, o que afetou a distribuição de espécies de árvores entre o Holoceno médio, mais seco, e o Holoceno tardio, mais úmido. São utilizados dados paleoecológicos (concentrações de pólen depositados nos sedimentos de lagos amazônicos), modelos de distribuição de espécies e modelos de abundância. Além disso, é testado se os dados paleoecológicos podem ser usados como representações da abundância relativa das espécies.

O capítulo 5 investiga os impactos das mudanças climáticas e do desflorestamento sobre todas as espécies de árvores amazônicas, baseado na lista de espécies arbóreas mais recente para a região. Esta investigação inclui uma análise dos impactos do clima, por meio da modelagem de distribuição de espécies no presente, e sob dois diferentes cenários futuros para o ano de 2050, um otimista (RCP 2.6) e um pessimista (RCP 8.5), combinados com uma análise dos impactos do desflorestamento histórico (até 2013) e dois cenários futuros de projeções de desflorestamento para o ano de 2050, também considerando um cenário otimista (“governança”) e um pessimista (“condições usuais”). São avaliados também os níveis de ameaças de extinção de espécies, baseados nas categorias de ameaça de extinção de espécies definidas pela IUCN, e a efetividade das áreas protegidas na Amazônia em mitigar os impactos sobre as espécies.

A síntese apresentada no capítulo 6 integra os resultados da tese, relatando os achados nos diferentes capítulos em relação aos impactos das mudanças globais sobre a biodiversidade Amazônica. Além disso, é discutida a distribuição de espécies no passado e presente, e como ela é moldada ao longo do tempo, e como pode determinar a resposta das espécies às mudanças climáticas no futuro. A conclusão apresenta as implicações para a conservação da biodiversidade e prospectos futuros para a investigação da conservação de espécies arbóreas amazônicas.

## CAPÍTULO 2 ESTIMATING SPECIES RICHNESS IN HYPER-DIVERSE LARGE TREE COMMUNITIES<sup>1</sup>

### Abstract

Species richness estimation is one of the most widely used analyses carried out by ecologists, and nonparametric estimators are probably the most used techniques to carry out such estimations. We tested the assumptions and results of nonparametric estimators and those of a logseries approach to species richness estimation for simulated tropical forests and five datasets from the field. We conclude that nonparametric estimators are not suitable to estimate species richness in tropical forests, where sampling intensity is usually low and richness is high, because the assumptions of the methods do not meet the sampling strategy used in most studies. The logseries, while also requiring substantial sampling, is much more effective in estimating species richness than commonly used nonparametric estimators, and its assumptions better match the way field data is being collected.

**Keywords:** Logseries, Nonparametric estimators, Species estimation, Tropical forests.

### 2.1 Introduction

Species-richness estimation is one of the most widely used analyses carried out by ecologists, either to compare samples obtained with different efforts, or by extrapolation, to predict the number of species present in an area larger than the one sampled. Extrapolation methods are frequently used for geographically large areas, where coverage of the complete range is out of reach, too labor intensive, or too expensive.

From a parametric point of view, species richness estimation is based on parameter inference for either one of the two main relationships describing assemblages: the number of individuals ( $N$ ) in a community or the area ( $A$ ) this community occupies. In these cases, the number of species ( $S$ ) only depends on the relative or rank abundance distribution of the species (RAD) (IZSÁK; PAVOINE, 2012) or the species-area relationship (SAR) (ROSENZWEIG, 1995).

---

<sup>1</sup>Publicado na revista *Ecology* (2017) 98: 1444–1454, Qualis A1 na Área de Avaliação de Ciências Ambientais.

As a general rule of thumb, in any number of random samples of an area, the number of species that remain undetected will increase with increased S and A (GOTELLI; COLWELL, 2001), precluding any attempt to directly quantify the RAD or the SAR from samples. This clearly poses a problem in tropical forests that are generally both large and rich.

There has been a long argument as to whether the logseries (FISHER; CORBET; WILLIAMS, 1943), the log-normal (PRESTON, 1948), or alternative distributions (MCGILL et al., 2007) give the best fit for Rank Abundance Distributions (RADs), how much the fit is dependent on scale or sampling completeness, and to which extent the best fitting model reflects the biological processes underlying the distribution. The use of nonparametric estimators of species richness such as Chao, ICE (Incidence-based Coverage Estimator of species richness), and Jackknifing, has been proposed as a way of dealing with this uncertainty, because they do not assume any underlying distribution. It would be wrong, however, to suppose that they are less sensitive to other assumptions than parametric methods or that they do not suffer from other drawbacks.

Brose et al. (2003) noted that sampling-theoretical methods of estimation require high sampling intensity to avoid what Wang and Linday (2005) call the “severe underestimation observed from popular nonparametric estimators due to the interplay of inadequate sampling effort, large heterogeneity and skewness.” Xu et al. (2012) also reported that nonparametric methods severely underestimate richness and emphasized that these methods should not be used across heterogeneous landscapes. This is largely because nonparametric estimators based on a sampling estimate of the rare-tail of the SAR are very sensitive to the shape of the abundance-distribution. As underlined by Harte and Kitzes (2015), “The rare tail is emphasized because the shape of the species-area relationship is especially influenced by the numbers of rare species”. Although the performance of estimators has been frequently compared (BROSE; MARTINEZ; WILLIAMS, 2003; CHIARUCCI et al., 2003; HORTAL; BORGES; GASPAR, 2006; WALTHER; MOORE, 2005; XU et al., 2012), much less of the ecological literature critically evaluates their assumptions and caveats.

Perhaps the most commonly used estimator for species richness is the Chao1 nonparametric estimator (CHAO, 1989; CHAO et al., 2009), which estimates the number of species as:

$$S_{estimated} = S_{observed} + \frac{f_1^2}{2f_2}$$

where  $f_1$  is the number of species with 1 individual in the sample (singletons) and  $f_2$  is the number of species with 2 individuals in the sample (doubletons). The Chao1 estimator and other nonparametric estimators make no assumptions about the underlying species-abundance distribution, but do assume that sampling is random with replacement across the whole area. When  $f_1 = 0$ , it is assumed that all species have been collected and  $S_{estimated} = S_{observed}$  (CHAO et al., 2009).

Chao Bunge (CHAO; BUNGE, 2002), Chao Lee ACE and Chao Lee ACEI (CHAO; LEE, 1992), and Jackknife (BURNHAM; GRAHAM, 1999) are variations on the original Chao 1 estimator are also dependent on the fractions of the rare or infrequent species, and require “a sufficiently high overlap fraction [...] to produce a reliable estimate of the species” (CHAO; BUNGE, 2002), and, finally, are all based on the capture-recapture principle that requires sampling with replacement.

The logseries in contrast is not based on a capture-recapture principle and was among the first attempts to mathematically describe the relationship between the number of species and number of individuals in a biological context by Fisher (FISHER; CORBET; WILLIAMS, 1943) and is given by:

$$\Phi_n = \frac{\alpha x^n}{n}$$

where:  $\Phi_n$  is the number of species with  $n$  individuals;  $\alpha$  is Fisher's  $\alpha$ ;  $x = N/(N + \alpha)$  ( $N$  being the number of individuals in the total sample;  $x$  being asymptotically equal to 1 with large sample sizes).

Hence, we expect  $\alpha$  from samples to quickly approach  $\alpha$  of the total landscape, after which it will be practically independent of sample size. Fisher's alpha can be calculated from the number of individuals (N) and species (S) in a sample by iteratively solving:

$$\alpha = \frac{S}{\ln(1 + \frac{N}{\alpha})}$$

The logseries is essentially a geometric summation, which builds up from the first term ( $\Phi_1$ ), the singletons. The number of singletons is thus predictable in a logseries ( $\Phi_1 = \alpha x$ ) and always the largest class. As  $x$  is very close to 1 for reasonably large samples,  $\Phi_1 \approx \alpha$  in such samples. Similarly, the number of doubletons is:  $\Phi_2 = \alpha x^2/2 \approx \alpha/2$ . When we assume that RAD's of communities follow the logseries, this has implications for the nonparametric Chao1 estimator. For large samples, the Chao1 estimator (note that  $f_1^2/[2f_2] = \Phi_1^2/[2\Phi_2]$ ) will simply become:  $S_{\text{estimated}} = S_{\text{observed}} + \alpha^2/[2(\alpha/2)] = S_{\text{observed}} + \alpha$ . Consequently, we predict that for reasonably large samples, for which  $\alpha$  is constant, Chao1 always estimates the number of unseen species as  $\alpha$ , regardless of the size of the samples.

Hubbell's neutral theory was the first ecological theory, deriving the logseries from the basic biological processes of birth rate (b) and death rate (d) (Hubbell 2001, Hubbell 2015). It can be shown that in this model  $x(N/[N + \alpha]) = b/d$ . NT derives a distribution, the Zero Sum Multinomial (ZSM), which for large communities with little drift approaches a logseries. For small local communities (limited immigration and drift), the ZSM approaches a lognormal (HUBBELL, 2001).

Here we compare commonly used nonparametric estimators of species richness to one parametric estimator based on the logseries for the purpose of estimating species richness in large areas of tropical forest. We specifically chose the logseries as we are trying to estimate richness in very large areas where the ZSM approaches this distribution. We show by simulations and comparisons with empirical data that the assumptions of the parametric estimator are less sensitive to deviations than those of the nonparametric estimators.

## 2.2 Methods

### 2.2.1 Simulations

We modeled forest communities of 100 x 100 1-ha plots (a 100 km<sup>2</sup> square area), each plot with 500 individuals. We initially filled each of the 10,000 hectares with a random sample of 500 individuals from a metacommunity (MC). The MC was constructed using a logseries of 15 million individuals and a Fisher's  $\alpha$  of 300, which is roughly equivalent to a rich central Amazonian rainforest (see data below). We used a logseries as this conforms to the structure expected (HUBBELL, 2001) and found in tropical forests (HUBBELL, 2001, 2015; TER STEEGE et al., 2013). After filling the plots randomly from the MC, the mean Fisher's  $\alpha$  of all plots and that of the virtual forest initially is, as expected, equivalent to that of the MC.

During the simulations, trees were randomly selected to be removed (1 per plot per time step) and new recruitment could come from dispersal (m) from 4 sources:

1. Recruitment from dispersal inside the plot ( $m_{\text{plot}}$ ), equivalent to local recruitment. Local recruitment is random within the plot, i.e. we assume no spatial structure inside the plots.
2. Recruitment from dispersal from the surrounding eight plots. Dispersal probability based on dispersal distance was based on the model of Chisholm and Lichstein (CHISHOLM; LICHSTEIN, 2009), modified by Pos et al. (POS et al., 2017). The dispersal probability from the adjacent plots ( $m_{\text{adjacent}}$ ) is computed from dispersal distance as (POS et al., 2017):

$$m_{\text{adjacent}} = 0.3 \times \frac{A - (1 - 2 \times d)^2}{A}$$

where: A is the area of the plot (10,000m<sup>2</sup>), l = length of the plot (100m), and d = the average dispersal distance. Assuming an average dispersal range of 10-40 meters  $m_{\text{adjacent}}$  is in the range of 0.108-0.288.

3. Recruitment from dispersal from the surrounding forest (10,000 ha), comparable to long-distance dispersal. Individuals for replacement were drawn randomly from the 10,000 ha. This assumes that long-distance dispersal is not spatially driven. We used a probability of  $m_{\text{forest}} = 0.1 * m_{\text{adjacent}}$ .

4. Recruitment from dispersal from the MC, this is comparable to infrequent very long-distance dispersal, also termed vagrancy. The individuals were drawn randomly from the MC, assuming that very long-distance dispersal too is not spatially driven. We used a probability of  $m_{MC} = 0.01 * m_{adjacent}$ .

And:

4. speciation ( $v$ ) as defined in the Unified Neutral Theory of Biodiversity and Biogeography (HUBBELL, 2001):

$$v = \frac{\theta}{2 \times J} = \frac{250}{2 \times 10,000 \times 500} = 2.5e^{-5}$$

Where  $\theta$  is the biodiversity number, asymptotically equivalent to Fisher's alpha and  $J$  is the size of the community.

Parameters 2-4 were calculated first. Local recruitment (1) was then calculated as:

$$m_{plot} = 1 - m_{adjacent} - m_{forest} - m_{MC} - v.$$

We ran 30,000-time steps for each model with mean dispersal distances of 10, 15, 20, 25, 30, and 40 meters. At each time step, 1 individual per plot was randomly selected to be replaced by another individual based on the 5 probabilities above. Thus, 10,000 individuals were replaced at each time step.

After each simulation, we plotted the RAD with a fit of the logseries and lognormal, the Species Area Curve with Chao1 estimator, the Fisher's  $\alpha$  to area curve, and the predicted richness based on Fisher's  $\alpha$  and the Chao1 estimator. All curves were based on the average of 50 draws from 1 to all 10,000 plots. We also plotted the results for the average of 50 random draws of 100 plots from our virtual forest.

We also ran the simulation model for a sample of 49 ha of forest (7x7 ha), using the field data of BCI (Table 2.1). We simulated a forest area of 49 plots, using a MC of 15km<sup>2</sup> (the size of BCI), an alpha of 50 and density of 429 ind ha<sup>-1</sup>, a dispersal distance of 40m (CHISHOLM; LICHSTEIN, 2009) for  $m_{adj} = 0.288$ , and  $v = 0.00119$ . Simulations and calculations were carried out with custom-made scripts in R (R CORE TEAM, 2011).

### 2.2.2 Field data

We used field data from 4 sites. 1) Barro Colorado Island (BCI), a 50-ha plot in old growth forest (CONDIT et al., 2002). This well-known dataset was also used in Chao et al. (2009); 2) Reserva Ducke (RD, Fig. S1), a forest reserve of 100 km<sup>2</sup> in central Amazonia, just north of Manaus (CASTILHO, 2004); 3) Piste de St Elie (PSE, Fig. S2), mixed forest in northern French Guiana (SABATIER et al., 1997); 4) the Monte Branco Plateau (MBP, Fig. S3), a large bauxite plateau of 3750 ha in Para, Brazil (SALOMÃO, 2015).

BCI tree data was extracted from vegan (OKSANEN, 2008), tree data for RD and PSE are integrated in the ATDN database (TER STEEGE et al., 2013) and extracted from that source, MBP tree data (R. P. Salomão, unpublished data) was taxonomically harmonized with the ATDN database.

We extrapolated the species richness for an area in which the plots were located; for RD for 7.2 million individuals (the area of the full 100 km<sup>2</sup> reserve); for PSE an imaginary 1500 ha forest area encompassing the plots; for MBP the 3750 ha that comprises the complete plateau (Table 2.1). The plots are well spread across these areas. For BCI we estimated richness for the 50-ha plot.

**Table 2.1.** Botanical inventories used for the analysis, with locality (Barro Colorado Island (BCI), Reserva Ducke (RD), Piste de St Elie (PSE), Monte Branco Plateau (MBP), number of plots sampled, plot area (ha), number of individuals sampled (N), number of species recorded (S), the target area for which estimates were made, number of individuals in the target area based on average density, and reference to the data source: 1) BCI; 2) RD; 3) PSE; 4) MBP.

Locality	# plots	area	N	S	target area	individuals	Reference
BCI	50	1	21,457	225	50 há	21,457	1
RD	72	0.5	25,066	1233	100 km <sup>2</sup>	7,200,000	2
PSE	20	1	12,450	574	1500 ha	933,750	3
MBP	301	0.25	36,546	703	3750 ha	1,821,229	4

For each of the plot datasets we carried out the following analyses:

1. plotted the RAD of the dataset with the exact logseries and lognormal for the number of individuals (N) and species (S) in the field sample,
2. constructed a curve of the mean species richness by area, based on 50 randomizations of the field data,
3. constructed a curve of the mean of Fisher's  $\alpha$  by area, based on the same 50 randomizations of the field data,
4. estimated species richness in the target area for all sub-samples of the 50 randomizations based on Fisher's  $\alpha$  of the sub-samples as follows:  $S = \alpha * \ln(1 + N/\alpha)$  (FISHER; CORBET; WILLIAMS, 1943); where  $\alpha$  = Fisher's  $\alpha$ , and N is the number of trees in the subsample and the variance of S as (FISHER; CORBET; WILLIAMS, 1943):  $\text{var}_S = \alpha \ln([2N + \alpha]/[N + \alpha]) - \alpha^2 N / (N + \alpha)^2$ ,
5. estimated species richness in the target area for all sub-samples of the 50 randomizations, based on Chao1:  $S_{\text{est}} = S_{\text{obs}} + f_1^2 / (2f_2)$ ,
6. estimated the species richness for the field dataset for a number of nonparametric estimators (Chao 1984, Chao Bunge, Chao Lee ACE, Chao Lee ACEI, Jackknife), as provided in the R-package SPECIES (WANG, 2011).

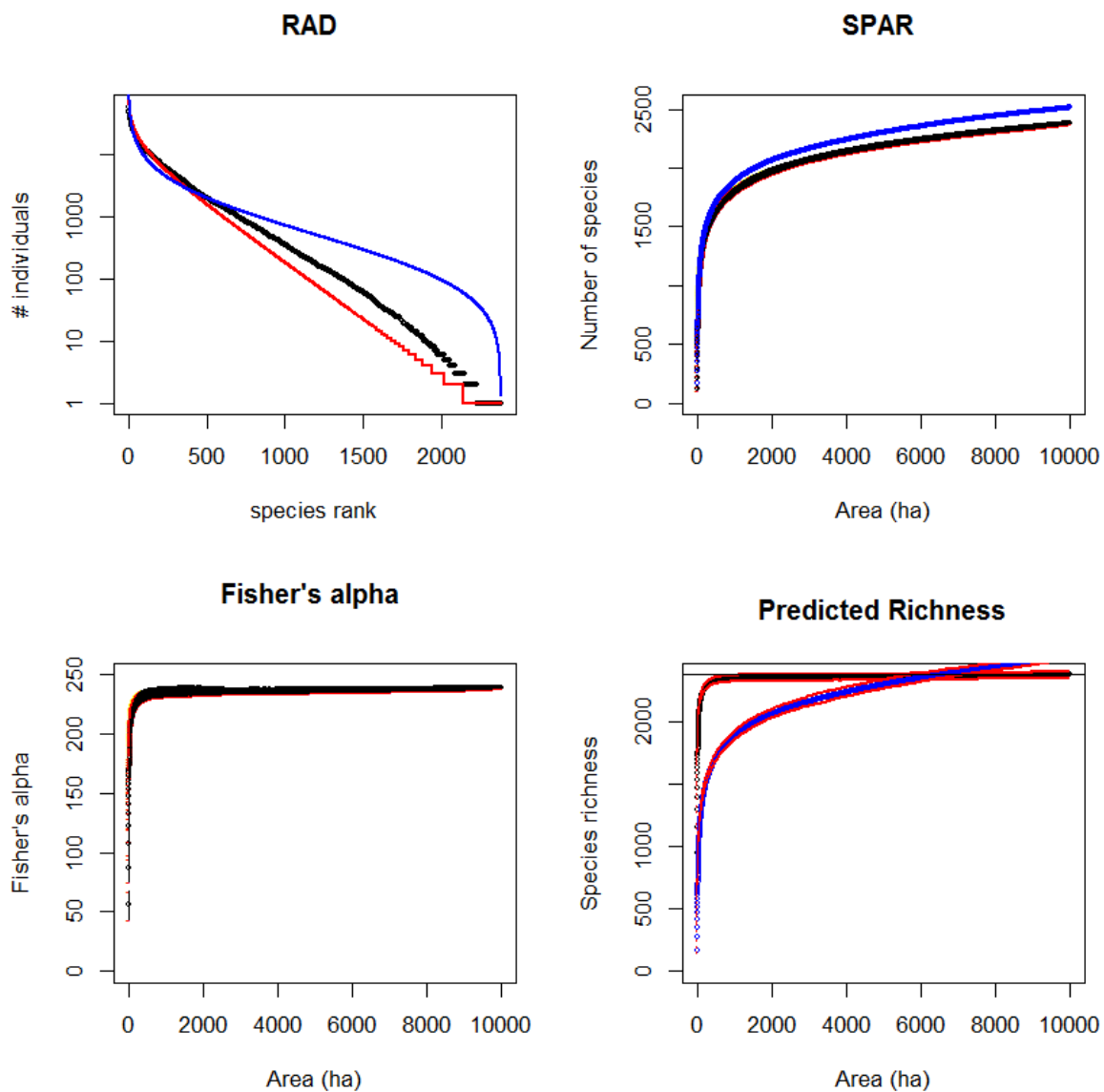
The 50 randomizations of the plot data were produced without replacement from one plot to the number of plots in the field dataset.

## 2.3 Results

### 2.3.1 Simulations

The simulations of our virtual forest with mean dispersal distance of 20 m produced a RAD that is close to a logseries (but not fully identical) (Fig. 2.1 A). Species richness calculated with the Chao1 estimator as predicted becomes  $S_{\text{observed}}$  plus  $\sim$ Fisher's  $\alpha$  for larger samples (Fig. 2.1 B). While Fisher's  $\alpha$  and species richness calculated with Fisher's  $\alpha$  tend to asymptotically approach the community value, species richness calculated with the Chao1 estimator follows the shape of the species area curve and finally overestimates the richness of the total sample by approximately Fisher's  $\alpha$ .

**Figure 2.1.** Simulation of a 10,000-ha virtual forest with mean dispersal distance of 20 m. Parameters used are  $m_{plot} = 0.78688$ ;  $m_{adjacent} = 0.192$ ;  $m_{forest} = 0.0192$ ;  $m_{MC} = 0.00192$ ;  $v = 10^{-4}$ . (A) Rank abundance distribution (RAD) of the total virtual (black) with logseries fit (red) and lognormal fit (blue). (B) Species area (SPAR) curve for the total virtual forest and estimated richness (Sestimated) based on Chao1 (blue). (C) Fisher's  $\alpha$  area curve for the virtual forest. (D) Species richness estimated with Fisher's  $\alpha$  (black), Chao1 (blue), each with 95% CI (red), and actual species richness of the simulated community (horizontal line).  $m_{plot}$  = local recruitment;  $m_{adjacent}$  = recruitment from adjacent plots;  $m_{forest}$  = recruitment from total forest;  $m_{MC}$  = recruitment from metacommunity;  $v$  = speciation.



All simulations ( $d = 1 - 40$  m) show similar results (Figs. S4-17, Appendix S1). With increasing mean dispersal distance and, hence, stronger input from the adjacent plots, Fisher's  $\alpha$  tends to be overestimated slightly before it reaches the value of the total virtual forest and the number of species in the full virtual forest increases from 2,071 to 2,098. The calculations for 50 samples of 100 plots suggest that although Fisher's  $\alpha$  predicts a richness closer to the known richness for the virtual forest, it is still an underestimate of 3-17% (Fig. 2.2, Figs. S5,7,9,11,13,15, Appendix S2). For a similar sample size, the Chao1 estimator provides an underestimate of 43-51%, depending on the dispersal distance chosen (Table S1).

### 2.3.2 Simulations of 49 ha of BCI

Simulations of a 49 ha virtual plot based on the BCI data produced a RAD (Fig. 2.3) very similar to that of the forest in the real 50 ha BCI plot (Fig. 2.4). Fisher's  $\alpha$  was very close to the final value for the simulated forest after 10 plots. Consequently, species richness was also close to its simulated richness after sampling 10 plots. Species richness calculated with Chao1 is, as predicted, the species area curve plus Fisher's  $\alpha$  of the sample. Thus, even when all individuals have been sampled, Chao1 still predicts unobserved species with a magnitude of Fisher's  $\alpha$ . This is because, as in real forests, the virtual forest of 49 ha still contains singletons.

### 2.3.3 Field data

In all cases: BCI (Fig. 2.2), RD (Fig. 2.3), PSE (Fig. 2.4), and MBP (Fig. 2.5), the RAD showed a hollow curve with few common and many rare species and, except for BCI, the logseries provided a reasonable fit. In all cases, Fisher's  $\alpha$  was very close to that of the full sample with less than 20 plots sampled. For small samples, Chao1 provided a severe underestimate for the richness in the sample, and even for the final sample,  $S_{\text{estimated}}$  was almost equivalent to  $S_{\text{observed}} + \text{Fisher's } \alpha$ .

**Figure 2.2.** Barro Colorado Island field data (BCI). A. Rank abundance distribution (RAD) of BCI with logseries fit (red) and lognormal fit (blue). B. Species area curve for BCI and estimated richness (Sestimated) based on Chao1 (blue). C. Fisher's  $\alpha$  area curve for BCI. D. Species richness estimated for a 50 ha area on BCI with Fisher's  $\alpha$  (black) and Chao1 (blue), each with 95% CI (red).

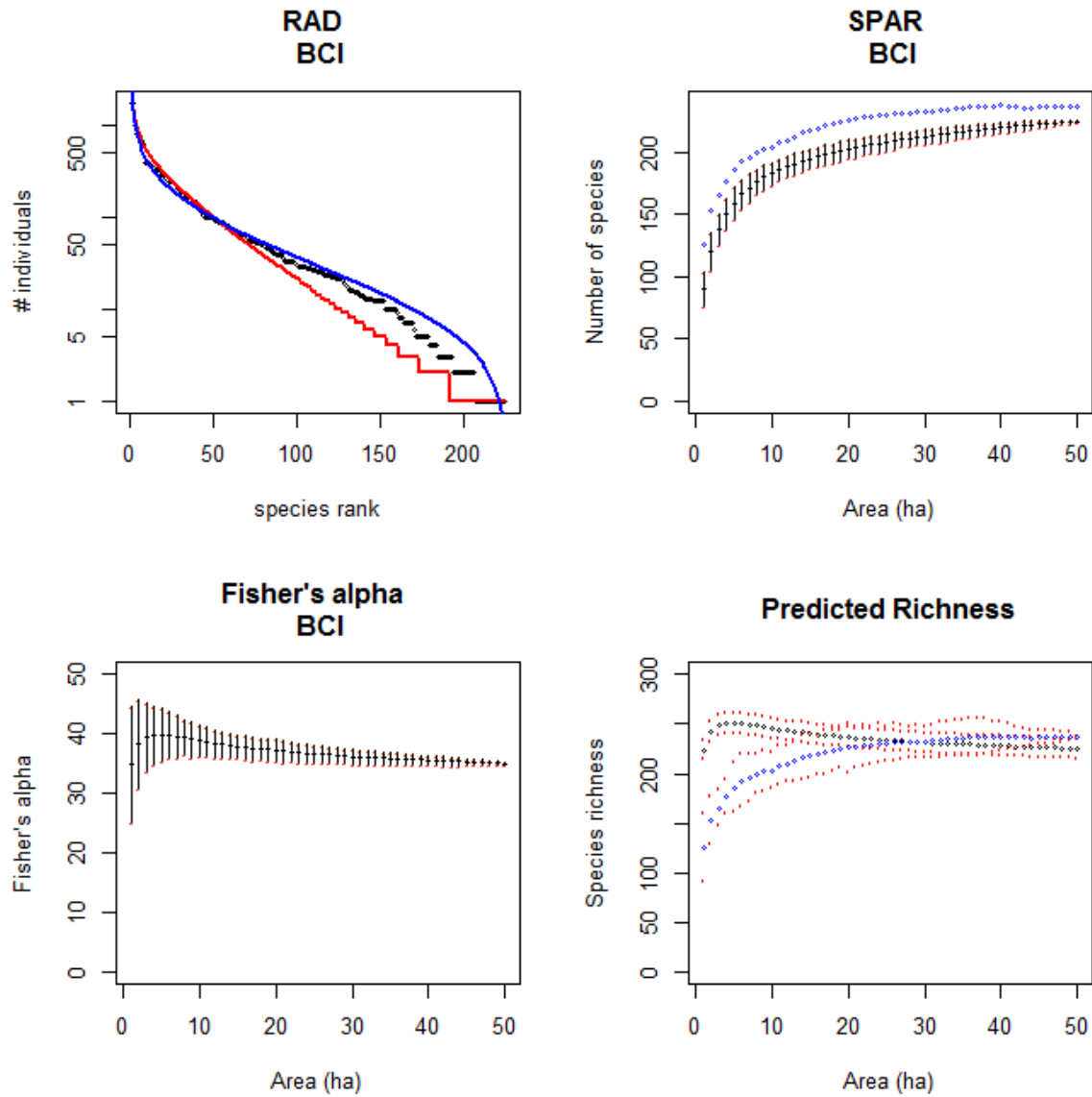


**Figure 2.3.** Reserva Ducke field data (RD). A. Rank abundance distribution (RAD) of RD with logseries fit (red) and lognormal fit (blue). B. Species area curve for RD and estimated richness (Sestimated) based on Chao1 (blue). C. Fisher's  $\alpha$  area curve for RD. D. Species richness estimated for the total 100km<sup>2</sup> RD area with Fisher's  $\alpha$  (black) and Chao1 (blue), each with 95% CI (red).

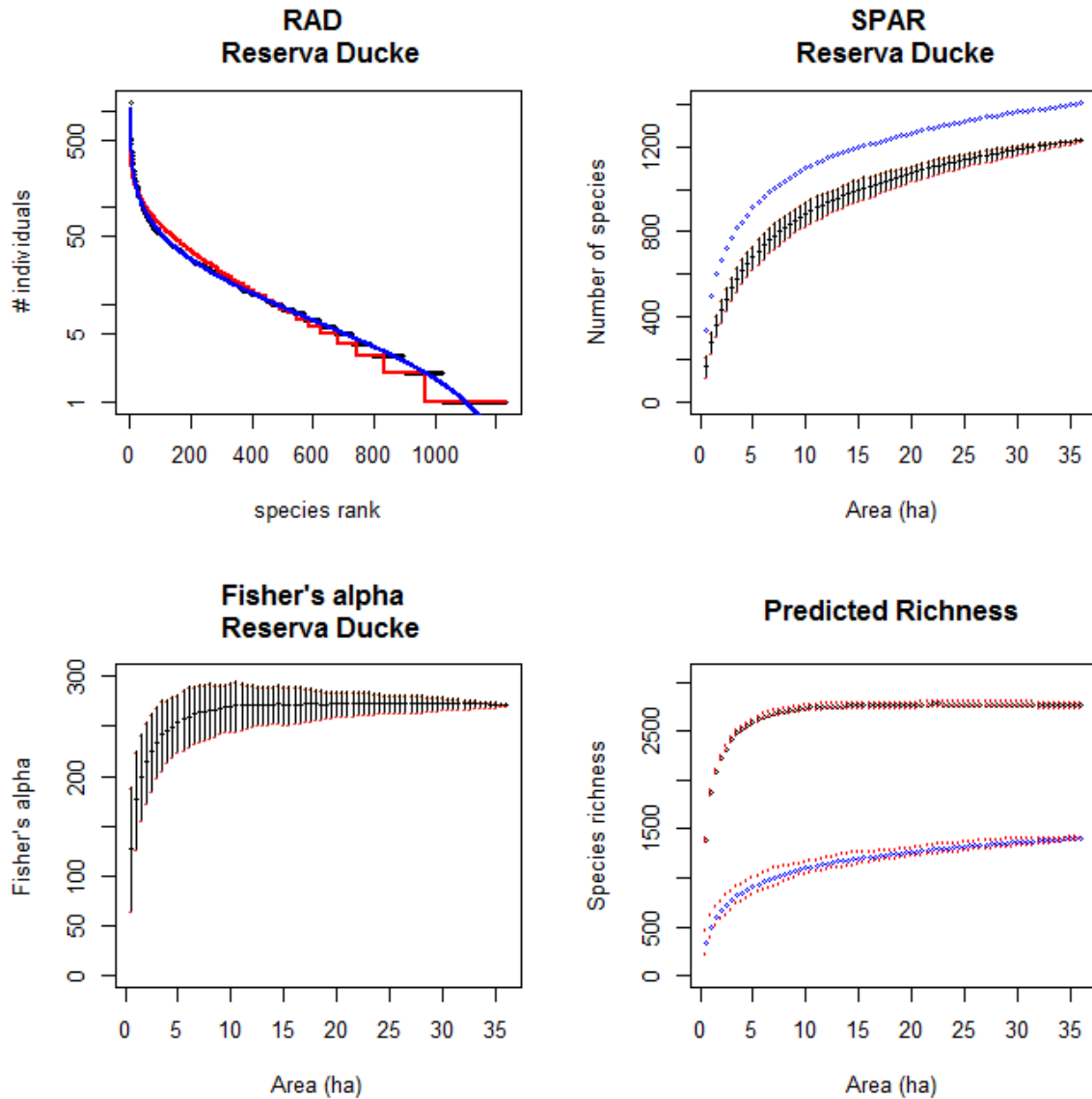


**Figure 2.4.** Piste de Saint Elie field data (PSE). A. Rank abundance distribution (RAD) of RD with logseries fit (red) and lognormal fit (blue). B. Species area curve for RD and estimated richness (Sestimated) based on Chao1 (blue). C. Fisher's  $\alpha$  area curve for RD. D. Species richness estimated for the total 15km<sup>2</sup> area surrounding the plots with Fisher's  $\alpha$  (black) and Chao1 (blue), each with 95% CI (red).

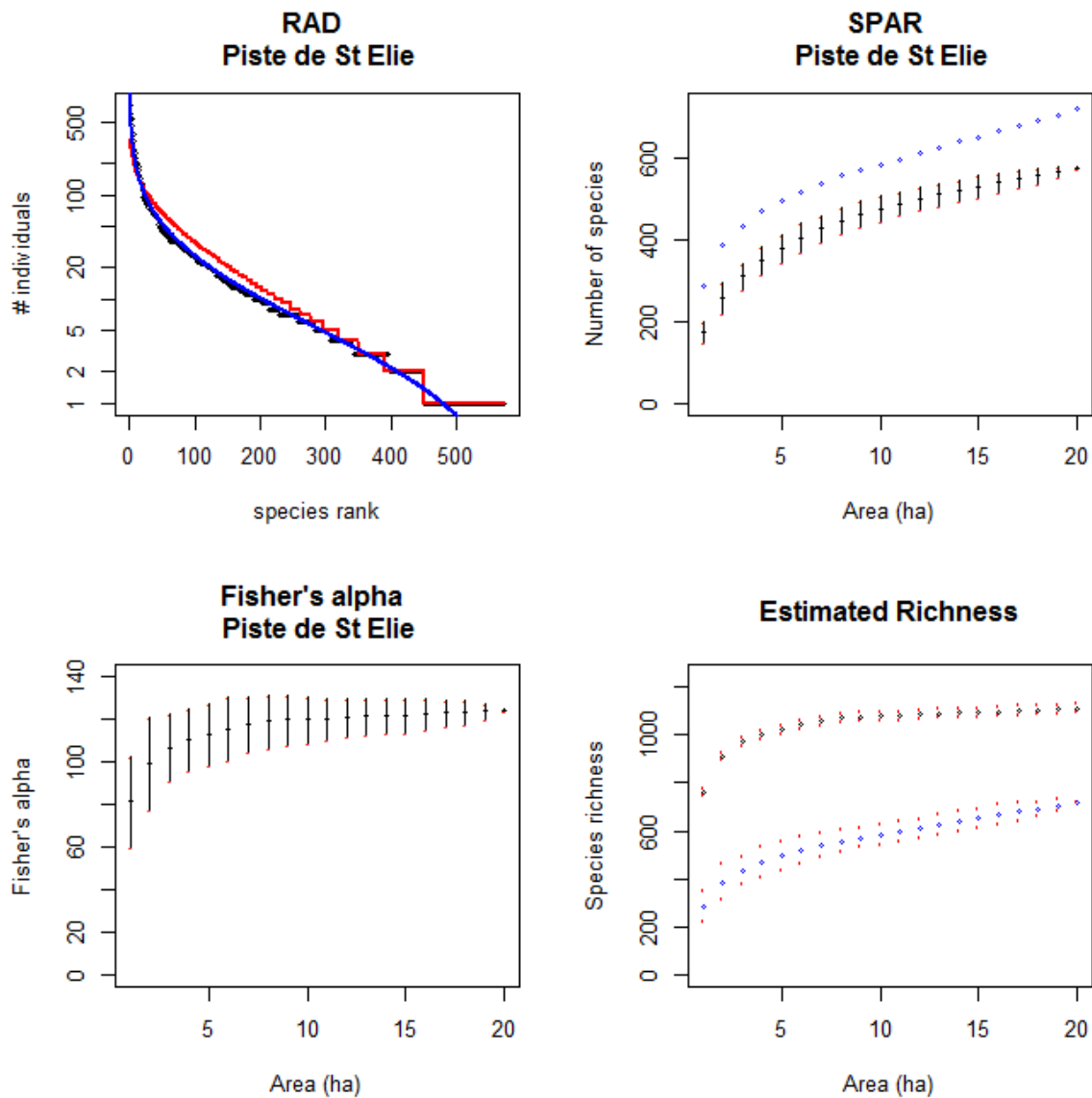
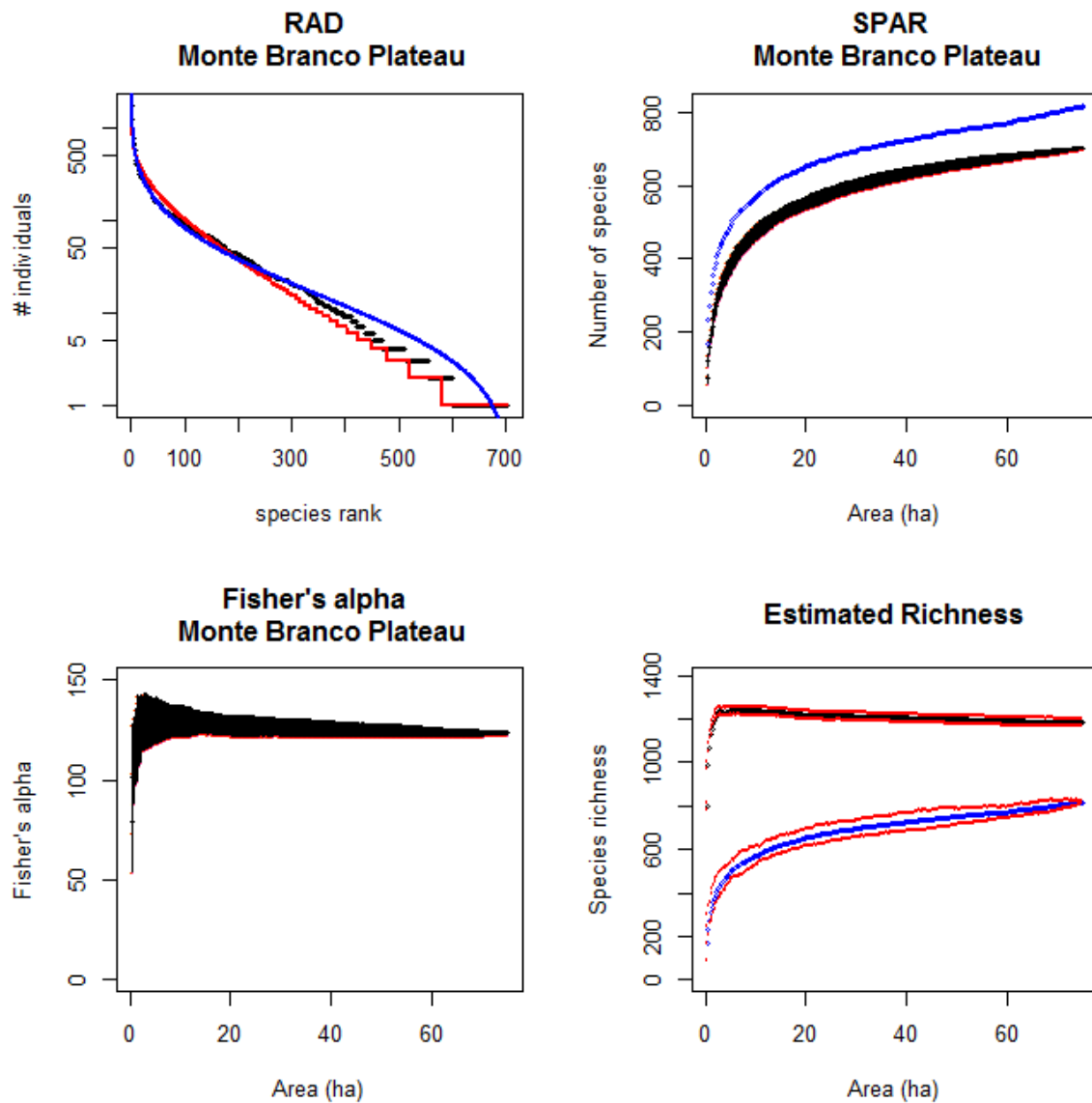


**Figure 2.5.** Monte Branco Plateau field data (MBP). A. Rank abundance distribution (RAD) of MBP with logseries fit (red) and lognormal fit (blue). B. Species area curve for MBP and estimated richness (Sestimated) based on Chao1 (blue). C. Fisher's  $\alpha$  area curve for MBP. D. Species richness estimated for the total 37.5 km<sup>2</sup> MBP area with Fisher's  $\alpha$  (black) and Chao1 (blue), each with 95% CI (red).



Species estimates for the target area made with Fisher's  $\alpha$  were much larger than those made with the asymptotic Chao1 estimator, which were close to  $S_{\text{observed}} + \text{Fisher's } \alpha$  of the measured data (Figs. 2.4-2.8). All other nonparametric estimators, too, predict much lower values for richness, comparable to the Chao1 estimator (Table 2.2). Only for BCI, where the area for which richness was to be estimated was similar to the actual sample, did the nonparametric estimators approach the estimate based on Fisher's  $\alpha$ .

**Table 2.2.** Species estimates based on plot samples in BCI, RD, PSE, and PMB.

	<b>BCI</b>	<b>se</b>	<b>RD</b>	<b>se</b>	<b>PSE</b>	<b>se</b>	<b>PMB</b>	<b>se</b>
Number of plots	50		72		20		301	
number of individuals	21,457		25,066		12,450		36,546	
number of species	225		1233		574		703	
target area	50 ha		100 km <sup>2</sup>		1500 ha		3750 ha	
target individuals	21,457		6,960,000		933,750		1,821,229	
Sestimated with								
Fisher's $\alpha$	225		2759		1110		1185	
Chao 1984	239	8.3	1,408	32	724	36	821	31
Chao Bunge	243	9.6	1,423	32	715	34	823	31
Chao Lee ACE	238	6.1	1,375	20	669	18	738	16
Chao Lee ACEI	241	8	1,405	26	694	25	805	23
Jackknife	244	6.1	1,591	59	1066	124	920	40

For the BCI and MBP data, and simulations with higher mean dispersal distances, Fisher's  $\alpha$  peaked before it leveled off to its final value similar to the simulations, i.e. it showed a hump (see Figs. 2.4 and 2.7). Fisher's  $\alpha$ , however, rose regularly for PSE, RD and for simulations with lower mean dispersal distances (Figs. 2.1, 2.2, 2.5 and 2.6).

## 2.4 Discussion

Based on our simulations with a spatially semi-explicit model, Fisher's  $\alpha$  provides a more accurate prediction of species richness in the virtual forest communities than does the nonparametric Chao1 and other nonparametric methods, especially if sample intensity is low. We believe that the failure of nonparametric methods to estimate diversity is mainly due to the resampling approach with its need of high sampling effort and its expected loss of singletons, and the lack of definition of the target area. We elaborate on this below.

Based on resampling the BCI plot data, Chao et al. (2009) found that, to detect 90% of the species, a median sample size of 80% of the area is necessary. Also Chiarucci et al. (2003), using modeled vegetation, found that nonparametric estimators need at least 15-30% of the area to be sampled for reasonable estimates of the species richness of the whole area. Using these methods with low sampling effort leads to serious underestimation as Brose et al. (2003) and our models clearly show. In real life, even though trees are not removed by our sampling (and resampling is thus statistically possible), the chances of resampling the same plot are negligible. In the Amazon with a sample of 1170 1-ha plots in an area of over 5 million km<sup>2</sup> (TER STEEGE et al., 2013), that chance would be just  $2 \cdot 10^{-9}$ . At the intensities at which tropical forests are sampled (0.0002% for the Amazon) nonparametric methods simply cannot accurately estimate the number of species in the whole area. On top of that when plot locations are known researchers are unlikely to resample a known area.

With capture and recapture techniques and the nonparametric estimators tested, sampling is considered complete when no singletons exist anymore in the data (CHAO et al., 2009). In tree plots the disappearance of singletons would be the result of sampling the data many times over with replacement (CHAO et al., 2009). This resampling results in the estimated richness asymptotically approaching true richness when the number of singletons is zero, as the total number of species cannot be larger than those observed in the total dataset (CHAO et al., 2009).

We argued above that in the case of research in tropical forests, plots are probably never sampled with replacement. Thus, the number of species is expected to increase with sample size as predicted by the ‘First Law of Biodiversity’ (ROSENZWEIG, 1995) (*‘larger samples yield more species’*) and many other theories of Biodiversity (HARTE, 2011; HARTE et al., 2008; HUBBELL, 2001; KIMURA, 1983; MACARTHUR; WILSON, 1967).

In addition, singletons will remain (often close in number to Fisher’s alpha). In the above theories, singletons are the representatives of the biological processes of immigration, extinction or speciation. Singletons might be species on their proverbial way out driven by extinction or new species coming in by speciation or migration. The latter are hence necessary to maintain richness. Without these processes, fixation will occur due to ecological drift, analogous to genetic drift from population genetics. Thus, when sampling without replacement: the lack of singletons in these systems would suggest incomplete rather than complete sampling. This inconsistency can be extracted from the description of the method itself, where authors (CHAO et al., 2009) mention that “given adequate sampling, lack of singletons indicates adequate sampling”.

Finally, as most tropical tree field data conforms to the logseries (see references in the introduction), the Chao1 index becomes scale invariant, always estimating the same number of missing species, in the case of Chao1, to exactly the amount of Fisher’s  $\alpha$ . This was shown mathematically in the introduction for Chao1 and is supported our simulations. While we did not show this mathematically for the other nonparametric estimators, they are derived from the same theoretical framework of capture-recapture and estimate similar richness (Fig. S18, Table 2.2) and thus also provide severe underestimates with low sampling intensities.

For the full Amazon area (~5.5 million km<sup>2</sup>), ter Steege et al. (2013) estimated ~16,000 tree species based on a sample of 1170 plots of 1-ha. They applied at least 18 different extrapolation methods from software packages SPECIES (WANG, 2011), and CatchAll (BUNGE et al., 2012) to their plot (TER STEEGE et al., 2013). Almost all were rejected, as they predicted the total number of Amazonian tree species to fall in the range 4015-6412, a demonstrably severe underestimation of the true species richness (FINE, 2001).

A new estimator, implemented in CatchAll (WLRM\_UnTransf) (BUNGE et al., 2012; ROCCHETTI; BUNGE; BÖHNING, 2011) gave an estimated total richness above 11,000, closer to that calculated with their logseries extrapolation, but was not selected by the program as the best estimator. The ACE1\_Max Tau estimator gave a result greatly exceeding the estimate with the log-series but its Tau was much higher (9048) than the recommended value (Tau < 10).

The failure of these models to fit the Amazonian data was not surprising. These estimators performed poorly because at least one of their assumptions, high sampling intensity, was not met - a condition unlikely to be met in any large forested area. Based on an extensive search in several data providers and herbaria, ter Steege et al. (2016) found that nearly 12,000 tree species have actually been collected in Amazonia, with a collecting density as low as 10 collections per 100km<sup>2</sup>. They conclude that the estimate of 16,000 is entirely plausible. Importantly, the number of species found is almost twice that estimated with most nonparametric methods.

Using different methods to estimate or extrapolate the SAR, like a Maximum Entropy inference (HARTE, 2011; HARTE; KITZES, 2015) or a power law based fitting from multi-scales sampling (KRISHNAMANI; KUMAR; HARTE, 2004; PLOTKIN et al., 2000), also showed that regional scale diversity of trees was estimated acceptably from small plots samples. Interestingly, the abundance distribution model arising from the MaxEnt approach is most often a logseries (HARTE; KITZES, 2015).

Using the logseries is not without assumptions either, however. Our virtual forest is neutral with regard to the environment, i.e. demographic probabilities for each individual, regardless of species identity, are equal. Hence, in addition, the only cause of aggregation is limited dispersal of individuals but given enough time, even ranges of very dispersal limited species can become large. In real life, species will segregate the environment based on ecological preferences as well. Hence, beta-diversity in real forests is higher than in our virtual-forest stand and a peak of Fisher's  $\alpha$  is expected when a large heterogeneous area is sampled over a range of sampling intensities.

BCI is known to have clear segregation of species based on soil moisture (HUBBELL; FOSTER, 1983) and the relationship Fisher's  $\alpha$  to area peaks at relatively low number of plots. We also expect the species on MBP to be similarly clumped because of the clear peak in Fisher's  $\alpha$  at low sample sizes. At MBP plot size may also influence the peaking of Fisher's  $\alpha$ . As the plots are smaller (0.25 ha), the recruitment to the plots will be more affected by the adjacent plots as  $m_{\text{adjacent}}$  is very much dependent on the ratio between the plot boundary and mean dispersal distance (CHISHOLM; LICHSTEIN, 2009). The peak modeled and observed can be explained by a relationship between beta-diversity and alpha-diversity. At low migration rates, recruits mostly come from within plots, hence beta-diversity is maximized but alpha-diversity is not because each plot is practically isolated and losing species due to ecological drift. This means that, for just sampling one plot, Fisher's  $\alpha$  will be much lower than the average of the whole forest.

Continuous sampling, however, will gradually result in the average Fisher's  $\alpha$ . There will be no peak because the probability for each plot bringing new species to the whole is the same and thus the increase will be gradual until Fisher's  $\alpha$  is equal to that of the virtual forest. When migration increases, however, plots close by exchange more species and beta and local alpha diversities increase simultaneously. In this case, sampling a few plots randomly will likely initially overestimate Fisher's  $\alpha$ , because each sample includes new species for the total sample due to the combined higher beta and alpha-diversity, creating a fast rise in Fisher's  $\alpha$ .

However, continuing the sampling at some point does add more individuals to the total sample, though species will be resampled, lowering Fisher's  $\alpha$  again. When dispersal is so high as to be similar across the complete virtual forest, composition would essentially be very similar for all plots with very high local alpha- and low beta-diversities and Fisher's  $\alpha$  would not peak but increase fast to its virtual-forest value (as in the virtual 49 ha BCI, Fig. 2.3).

#### 2.4.1 Is estimating species richness still a long way off?

Chiarucci (2012) suggested that '*estimating species richness is still a long way off!*' Nonparametric estimators underestimate richness (see above and XU et al., [2012]), while area-based estimators tended to overestimate richness (XU et al., 2012). Xu et al. (2012) concluded that Maxent greatly overestimated richness. However, their perceived overestimate is based on the richness they expected, which was based on a list of species found in their area. We believe that many of us do not fully comprehend the consequences of the logseries model. One of us was also surprised when we estimated the expected species for RD, which was much more than was expected based on extensive fieldwork for the Flora of the area (RIBEIRO et al., 1999) and ecological fieldwork. However, with an Fisher's  $\alpha$  of 271 for the plots of RD, assuming that this is close to the correct Fisher's  $\alpha$  for the area, we expect 271 species with only 1 individual, 135 with two individuals, 62 with 3 individuals, 31 with 4 individuals, etc. RD covers 100 km<sup>2</sup>, with an average tree density of 696 trees ha<sup>-1</sup> (TER STEEGE et al., 2013). That indicates a total of 6.96 million individuals. The chance of finding a singleton species there with feasible sampling intensity is thus very, very small. This is the consequence of using this theoretical framework (see also HUBBELL, [2015]).

Because many researchers using nonparametric estimators assume that sampling is complete when the samples contain no singletons, an assumption that does not agree with ecological theory or with most ecological sampling, they are likely to severely underestimate richness when sampling level is low. Therefore, we suggest that the use of nonparametric estimators should be discouraged in studies with low sampling intensity in large remote areas. If the data can reasonably be assumed to follow a logseries, species estimation by means of Fisher's  $\alpha$  is likely a better option.

Other methods that produce abundance distributions with many singletons, matching most observational data, such as various parametric methods (BUNGE; BARGER, 2008) or phenomenological theories, such as Maximum Entropy (HARTE, 2011) are probably also good alternatives.

#### 2.4.2 Fisher's paradox

The term Fisher's paradox was coined by Hubbell (2015):

“The logseries is an infinite series that mathematically goes on forever. But the world's forests are finite in size. So, what happens to estimates of species abundance when the entire world is your sample? [...] The paradox would seem to run even deeper, because Fisher's logseries predicts that many more of the world's tropical tree species are hyper-rare. [...] The truth is, we still have inadequate data to definitively answer the “how many tropical tree species?” question. Ecologists at present are forced to make huge extrapolations from existing inventory plot data to the entire world.”

Hubbell (2015) believes hyper-rare species do exist, as do we and in the case of areas smaller than the world, so do singletons. What are then those singletons. For an area like the Amazon, a huge and open system, singletons are the result of species (locally) going extinct or new immigrants. Ter Steege et al. (2016) (Fig. S7) showed that several singleton species are in fact species found only once in the Amazon but common in the Cerrado, Andes and even Atlantic forest, ‘vagrants’ in the viewpoint of Magurran and Henderson (MAGURRAN; HENDERSON, 2003). However, this may suggest that singletons or other hyper rare species are found mainly on the edges of an area. In the Amazon they were not and include such iconic species as *Asteranthos braziliensis* (endemic to the middle and upper Rio Negro) and *Duckeodendron cestroides* (endemic to an area around Manaus, central Amazon).

We believe that even if all individuals of the Amazon forest could be measured and identified, the biological processes of extinction and immigration would lead to the presence of at least ~750 singleton species, based on the Fisher's  $\alpha$  found for the area (TER STEEGE et al., 2013) and a huge amount of hyper-rare species, some of which may have small contracted ranges, some of which may even be spread over large areas (ZIZKA et al., 2018).

One of the most important merits of NT is to emphasize the role of migration in building and maintaining community structures. However, the underlying mathematical model is based on a discretization down to the individual level, where a random process is supposed to play and can be expressed as per capita probabilities. In a complex system such as tropical forests, clearly not only chance acts upon birth, death, dispersal and migration. This could result from acquiring a new competitive advantage, losing a competitor because a pest, losing a pest because a super-pest develops. A manifold of combinations is possible. The processes involved at local scale are not exclusively random but from local to global their combined effects on species abundances may sometimes appear to be.

## **2.5 Conclusion**

To evaluate diversity of a rich, complex, large, open system, a parametric approach based on a probabilistic model, such as Fisher's logseries, seems to be more applicable than a non-parametric one, because such a system is driven by the random walk resulting from an infinity of processes that vary among scales, and where chance affects many biological processes, and not just the random sampling context considered by non-parametric methods.

## CAPÍTULO 3 SPECIES DISTRIBUTION MODELLING: CONTRASTING PRESENCE-ONLY MODELS WITH PLOT ABUNDANCE DATA<sup>2</sup>

### Abstract

Species distribution modeling (SDM) is widely used in ecology and conservation. Presence-only models such as MaxEnt frequently use natural history collections (NHCs) as occurrence data, given their huge numbers and accessibility. NHCs data are, however, often spatially biased, and may generate inaccuracies in SDMs. Moreover, NHCs data distribution may differ from the actual distribution, due to differences in the collection effort between common and rare species. Here, we test how the distribution of NHCs relates to species relative abundance. We compared NHC data and MaxEnt predictions to a spatial abundance model, based on a large plot dataset for 227 Amazonian hyperdominant species, using inverse distance weighting (IDW). We also propose a new pipeline to deal with inconsistencies in NHC data. We found no positive relationship between the distribution of NHCs and species relative abundance for 33% of the species. Furthermore, the relationship between SDMs and relative abundance maps was positively weak for 84% of the species. Presence-only SDM applications should consider this limitation, especially for large biodiversity assessments projects, when they are automatically generated without subsequent checking. Nevertheless, sensitivity for both analyses was high, where IDW predicted 91% of the NHCs records, and MaxEnt 87% of plots presence data.

**Keywords:** Amazonia, environmental suitability, IDW, MaxEnt, relative abundance, species distribution modelling, tree species.

---

<sup>2</sup>Publicado na revista *Scientific Reports Ecology* (2018) 8:1003, Qualis A1 na Área de Avaliação de Ciências Ambientais.

### 3.1 Introduction

Species distribution models (SDMs) are widely used in the fields of macroecology, biogeography and biodiversity research for modelling species geographic distributions based on correlations between known occurrence records and the environmental conditions at occurrence localities (ELITH; LEATHWICK, 2009; PHILLIPS; ANDERSON; SCHAPIRE, 2006). SDMs generate geographical maps of a species' environmental suitability, its likelihood of being collected, and its local abundance (MILLER, 2010). Their application includes selecting conservation areas, predicting the effects of climate change on species ranges and determining the risk of species invasions (ARAÚJO; PETERSON, 2012; PEARSON, 2010). The wide use of SDMs in ecological and conservation research can partly be explained by the growing availability of georeferenced species records (e.g. GBIF, SpeciesLink) and environmental data (e.g. WorldClim, CliMond) (HIJMANS et al., 2005; KRITICOS et al., 2012) on the web, together with the user-friendly character of some of the modelling methods.

One of the most commonly used SDMs is MaxEnt, which has become increasingly popular since its introduction (RENNER; WARTON, 2013). This machine-learning algorithm estimates a species' probability distribution that has maximum entropy (closest to uniform), subject to a set of constraints based upon our knowledge of the environmental conditions at known occurrence sites (PHILLIPS; ANDERSON; SCHAPIRE, 2006). MaxEnt is a presence-only model, enabling scientists to utilize the abundant data sources of natural history collections (NHCs), avoiding the high costs of sampling the species throughout their extent of occurrence. Presence data are abundant, but absence data are hard to obtain and often unreliable due to insufficient survey effort. To counter the lack of absences, MaxEnt uses a background sample to contrast the distribution of presences along environmental gradients against the distribution background points, randomly drawing from the study area.

NHCs, however, may not be independently drawn from the investigated populations due to the non-random nature of collecting (HARIPERSAUD, 2009; TOBLER et al., 2007). Because collectors aim to collect as many species as possible, rare species are often overrepresented in herbaria, whereas common species are underrepresented, producing collectors' bias (TER STEEGE et al., 2011).

Therefore, the relative number of specimens per species in herbaria is not a good representation of the species' relative abundance in the field. Additionally, NHCs have spatial bias due to geographical differences in survey effort, data storage and mobilization (BECK et al., 2014; HARIPERSAUD, 2009; TOBLER et al., 2007). This may have negative impacts on the performance of presence-only SDMs if this results in environmentally biased sampling (BECK et al., 2014; FOURCADE et al., 2014; PHILLIPS et al., 2009; SYFERT et al., 2013). Negative impact of spatial bias is not always present, however (KADMON; FARBER; DANIN, 2004; LOISELLE et al., 2008).

MaxEnt has shown to outperform other SDMs in several studies (AGUIRRE-GUTIÉRREZ et al., 2013; ELITH et al., 2006; GIOVANELLI et al., 2010; MERCKX et al., 2011; WISZ et al., 2008). Nevertheless, some drawbacks have been identified. For example, MaxEnt may underestimate the probability of occurrence within areas of observed presence, while overestimating it in areas beyond the species' known extent of occurrence (FITZPATRICK; GOTELLI; ELLISON, 2013). Like other SDMs, one essential assumption of MaxEnt is that the presence-data are an independent sample from the species' unknown probability distribution of occurrence over the study area (PHILLIPS; ANDERSON; SCHAPIRE, 2006). Given the shortcomings of NHCs due to collectors' bias mentioned above, this assumption may not be met.

With a large set of plots with quantitative data species abundances may be estimated by a spatial interpolation of local species' abundances (TER STEEGE et al., 2013). Based on plot data, where all species are collected (regardless of commonness or rarity), the interpolation method arguably suffers less from the collectors' bias and is exclusively based on location. The abundance maps may serve as the species' estimated probability distribution and a higher local abundance implies a higher probability of collecting. That is, the chance of encountering a species is higher in a region where the relative abundance of that species is high, than where the relative abundance is low. With spatially interpolated abundances we may thus test whether NHCs can actually be considered a random sample of the unknown probability distribution.

Here we test how the geographic distribution of NHCs relates to the species relative abundance. To achieve this, we address the following questions: 1) Do NHCs represent an independently drawn sample from the unknown probability distribution of a species? And 2) how does MaxEnt's predicted environmental suitability compare to plot abundance data and spatial interpolation of species abundances? To answer these questions, we used NHCs and abundance plot data of 227 hyperdominant Amazonian tree species, which are the most common tree species that together make up half of all trees with a diameter (dbh) over 10 cm in Amazonia (TER STEEGE et al., 2013, 2016), the most biodiverse rainforest on Earth. We used NHCs and MaxEnt to construct presence-only SDMs for all 227 species and constructed the abundance maps by spatial interpolation of the plot abundance data for all species as well. To answer the first question, we compared the collection records to the interpolated abundance maps for each species. Secondly, we compared MaxEnt's predicted environmental suitability maps to the same interpolated abundance maps for each of the 227 species.

## **3.2 Methods**

### **3.2.1 Species**

We focused our analysis on 227 hyperdominant Amazonian tree species. The hyperdominant species are the most common tree species in Amazon, and together make up half of all trees with a dbh over 10 cm (TER STEEGE et al., 2013). We chose only hyperdominant species to reduce the emergence of too many 'false absences' when plot data are interpolated into abundance maps. They present the largest probability of occurrence in the plots where they are present in the surrounding area.

### **3.2.2 Collections**

Species collections were downloaded from GBIF (August 2017, [www.gbif.org](http://www.gbif.org)). We used data from the species' complete extent of occurrence to prevent deficiencies that are associated with SDMs based on a species' partial geographic range, such as under-prediction (RAES, 2012). All individuals were assigned to species level; intraspecific levels were ignored.

Taxonomic names were checked with the Taxonomic Name Resolution Service (TNRS, <http://tnrs.iplantcollaborative.org/>). Although misidentification may represent a major problem in tree plots, we assume it is less severe in common species such as the hyperdominants; which are better represented in herbaria and more likely to be collected fertile (TER STEEGE et al., 2016). We assume that misidentification is within acceptable limits.

### 3.2.3 Collections cleaning pipeline

The cleaning pipeline consisted of a two-step process to remove inconsistencies from GBIF downloaded data (GBIF records). The first step consisted of removing all records with missing latitude, longitude or locality information (imprecise georeferences) (MALDONADO et al., 2015) and all duplicates at 0.5-degree spatial resolution (BOYLE et al., 2013). With the GeoClean function from speciesgeocodeR R Package (ZIZKA; ANTONELLI, 2015) we also removed coordinates assigned to capital cities, coordinates with latitude equal to longitude, coordinates equal to exactly zero; coordinates based on centroids of provinces, and corrected country references (cleaned GBIF records).

In the second step we used a kernel-density estimate function to remove spatial outliers from the cleaned GBIF data, assuming that these are misidentifications or incorrect coordinates not filtered by the step described above. This function calculates a fixed-bandwidth kernel-density estimate of the point process density function that produced the point patterns (DIGGLE, 1985), using the `density.ppp` function from `spatstat` R Package (BADDELEY; RUBAK; TURNER, 2015) to generate a kernel-density estimate. Outliers were identified and removed based on the kernel-density values for each species coordinate, using a threshold based on a quantile function from `stats` R Package (R CORE TEAM, 2016) (kernel-density estimate GBIF records).

The quantile threshold was set according to the number of Amazonian regions in which a species occurred, six in total as defined by ter Steege et al. (2013). The quantile threshold was larger for species with narrow distribution (occurring in one to three Amazonian regions) and smaller for species with wide distribution (occurring in more than three Amazonian regions).

As some hyperdominants are very widely distributed in Amazonia a larger quantile threshold cuts off too many occurrences, removing not only outliers, but also potential correct occurrence or entire occurrence clusters. Both steps reduced the number of species collection records (Appendix S4), and the predicted area of occupancy (Appendix S5).

#### 3.2.4 Plot abundance data

Abundance maps were constructed using 1675 1-ha tree inventory plots well distributed across Amazonia (defined as the tropical rain forest of the Amazon basin and the Guyana Shield) from the Amazon Tree Diversity Network (ATDN) (<http://atdn.myspecies.info/>). All individuals with  $\geq 10$  cm diameter at breast height (dbh) were recorded within the plots (TER STEEGE et al., 2013). Because a relatively small number of collections from these plots have been deposited in herbaria, they constitute a dataset nearly independent from the NHCs.

#### 3.2.5 Constructing abundance maps

Inverse distance weighting (IDW) interpolation was used to create abundance maps from the plot abundance data. First, Amazonia was divided into 2193 0.5-degree grid cells. We then constructed the inverse distance weighting (IDW) models based on relative abundance following ter Steege et al. (2015). Then, the relative abundance (RA) for each cell was defined as  $RA_i = n_i/N$ , where:  $n_i$  = the number of individuals of species  $i$ , and  $N$  = the total number of trees. IDW models were based on the nearest 150 plots within a limit of 300 km distance. Each plot weight was calculated by taking the square root of the distance in degrees. The 150 plots that were taken into account ensured that within an area consisting of absence plots only, the species is predicted to be absent. In addition, the 3-degree distance limit causes the model to predict the absence of a species when no occurrence plots are present within a radius of 3 degrees. This setting is based on the notion that within a non-environmental model a species' extent of occurrence is restricted by dispersal limitation only (GASTON, 2009). The maximum dispersal distance has been optimized to a 3-degree distance by determining the best match between the IDW maps and the Fisher's Alpha diversity map of all species (TER STEEGE et al., 2003).

### 3.2.6 Constructing presence-only SDMs using MaxEnt

We used MaxEnt version 3.3.3k (PHILLIPS; ANDERSON; SCHAPIRE, 2006; PHILLIPS; DUDÍK; SCHAPIRE, 2004), to construct presence-only SDMs for all the 227 species. Data of 19 environmental variables were downloaded from WorldClim (HIJMANS et al., 2005). These included variables related to temperature and precipitation. Since collinearity, the non-independence of predictor variables, potentially leads to the wrong identification of relevant predictors for the model, we used the common Spearman's rank correlation coefficient threshold of  $|\rho| > 0.7$  to identify correlated variables (DORMANN et al., 2013).

Subsequently, we selected least correlated variables ( $|\rho| < 0.7$ ) based on biological relevance and their loadings in a principal component analysis (PCA). The PCA consisted of all environmental variables for all collection localities of the 227 species. For temperature, we selected isothermality, temperature seasonality, and maximum temperature of warmest month. For precipitation we chose annual precipitation, wettest month precipitation and driest month precipitation. All the environmental variables were cropped to the extent of the Neotropics (RAES, 2012), and aggregated to a 0.5-degree spatial resolution, using the function 'mean' from R package 'raster' (HIJMANS; VAN ETTEN, 2016). We used precipitation and temperature variables to assess MaxEnt's predicted environmental suitability based on climate only. In the MaxEnt feature settings we excluded the product, threshold and hinge features given their lack of biological justification with the variables used (BOUCHER-LALONDE; MORIN; CURRIE, 2012; MEROW; SMITH; SILANDER, 2013).

Correcting for geographical sampling bias has been found to improve the predictive performance of MaxEnt (SYFERT et al., 2013). Also, environmental bias can be assessed by environmental filtering, which improves MaxEnt discriminatory ability (VARELA et al., 2014). We produced a bias file to employ the target-group background method recommended by Phillips and Dudík (PHILLIPS; DUDÍK, 2008), an option which is implemented in MaxEnt.

The bias file consisted of a binary raster grid based on all Amazon tree species collections (TER STEEGE et al., 2016), at each grid cell downloaded from GBIF, which reflects local survey effort. This is an essential step in the analysis, given MaxEnt's assumption that the occurrences are independently drawn from the unknown probability distribution of the species. Without a bias file, sampling bias could severely reduce model's accuracy. We used the bias file to produce a background file according the efforts of collection. Finally we used a convex hull around cleaned occurrences (kernel-density estimate GBIF records) of each species to estimate their extent of occurrence (IUCN, 2012), plus a buffer of 300 km, equal to the buffer set for the IDW analysis, to crop the area of predicted environmental suitability . The latter is our predicted area of occupancy.

### 3.2.7 Data analysis

We compared collection presences and absences to IDW relative abundance to answer our first question whether NHCs are independent drawn from the unknown probability distribution. A binomial generalized linear model (logit regression) was used to determine if a significant positive relationship existed between the probability of being collected and predicted local relative abundance.

To answer the second question, how MaxEnt's predicted environmental suitability compares to IDW relative abundance, we first tested which species' MaxEnt maps were significantly different from random expectation with a bias corrected null-model (RAES; TER STEEGE, 2007a). For each species, 99 null-models were generated by randomly drawing  $n$  collection localities without replacement from the same spatial grid as the environmental layers, with  $n$  being the number of geographically unique collections for that species. Using an upper one-sided 95% confidence interval, we determined the probability value of the observed AUC as calculated by MaxEnt against those generated by the null distribution. If the species' observed AUC value ranks 95 or above, the chance that a random set of  $n$  points could generate an equally good model is less than 5%, hence considered significantly different from random expectation. All species for which the SDM prediction did not deviate significantly from random expectation were excluded from further analysis. Second, a Spearman Rank Correlation test was used to test the relationship between MaxEnt logistic output and IDW relative abundance at plot localities.

Additionally, following VanderWal et al. (2009), we determined the linear 90<sup>th</sup> percentile quantile regression between the IDW relative abundance and MaxEnt logistic outputs at plot localities. The confidence intervals of the linear quantile regressions were calculated with the Markov chain marginal bootstrap method as suggested by Kocherginsky et al. (2005). We computed the correlations and regressions for all plots separately, even if multiple plots were present in one grid square.

Third, we tested the predictive performance of MaxEnt and IDW. For MaxEnt, its logistic output was transformed into binary maps with a 10% training presence threshold. Although the maximum sum of sensitivity and specificity is considered to be the best threshold method for presence-only SDMs by Liu et al. (2013), we followed the advice of Merow et al. (2013) to avoid measures with specificity because they are based on absences that are unknown in this analysis. Then we tested its sensitivity by calculating true positive rate of the binary maps against plot presence. That is, the fraction of the grid cells with a plot for which MaxEnt predicted the species correctly to be present. Finally, we calculated the median predicted area of occupancy.

For IDW, its output was transformed into binary maps by converting the grids cells with  $RA > 0$  into 1. Last, naturally non-forested areas were excluded from the maps based on Soares-Filho et al. (2013). We then calculated its output true positive rate against collections presences and absences. That is, the fraction of the grid cells with a collection for which the IDW relative abundance predicted the species correctly to be present. Finally, we also calculated the median predicted area of occupancy for IDW.

All calculations and analyses were performed with R version 3.0.3<sup>3</sup>, including the R packages raster (HIJMANS; VAN ETTEN, 2016), rgdal (BIVAND; KEITT; ROWLINGSON, 2014), gstat (PEBESMA; GRAELER, 2014), dismo (HIJMANS et al., 2017b), vegan (OKSANEN et al., 2015), quantreg (KOENKER, 2013), sp (PEBESMA; BIVAND, 2014), rJava (URBANEK, 2013) and SDMTools (VANDERWAL et al., 2014).

### 3.3 Results

#### 3.3.1 NHCs data distribution and relative abundance analysis

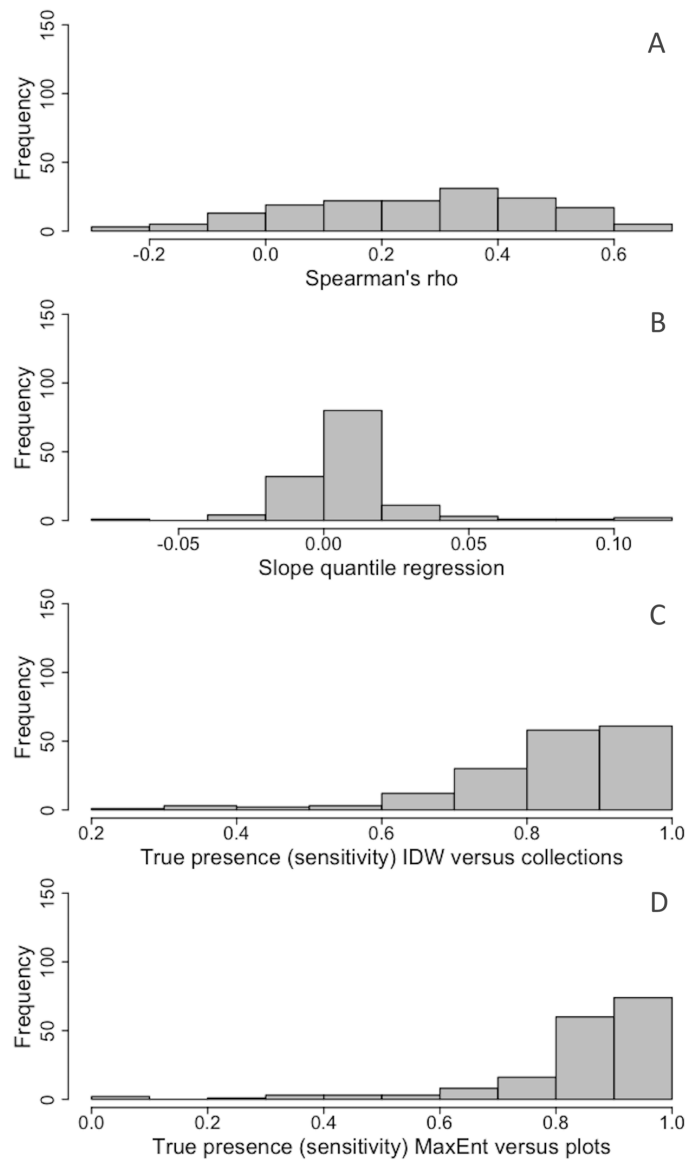
The analysis testing our first question, whether NHCs are an independent draw from the unknown probability distribution, resulted in a significant ( $P < 0.05$ ), but very weak positive relationship for 149 (66%) species of the 227. For these species the chance of being collected indeed increased slightly with higher interpolated relative abundance. For the other 78 species (34%), this relationship was non-significant or negative (Appendix S1).

#### 3.3.2 Predicted environmental suitability compared to species relative abundances

Further analyses were carried out using only 170 species. Species, that had MaxEnt's predicted environmental suitability not significantly different from a random expectation tested with bias corrected null models, were excluded (57 species). For 161 of the 170 species (95%), MaxEnt's predicted environmental suitability was also significantly correlated with interpolated abundance ( $P < 0.05$ ). The correlations and, thus the biological significance, were low however, with a mean rho (Spearman rank correlation) of 0.26 (Fig. 3.1 A).

A linear 90<sup>th</sup> quantile regression revealed that for 135 (79%) of the 175 species, the logistic output of MaxEnt could significantly ( $P < 0.05$ ) predict the highest 10% of the local relative abundance values. The slope of the regression and thus the biological significance was very low, with a mean slope of only 0.01 (Fig. 3.1 B).

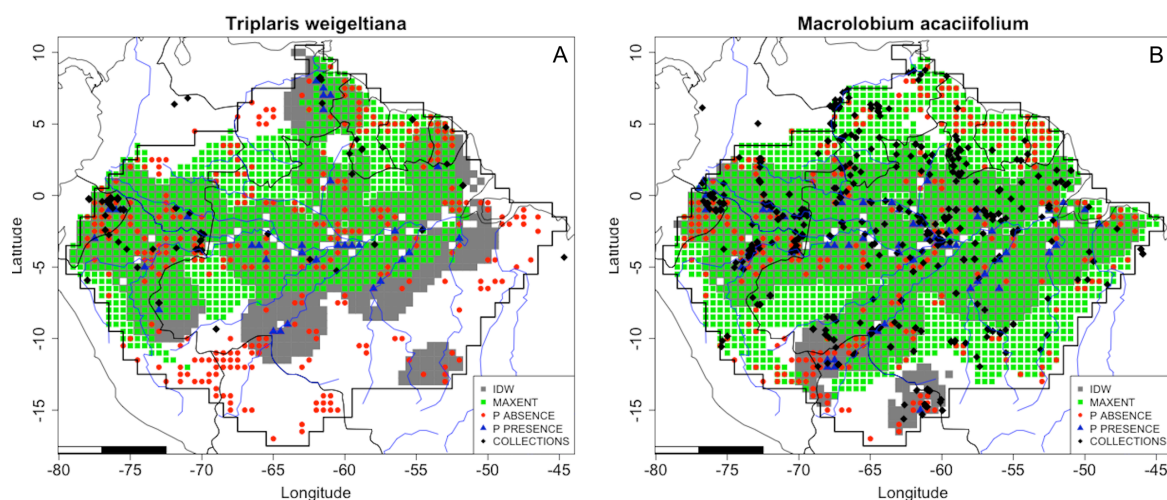
**Figure 3.1.** Frequency distributions for 189 significant hyperdominant Amazonian tree species of (A) the Spearman's correlation index  $\rho$  between MaxEnt's predicted environmental suitability and relative local abundance of the plots; (B) The slopes of the linear 90th percentile quantile regression between MaxEnt's predicted environmental suitability and the relative local abundance of the plots; (C) The true presence (sensitivity) of the distribution predicted by the IDW maps compared to the collection localities; and (D) The true presence (sensitivity) of the distribution predicted by the MaxEnt maps compared to the plot presence.



We also investigated the performance of the IDW output against NHCs data and the MaxEnt output against plot presence (sensitivity), to check whether the models were accurate references to the occurrence data of each other (Appendix S2). Approximately 87% of the grid cells with species' NHCs were correctly predicted as present by the IDW maps with a median true positive rate of 0.87 (Fig. 3.1 C). The same analyses for MaxEnt showed that 88% of the grid cells with plot presence were correctly predicted by MaxEnt maps, with a median true positive rate of 0.88 (Fig. 3.1 D). Sensitivity for both analyses was high.

We provide maps (combined MaxEnt and IDW maps [as in Fig. 3.2]) for all species in the supplementary material S3. The predicted environmentally suitable region and the abundance distribution were similar for very abundant species with a large extent of occurrence, such as *Brosimum rubescens* Taub. (Fig. S3\_14A), *Conceveiba guianensis* Aubl. (Fig. S3\_32A) and *Eschweilera coriacea* (DC.) S.A.Mori (Fig. S3\_49A). The same was true in the case of the species *Clathrotropis glaucophylla* Cowan (Fig. S3\_30A) and *Cenostigma tocaninum* Ducke (Fig. S3\_26A), despite the fact that neither species has a wide extent of occurrence.

**Figure 3.2.** The predicted area of occupancy by MaxEnt (green) and the IDW map (grey) of (A) *Triplaris weigeltiana* (Rchb.) Kuntze; and (B) *Macrolobium acaciifolium* (Benth.) Benth. The localities of the collections, presence and absence plots are also indicated. Maps created with custom R script. Base map source (country.shp, rivers.shp): ESRI.



Fonte: ESRI (2016); R Core Team (2018).

Moreover, MaxEnt also correctly predicted the environmental unsuitability of non-forested savanna areas, which are located in the north (Brazil, Guianas and Venezuela) and south of the map (northern Bolivia). These close matches apply to very abundant species with a large extent of occurrence, such as *Licania micrantha* Miq. (Fig. S3\_87A), and *Ocotea aciphylla* (Nees & Mart.) Mez (Fig. S3\_111A).

For *Triplaris weigeltiana* (Rchb.) Kuntze, a species with a northern Amazonian distribution, MaxEnt also correctly predicted its absence in these northern non-forested areas (Fig. 3.2 A, S3\_160 A, B). In this case MaxEnt was able to establish a relationship between species distribution and vegetation type, based on climate variables (temperature and precipitation) and species occurrence. For *Macrolobium acaciifolium* (Benth.) Benth., a riverine species, the IDW presented limitations. This species is rarely recorded in plots, because the plots are mostly far from river edges. Thus, the species was found only in plots near to major rivers such as the Amazon. In this case NHCs provided better information about species occurrence, as collectors can reach areas closer to other smaller rivers aiming to collect more species. In such a case, MaxEnt maps presented a wider distribution for the species (Figs. 3.2 B, S3\_92 A-C).

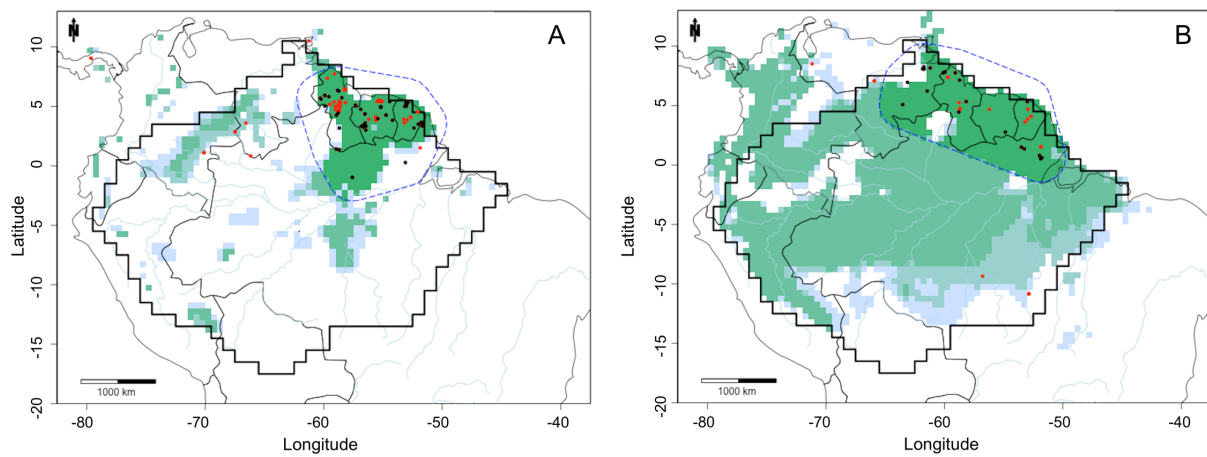
IDW maps predicted widespread distributions for palms, for which the MaxEnt estimates were in sharp disagreement. Palms species are more difficult to collect, which can result in a lack of specimens in NHCs (TER STEEGE et al., 2013). IDW maps appear to be more accurate for these species, because all species are recorded inside plots. In eastern Amazonia this was particularly severe because NHCs showed a large lack of occurrence in comparison with plot data but also proper locations were rejected by the KDE because of the huge amount of palm occurrence data from the Aarhus University Palm Transect Database in western Amazonia. Some of the species affected were *Attalea butyracea* (Mutis ex L.f.) Wess.Boer (Fig. S\_8A), *Euterpe precatóriaria* Mart. (Fig. S3\_60A), *Iriarteia deltoidea* Ruiz & Pav (Fig. S3\_72A), *Oenocarpus bacaba* Mart. (Fig. S3\_13A), *Oenocarpus bataua* Mart. (Fig. S3\_114A) and *Socratea exorrhiza* (Mart.) H.Wendl. (Fig. S3\_150A).

### 3.3.3 NHCs data cleaning treatment and MaxEnt map building

All 227 hyperdominant species had records excluded by the data cleaning treatment, the consequence of records that either lack geographic information, are duplicates at the used grid cell resolution of 0.5 degree or were outliers based on a kernel-density estimate (Appendix S4). An average of 50% of the records was excluded. The first twelve species with the most excluded records were palms, with a mean of 96% of excluded records. The total average of excluded records decreased to 43% when palms were taken out of the analyses (Appendix S4). This high percentage is due to the huge amount of palm occurrence data of the Aarhus University Palm Transect Database (CÁMARA-LERET et al., 2016). At this moment this database contains 543,000 records, all available in GBIF. Most of these records represent observations in many plots inside the same grid cell, thus these records were removed and considered as a single observation.

After the kernel density estimate treatment the average of excluded records was 57%, presenting an increment of 6.7% in the total amount of records excluded. *Eperua purpurea* Benth. and *Eperua leucantha* Benth. collections were in good agreement with plot data distribution, after outliers were excluded by the kernel density estimate (Appendix S5). In the case of *Eperua falcata* Aubl., some occurrences in Colombia and Venezuela were in fact misidentifications of *Eperua leucantha* Benth., since this species occurs only in the Guianas (H. ter Steege, pers. obs.). The kernel density estimate function correctly removed these occurrences outside the *E. falcata* cluster observed in the Guianas (Fig. 3.3 A). Some occurrences of *Licania alba* (Bernoulli) Cuatrec. in southeast Amazonia, an area with no plot data, were also removed by the kernel-density estimate function (Fig. 3.3 B).

**Figure 3.3.** MaxEnt environmental suitability maps for (A) *Eperua falcata* Aublet.; (B) *Licania alba* (Bernoulli) Cuatrec.. MaxEnt maps constructed using GBIF records, cleaned GBIF records, kernel-density estimate GBIF records, and kernel- density estimate GBIF records plus the buffer clip. Black dots: GBIF records. Red dots: GBIF records after the use of the cleaning pipeline. Dashed blue line: buffer based on a convex hull around species cleaned collections. Light blue: predicted environmental suitability using GBIF records. Light green: predicted environmental suitability using cleaned GBIF records. Medium green: predicted environmental suitability using kernel density estimate GBIF records. Dark green: predicted environmental suitability using kernel density estimate GBIF records and the buffer clip, resulting in the final predicted area of occupancy. Maps created with custom R script. Base map source (country.shp, rivers.shp): ESRI.



**Fonte:** ESRI (2016); R Core Team (2018).

Because of the use of the buffer treatment to limit MaxEnt predictions around the species' extent of occurrence, MaxEnt maps predicted an area of occupancy close to that of the IDW maps., The median value for MaxEnt's area of occupancy was 1354 0.5-degree grid cells, and the median for IDW was 1217. For 98 (58%) of the 170 species, MaxEnt predicted an area of occupancy bigger than the that predicted by IDW, and for 115 (42%) of the species IDW had a predicted area of occupancy bigger than MaxEnt. In 15% of the cases (26 species) the size difference in area of occupancy was smaller than 5% (Appendix S2).

### 3.4 Discussion

#### 3.4.1 Using NHCs for presence-only SDMs

Collection density was weakly related to relative abundance in most tree species, and for 34% there was no positive relationship between the chance of being collected and local abundance, violating the assumption of MaxEnt that collection localities are an independently drawn sample from a species' unknown probability distribution (PHILLIPS; ANDERSON; SCHAPIRE, 2006). The differences between the distribution of NHCs and local abundance could limit the ability of presence-only SDMs to predict species probability of distribution as predicted by spatial interpolation of local species' abundance.

MaxEnt's premise that species occurrences are drawn randomly from the unknown probability distribution (PHILLIPS; ANDERSON; SCHAPIRE, 2006) may not be met for two reasons: 1) collections are spatially biased with regard to environmental conditions (PHILLIPS et al., 2009); 2) and collections are spatially biased with regard to areas of high abundance, with underrepresentation of in areas of high abundance and overrepresentation in areas of low abundance. Much attention has been given to the possible impacts of spatial bias on the performance of presence-only SDMs, with some showing a negative impact on these models (FOURCADE et al., 2014; PHILLIPS et al., 2009; SYFERT et al., 2013), and others arguing for the robustness of MaxEnt against spatial bias (GRAHAM et al., 2008; LOISELLE et al., 2008). However, little attention has been given to the second issue. With our plot dataset, we addressed the relationship between collection localities and the predicted spatial abundance distribution.

In 66% of the cases we found that a higher local relative abundance indeed increased the chance of being collected, although the correlations were very weak (Fig. 3.1 A), and the majority of collections originated from areas with a low relative abundance due to the large areas where a given species' abundance is low. Even hyperdominant species are usually only dominant in one or two of the six regions of Amazonia, most hyperdominant have a large geographic extent of occurrence but are habitat specialists (TER STEEGE et al., 2013). Steege et al. (2016) also found that abundance is a poor predictor for the number of collections of a species compared to the size of its extent of occurrence. Additionally, herbaria are characterized by the earlier

discussed collectors' bias (TER STEEGE et al., 2011). Although we addressed the spatial bias of survey effort by including a bias-based background file in our MaxEnt modelling, the lack of a significant positive relationship between relative abundance estimated by IDW and collection density for many species suggests that this assumption of MaxEnt is not met because of the way species are collected.

#### 3.4.2 MaxEnt maps vs. IDW maps

We also asked if MaxEnt maps would be a close match to the IDW maps. In general, environmental suitability does not reflect a species abundance. Presence-only SDMs, such as MaxEnt, are based on correlations between species presence and environmental conditions, predicting the environmental suitability for a species, and not their realized distribution (ARAÚJO; PETERSON, 2012). Relative abundance in the other hand is based solely on abundance, estimating the number of trees belonging to each species in the grid cells (STEEGE et al., 2015). The Spearman's rank correlation and the linear 90<sup>th</sup> percentile quantile regression showed a very weak positive relationship between MaxEnt's predicted environmental suitability and IDW relative abundance prediction at plot localities, contrary to the results of VanderWal et al. (2009), who found a strong relationship between the two. Their research differs in that they modelled a biogeographical region with tropical and subtropical rainforests, and also drier and warmer environments. The relationship between environmental suitability and local abundance is likely to be stronger when more (extreme) divergent conditions are included, such as areas from different biomes. Perhaps Amazonia's less divergent conditions, representing perhaps a one single biome, in a much larger area, are potentially responsible for this weak relationship.

To test their further predictive performances, we also converted both outputs to binary maps. Some studies have addressed questions about the transformation of SDM predictions into discrete representations such as binary maps, aiming to estimate area of occupancy, species richness and others applications (CALABRESE et al., 2014; GUILLERA-ARROITA et al., 2015; LAHOZ-MONFORT; GUILLERA-ARROITA; WINTLE, 2014; LAWSON et al., 2014).

Binary maps can add more uncertainties to model predictions, especially because it is necessary to set a threshold to distinguish between species presence and absence, which can be selected arbitrarily or without taking into account the context of the study. However, we avoided thresholds based on specificity (prediction of absences) because of the lack of absence data (MEROW; SMITH; SILANDER, 2013). In many cases our MaxEnt binary maps presented an area of occupancy close to those made with IDW, presenting a high median sensitivity (88%). Moreover, our MaxEnt binary maps also correctly predicted absence in naturally non-forested areas in northern Amazonia for many species (Appendix S3).

MaxEnt's environmental suitability mostly predicted much larger area of occupancy than those predicted with the IDW relative abundance. We reduced this effect estimating species extent of occurrence using a convex hull around each species records, plus a buffer of 300 km. This approach minimized MaxEnt's overestimation of the area of occupancy beyond the species' known geographical range (extent of occurrence), over climatically suitable areas, by restricting the species' predicted suitable habitat, providing a more conservative estimate for the species' area of occupancy (Appendix S5) (BOUCHER-LALONDE; MORIN; CURRIE, 2012; IUCN, 2012).

The IDW relative abundance models showed an opposite behavior, underpredicting areas where collections are present but where no plots have recorded the species. The high sensitivity of the MaxEnt compared to those of the IDW is in agreement with a previous study (MAHER et al., 2014), where models fit to presence-only data yielded higher sensitivity but a lower specificity than presence-absence models. Nevertheless, in our case, the IDW relative abundance yielded sensitivity rates based on collection localities that were as high as the sensitivity rates of MaxEnt's predicted environmental suitability based on plot presence localities (87%). Thus, both models function similarly in predicting species presences.

### 3.4.3 Collections versus abundance plot data

In some cases, collections were located outside the species' extent of occurrence predicted by the IDW maps. This divergence follows from the methodical differences between collections and plot assessments. The distributions as predicted by the IDW do not always cover the whole species' extent of occurrence. Because there are only 550 individuals (on average) in one plot, and 16,000 tree species in Amazonia (TER STEEGE et al., 2013), one plot obviously cannot contain all species that are present in the surrounding area.

Furthermore, many plots, lacking a given species, are within the extent of occurrence predicted by IDW, and many plots with absences are located in near proximity of plots with presence data. This results in low specificity values. NHCs comprise a species' range including areas of low abundance; while plot data have information on abundance, but may miss areas of low abundance, and, thus, may miss rare species more easily.

### 3.4.4 Environmental suitability versus dispersal limitation

The second large difference between the two models is the theoretical principles they are based upon. MaxEnt is based on environmental suitability, which is appropriate since correlations between species' distributions and climate are evident (ARAÚJO; PETERSON, 2012; BOUCHER-LALONDE; MORIN; CURRIE, 2012). Nevertheless, predicting actual (realized) distributions also requires information on biotic interactions, dispersal limitation, and other environmental variables, which are beyond presence-only SDM (ARAÚJO; PETERSON, 2012). IDW, on the other hand, is based on location only. Thus, both models cover only one of the three explanatory variables for species distributions. Again, it will depend on the aim of the research which type of model is most suitable. In either case predicted species distributions need to be interpreted with caution.

### 3.4.5 Collection data and cleaning pipeline

We propose a cleaning pipeline to remove possible inconsistencies in collection data. Unlike species-specific approaches, many studies use large numbers of species, lacking correction because of the great number of references and specialists to be consulted (ZIZKA; ANTONELLI, 2015). Collection data available in global datacenters, such as GBIF, cannot carry out thorough data-correction procedures, and the quality of the records has been debated and tested in some cases (MALDONADO et al., 2015). Some records have no locality information, or coordinates are based on cities close to the observed distribution, and may contain duplicated data or zeros as information (BOYLE et al., 2013; MALDONADO et al., 2015; ZIZKA; ANTONELLI, 2015).

We used a pipeline that cleans collection data by removing records with a lack of geographic information (ZIZKA; ANTONELLI, 2015), and we strongly recommend the use of analytical tools to correct inconsistencies present in global databases. The cleaning process also removed coordinates considered spatial outliers by a kernel-density estimate, omitting locations too far from the central part of the distribution, which we assume to be misidentifications. Our results suggest that half of the species records are likely inconsistent, missing geographical information, such as latitude, longitude or locality. Palms were the most impacted species, because the huge amount of records available with high levels of redundancy.

We used a kernel density estimate (KDE) to remove geographical outliers of the NHCs. This function removed e.g. occurrences outside the *Eperua falcata* Aubl. cluster observed in the Guianas (Fig 3.3 A), and *Licania alba* (Bernoulli) Cuatrec. in southeast Amazonia (Fig. 3.3 B). Although the KDE excluded only a small number of records compared to the previous cleaning step, it was able to identify some isolated occurrences, which we considered likely misidentifications. The KDE, however, showed limitations with palm species, removing some eastern Amazonia records, simply caused by the great number of collections in the Aarhus University Palm Transect Database in western Amazonia.

### 3.5 Conclusion

We have shown that the NHCs violate the assumption of MaxEnt that collection localities are an independently drawn sample from a species' unknown probability distribution. Although we found a relationship between NHCs and relative abundance for some species, it was very weak. Additionally, we found that the majority of MaxEnt's predicted environmental suitability values differ from those of the IDW relative abundance values, and its results cannot be interpreted as an abundance estimate. Nevertheless, MaxEnt predicts probability of occurrence well, and both models largely overlap and predict similar areas of occupancy, showing high sensitivities. Furthermore, NHCs data should undergo cleaning processes before being used to represent occurrences in species distribution models.

We showed that, half of the species records are likely inconsistent, missing geographical information, such as latitude, longitude or locality, and it also may represent misidentifications of the species. We therefore conclude that distribution maps as generated by MaxEnt should be used with caution. Their application should not be based solely on unsupervised models, especially because their easily constructed distribution maps are tempting to utilize without indication of probable errors. This outcome is particularly important for biodiversity assessments, for which SDMs of a large number of species are automatically generated without subsequent checking. Our pipeline provides a conservative means to do so. As our pipeline removes inconsistencies from NHCs data and estimates area of occupancy in an area slightly larger than the extent of occurrence of a species, compatible with IUCN red list assessments (IUCN, 2012; SYFERT et al., 2014).

## CAPÍTULO 4 MODELING THE DISTRIBUTION OF TREE SPECIES OF THE AMAZONIAN RAINFOREST TO LONG-TERM CLIMATE CHANGE DURING THE MID-LATE HOLOCENE<sup>3</sup>

### Abstract

Fossil pollen records from ecotonal southern Amazonia show that humid evergreen rainforest expanded southwards, at the expense of dry forest and savanna, in response to an increase in late Holocene rainfall. Using species distribution modelling, we model environmental suitability for species of two Amazonian tree families, Moraceae and Urticaceae, in the mid and late-Holocene, to test the responses of rainforest species to long-term climate change. We also test whether modern pollen assemblages of Moraceae/Urticaceae from Amazonian paleoecological sites are a good proxy for the current abundance of these families, using spatial abundance models based on a large plot dataset for Amazonian trees. Mean environmental suitability for species of Moraceae and Urticaceae showed a slight increase (2.5%) during the mid-late Holocene (since 6,000 yr BP) in Amazonia, in response to rising precipitation. This increase was highest in the ecotonal southern part of Amazonia. The accompanied modelled mean species richness increased by as much as 132% throughout Amazonia. The total abundance of Moraceae and Urticaceae correlated significantly with the modern pollen assemblages for these families ( $R^2 = 0.54$ ). Increased precipitation during the late Holocene increased the environmental suitability for species of Moraceae and Urticaceae, thus leading to an expansion of their ranges in ecotonal southern Amazonia, consistent with previously published fossil pollen data. This study establishes links of how the distribution of Amazonian tree species changed between past (drier) and current (wetter) climatic conditions, favoring ecotonal shift in southern Amazonia. It also inspires questions about the future of those species in global change scenarios, especially facing drier conditions.

**Keywords:** Climate change, Holocene, Pollen records, Species distribution.

---

<sup>3</sup>Em processo de submissão à revista *Journal of Biogeography*, Qualis A1 na Área de Avaliação de Ciências Ambientais. Material suplementar (Appendices S4.1 - S4.4) disponível em: [https://drive.google.com/file/d/172MpnO6g-i2cD\\_zS9ANWIoJNtZw6p44I/view?usp=sharing](https://drive.google.com/file/d/172MpnO6g-i2cD_zS9ANWIoJNtZw6p44I/view?usp=sharing).

## 4.1 Introduction

Tropical South America was influenced by long-term climate change during the late Holocene (REIS et al., 2017; RODRÍGUEZ-ZORRO et al., 2018; ROUCOUX et al., 2013). Significant changes occurred southern Amazonia, as well as several other Amazonian regions, driving the rainforest into wetter climatic conditions (BURNHAM; GRAHAM, 1999; COHEN et al., 2012; GRAHAM; MORITZ; WILLIAMS, 2006; MARTIN et al., 1997; SMITH; MAYLE, 2017), changing seasonality and precipitation patterns (BUSH; SILMAN, 2004). The responses of the vegetation to higher late Holocene precipitation, associated with a less prolonged and pronounced dry season, resulted in a long-term trend of climate driven rainforest expansion in ecotonal areas, between Amazonian rainforest, semi-deciduous dry forest, and Cerrado savannas (BEERLING; MAYLE, 2006; LATRUBESSE; RAMONELL, 1994; MAYLE et al., 2004).

This southward, late Holocene, rainforest expansion is inferred from fossil pollen data obtained from lake sediment cores, whereby higher pollen percentages of herbaceous taxa (e.g. Poaceae) and indicator tree taxa (i.e. *Curatella mericana* L.) are representative of savannas, and high pollen percentages of evergreen rainforest taxa (in particular > 40% Moraceae/Urticaceae type) signify humid evergreen rainforests (BURN; MAYLE; KILLEEN, 2010; COLINVAUX; DE OLIVEIRA, 2001; LIU; COLINVAUX, 1988).

The clearest evidence for late Holocene, climate-driven, rainforest expansion comes from fossil pollen data from two lakes – Lagunas Bella Vista and Chaplin – in Noel Kempff Mercado National Park in ecotonal Northeastern Bolivia. Surface-sediment pollen assemblages reflect the closed-canopy humid evergreen rainforest surrounding both lakes today; i.e. 40-50% Moraceae/Urticaceae pollen, and < 10% grass pollen. This contrasts with < 20% Moraceae/Urticaceae and ca. 40% Poaceae pollen during drier conditions of the middle Holocene, consistent with a mosaic of semi-deciduous dry forest and savanna, which dominates the Brazilian Cerrado biome south of Amazonia today (MAYLE; BURBRIDGE; KILLEEN, 2000).

At Laguna Bella Vista the abundance of Moraceae/Urticaceae pollen increased steeply between 2790 cal yr and 1530 cal yr (before present). At Laguna Chaplin, a lake 100 km further to the south, this rainforest expansion occurred later, between 2240 cal yr and 660 cal yr (BURBRIDGE; MAYLE; KILLEEN, 2004; BURN; MAYLE; KILLEEN, 2010).

Moraceae and Urticaceae are commonly found in Amazonian rainforests (TER STEEGE et al., 2006, 2015), and Moraceae is among the 10 most abundant families in Amazonia (TER STEEGE et al., 2013). In the Bolivian wet forests Moraceae are the most dominant family in the forest. Modern pollen assemblages of southern Amazonian rainforest also show high percentages of Moraceae/Urticaceae pollen (BEHLING; DA COSTA, 2000; BEHLING; HOOGHIEMSTRA, 1999). The pollen of these two families is well-represented in Amazonian fossil records, but it is difficult to reliably distinguish between the genera within the families or even between these two families (BURN; MAYLE, 2008). The majority of the grains of pollen identified as Moraceae/Urticaceae in southern part of Amazonia have been attributed to Moraceae rather than Urticaceae, because Moraceae is much more common than Urticaceae in inventories of vegetation plots (BURBRIDGE; MAYLE; KILLEEN, 2004; MAYLE; BURBRIDGE; KILLEEN, 2000).

## **4.2 Aims and approach**

Long-term climate change may have increased the environmental suitability for individual species of Moraceae and Urticaceae during the mid-late Holocene. Here, we model the distribution of the tree families Moraceae and Urticaceae throughout Amazonia, to increasing precipitation during the mid-late Holocene, using species distribution modelling, and thereby quantify the spatial scale of climate-driven range distribution. To achieve this, we model the environmental suitability based on species potential distribution using a conservative pipeline (GOMES et al., 2018) to define the area of occupancy (AOO) (IUCN, 2012) of species. We do this for current climate conditions and mid-Holocene projections of seven global circulation models (GCMs) (HIJMANS et al., 2005). Furthermore, we test if the modern pollen assemblage of Moraceae and Urticaceae obtained from the pollen diagrams of the paleoecological sites, are a good proxy for the current (relative) abundance of these families.

## 4.3 Methods

### 4.3.1 Amazonian base map

We based Amazonian lowland forest on ter Steege et al (2015). The base map consists of 2191 0.5-degree cells (Fig. S4.7). We also followed ter Steege et al (2013) and divided the Amazonia area into six regions, Guiana Shield (GS), northwestern Amazonia (WAN), southwestern Amazonia (WAS), southern Amazonia (SA), eastern Amazonia (EA) and central Amazonia (CA).

### 4.3.2 Tree families

We used the abundance data of Moraceae and Urticaceae provided by the Amazon Tree Diversity Network (ATDN, <http://atdn.myspecies.info/>) to model the relative abundance of the two families spatially. To model species distribution based on environmental suitability we downloaded collections of Moraceae/Urticaceae from Global Biodiversity Information Facility (GBIF, <http://www.gbif.org/>), based on the most recent Amazonian tree species list (TER STEEGE et al., submitted). Taxonomic names were checked with the Taxonomic Name Resolution Service (TNRS, <http://tnrs.iplantcollaborative.org/>) and also with the list of ter Steege et al. (submitted), to correct for synonyms and non-Amazonian species. All collections were also checked for inconsistencies using a cleaning pipeline (GOMES et al., 2018).

### 4.3.3 Collections

We downloaded species collections from GBIF (January 2018) using ‘gbif’ function from R package ‘dismo’ (HIJMANS et al., 2017b). We used data from all ‘Neotropic’, using the complete extent of occurrence of the species to prevent SMDs deficiencies that are associated with models based on a species’ partial geographic range (RAES, 2012). We assigned all individuals to species level and intraspecific levels were ignored. We used a cleaning pipeline to deal with data inconsistencies, possible outliers and imprecise georeferences (BOYLE et al., 2013; GOMES et al., 2018; MALDONADO et al., 2015; ZIZKA; ANTONELLI, 2015).

#### 4.3.4 Environmental suitability

We estimate mean environmental suitability based on species potential distribution as predicted by species distribution modelling, constrained by species extension of occurrence (EOO) plus a buffer of 300 km, resulting in the used species distribution models to estimate mean environmental suitability, based on the area of occupancies (AOO) of the species (GOMES et al., 2018; IUCN, 2012). For that, we used MaxEnt version 3.3.3k (PHILLIPS; ANDERSON; SCHAPIRE, 2006; PHILLIPS; DUDÍK; SCHAPIRE, 2004). We downloaded 19 environmental variable data from WorldClim (HIJMANS et al., 2005), based on average monthly interpolated climate data. Species' original AOO was based on current conditions (average for 1950-2000). Species' past AOO for mid-Holocene (ca. 6,000 yr BP) was based on seven IPCC5 global climate model (GCM) projections, BCC-CSM (XIAO-GE; TONG-WEN; JIE, 2013), CCSM4 (YEAGER et al., 2012), HadGEM2-ES (JONES et al., 2011), IPSL-CM5A-LR (SWINGEDOUW et al., 2013), MIROC-ESM (WATANABE et al., 2011), MPI-ESM-LR (GIORGETTA et al., 2013) and MRI-CGCM3 (TATEBE et al., 2012).

We based the selection of the variables on their biological relevance and on their scores using a Spearman's rank correlation coefficient threshold of  $|\rho| > 0.7$  (DORMANN et al., 2013). We focused on variables related to precipitation and seasonality, since seasonal climate produced by latitudinal shifts of the South American Summer Monsoon is the overriding control over the geographical limit of the Amazonian rain forest (LATRUBESSE; RAMONELL, 1994; MARTIN et al., 1997). Furthermore taxa range limits are defined by their ability to endure dry conditions, where the threshold for the studied families presence is ~2,000 mm mean annual precipitation and ~-200 mm cumulative water deficit (ESQUIVEL-MUELBERT et al., 2016). We selected isothermality, temperature seasonality, max temperature of warmest month, precipitation seasonality, precipitation of driest quarter and climatologic water deficit (CWD). We followed Chave et al. (2014) to estimate CWD, which is a measure to calculate how much evapotranspiration exceeds rainfall.

We cropped all environmental variables to Neotropics extent (RAES, 2012). We also used the function ‘mean’ from R package ‘raster’ (HIJMANS; VAN ETTEN, 2016) to aggregate all variables to 0.5-degree spatial resolution. We corrected the SDMs for geographical sampling bias (GOMES et al., 2018) and used only product, threshold and hinge MaxEnt features (BOUCHER-LALONDE; MORIN; CURRIE, 2012; MEROW; SMITH; SILANDER, 2013). Species with a small number of collections (<6) were not used to model environmental suitability since they may develop inaccurate predictions (VAN PROOSDIJ et al., 2015).

#### 4.3.5 Species relative abundance

Abundance maps were constructed using 1912 1-ha tree inventory plots distributed across Amazonian rainforest (Amazon basin and the Guyana Shield) from the Amazon Tree Diversity Network. We recorded all individuals with  $\geq 10$  cm diameter at breast height (dbh) within the plots (TER STEEGE et al., 2013).

#### 4.3.6 Constructing abundance maps

We used inverse distance weighting (IDW) interpolation to produce abundance maps from the plot abundance data. We produced the inverse distance weighting (IDW) models based on relative abundance (STEEGE et al., 2015). We defined the relative abundance (RA) for each cell as  $RA_i = n_i/N$ , where:  $n_i$  = the number of individuals of species  $i$ , and  $N$  = the total number of trees. IDW models were based on the nearest 150 plots within a 300 km distance limit (GOMES et al., 2018). The plot weights were calculated by taking the square root of the distance in degrees.

#### 4.3.7 Pollen data

We analyzed pollen diagrams from 45 Amazonian paleoecological sites (BEHLING, 1996, 1998, 2001; BEHLING et al., 2001a; BEHLING; DA COSTA, 2000; BEHLING; HOOGHMSTRA, 2000; BERRÍO et al., 2002; BURBRIDGE; MAYLE; KILLEEN, 2004; BUSH et al., 2000; BUSH; COLINVAUX, 1988; COLINVAUX et al., 1997; DA SILVA MENESES; DA COSTA; BEHLING, 2013; IRION et al., 2006; LEDRU, 2001; LEDRU et al., 1997; LIU; COLINVAUX, 1988; MAYLE; BURBRIDGE; KILLEEN, 2000; ROUCOUX et al., 2013; TAYLOR et al., 2010; URREGO et al., 2013; WENG; BUSH; ATHENS, 2002; WENG; BUSH; SILMAN, 2004) to assess the percentage of modern pollen assemblages in the sediment cores of the paleoecological sites for both, Moraceae and Urticaceae families (Appendix S4.1; Fig. S4.8). The paleoecological sites are distributed within Amazonian lowland rainforest (Amazonian base map).

#### 4.3.8 Data analysis

To test the responses of Amazonian rainforest species to long-term climate change, we modelled current and past tree species distribution to assess increments in its environmental suitability between the drier middle Holocene and wetter present day (6,000 yr BP). We statistically validated species' models, testing which of them were significantly different from a random expectation using bias corrected null-models (RAES; TER STEEGE, 2007a). We then excluded all species which models were not significantly different from the null-models. We produced two SDMs for each species: 'current' and 'mid-Holocene'. For mid-Holocene we considered only grid cells predicted by all IPCC5 GCMs. To estimate the environmental suitability for Moraceae and Urticaceae we averaged the models of the top 20 most dominant species of each family (STEEGE et al., 2015), since they represent most of the individuals of the families (more than 50% for both families).

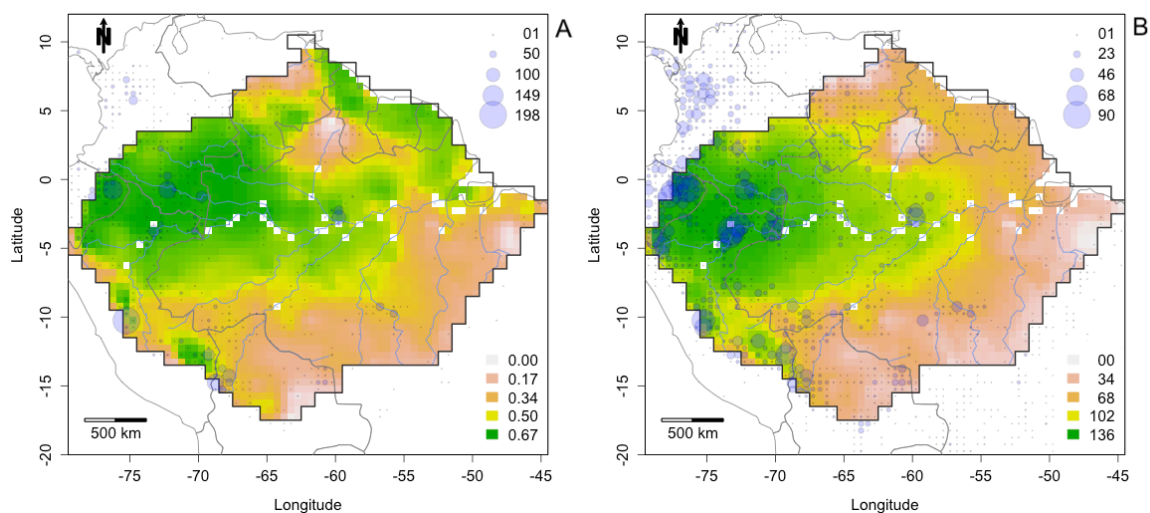
We also estimated species richness and its increment between mid-Holocene and current climate. To assess species richness we transformed MaxEnt logistic output of each species into binary maps with a 10% training presence threshold, using a convex hull plus a buffer of 300 km around species records to estimate their area of occupancy (AOO) (GOMES et al., 2018; IUCN, 2012; SYFERT et al., 2014). Then, we stacked the thresholded maps of all species (GOMES et al., submitted). Finally, fitted a linear model to test how pollen records of Moraceae/Urticaceae related to the relative abundance of both families on the paleoecological sites used.

#### **4.4 Results**

The 20 most abundant Moraceae and Urticaceae species included 13 species of Moraceae and 7 species of Urticaceae (Appendix S4.1). Moraceae are generally more abundant and the 20 most abundant Moraceae species are roughly 60% more abundant than the 20 most abundant Urticaceae species in Amazonia (Appendix S4.1).

Mean species richness for current and past climate was estimated using 176 Moraceae and Urticaceae species (113 Moraceae and 63 Urticaceae), which had available records in the GBIF database (>5), and models significantly differed from a random expectation, tested using null models (Appendix S4.2). Current mean environmental suitability and mean species richness were higher in northwestern and central Amazonia (Appendix S4.3; Fig. 4.1 A, B). Current environmental suitability was also high in a narrow band in the Guiana Shield. Both families showed roughly the same pattern (Appendix S4.3; Fig. S4.1; S4.2).

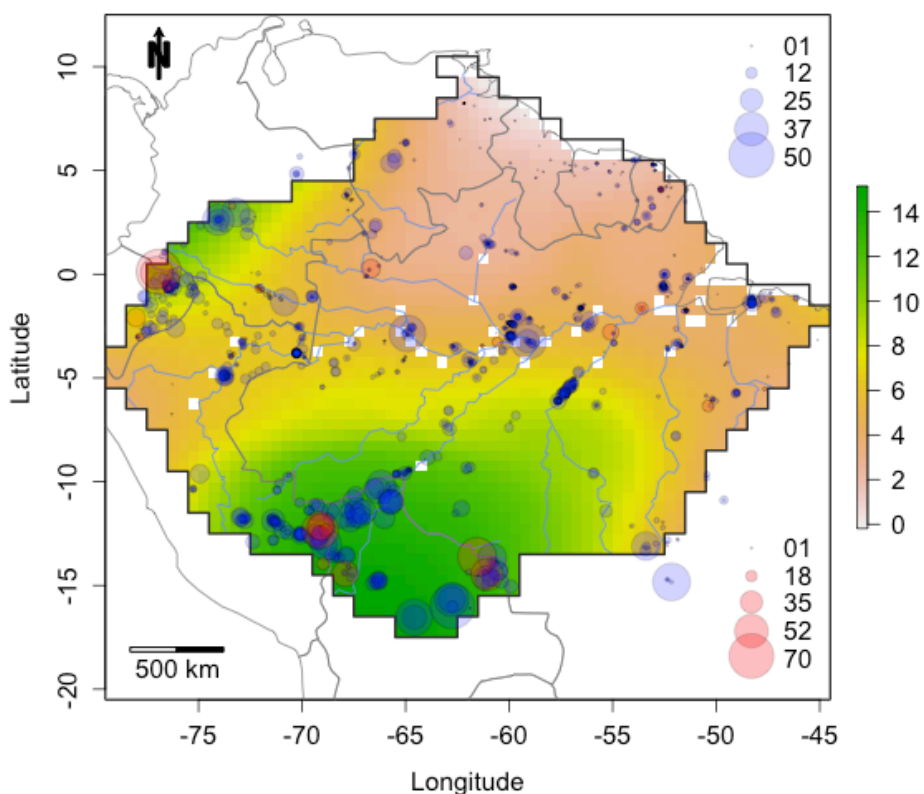
**Figure 4.1.** Current mean environmental suitability and current mean species richness for Moraceae and Urticaceae. a, Map for current mean environmental suitability. b, Map for current mean species richness. circles in blue, Numbers of species collections by 0.5-degree cell (a); Number of single species collected by 0.5-degree cell (b). gray line, Amazonian rainforest. Maps created with custom R script. Base map source (country.shp, rivers.shp): ESRI.



**Fonte:** ESRI (2016); R Core Team (2018).

Moraceae and Urticaceae are currently common in Amazonian forests in general, accounting for 7% of all individuals in the forest on average (Appendix S4.1), but are distinctly more dominant in southwestern Amazonia (16%, Appendix S4.1) (Fig. 4.2). Southwestern Amazonia showed the highest current mean relative abundance (16%) followed by southern Amazonia (8.6%) and northwestern Amazonia (7%). The lowest current relative abundance was found in the Guyana shield (3.5%). This contrasts strongly with the current environment suitability and species richness patterns (Fig. 4.1 A, B; 2). Moraceae, the most common family between the two, dominates this pattern, and showed highest current abundance in southern, southwestern, ranging between 0-10.9% (mean of 4.9%) (Fig. S4.3 A). Urticaceae is more evenly spread with peaks, including parts of eastern, southwestern and northwestern Amazonia. Its current relative abundance ranged between 0.1-6.3% (mean of 2.0%), with higher mean values in southwest and eastern Amazonia (3.5% and 2.5%, respectively) (Fig. S4.3 B).

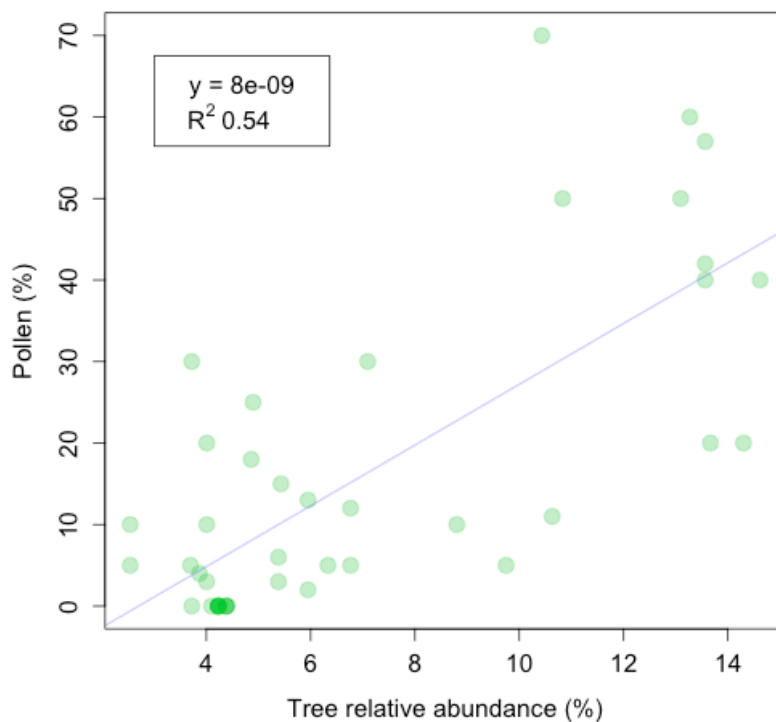
**Figure 4.2.** Relative abundance for Moraceae and Urticaceae families. circles in blue, number of plots with presence of the families. circles in red, percentage of modern pollen assemblages in the core's sediment of the paleoecological sites corresponding to the values in Appendix S4.4. gray line, Amazonian rainforest. Maps created with custom R script. Base map source (country.shp, rivers.shp): ESRI.



**Fonte:** ESRI (2016); R Core Team (2018).

Modern pollen assemblages of Moraceae/Urticaceae in the surface sediments of lake cores were a good proxy for the modelled relative abundance of these families ( $R^2 = 54\%$ ,  $P < 0.05$ ; Fig 4; Appendix S4.4). The Moraceae/Urticaceae pollen assemblages showed a high correlation when compared with the relative abundance of Moraceae ( $R^2 = 59\%$ ,  $P < 0.05$ ). The same analysis using the relative abundance of Urticaceae showed only a very weak ( $R^2 = 12\%$ ,  $P < 0.05$ ) (Appendix S4.4; Fig S4.6 A, B).

**Figure 4.3.** Relationship between the tree relative abundance of Moraceae and Urticaceae species in modern vegetation versus their modern pollen assemblages. Graph created with custom R script.



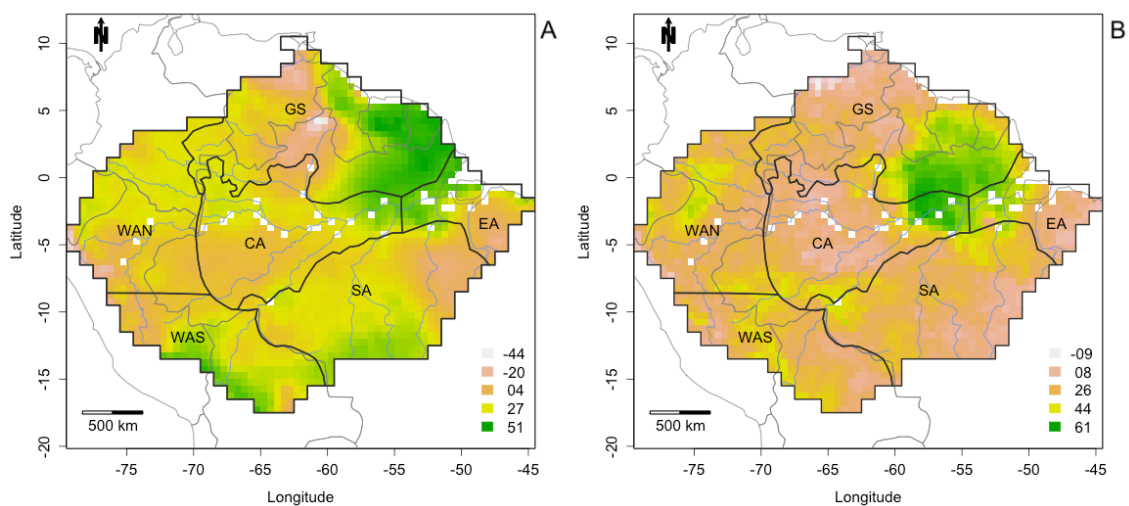
**Fonte:** R Core Team (2018).

The mean relative abundance of Moraceae/Urticaceae was higher in the paleoecological sites locations in southwestern Amazonia, followed by northwestern, central, southern Amazonia, Guiana Shield and eastern Amazonia (Appendix S4.4; Fig. 4.1). The modern pollen assemblage in the paleoecological sites was higher in southwestern Amazonia, followed by northwestern, southern Amazonia, Guiana Shield, central and eastern Amazonia.

During the mid-late Holocene environmental suitability for Moraceae/Urticaceae increased over all Amazonia (2.5%). The increment was positive in the Guiana Shield (7.4%), eastern Amazonia (4.7%) and in the rainforest–savanna boundaries in southwestern (4.0%) and southern Amazonia (0.8%), but negative in central (-0.3%) and northwestern Amazonia (-1.6%) (Appendix S4.3; Fig. 4.3). Although the mean increment was weak, it ranged widely between -44.2 and 51.2%.

The mean increment for Moraceae was positive for all of Amazonia on average (4.0%), for the Guiana Shield (11.7%), eastern (6.9%), southwestern (4.1%) and southern Amazonia (1.5%), but negative for central (-0.02%) and northwestern Amazonia (-0.8%) (Appendix S4.3; Fig. S4.4 A). The mean increment for Urticaceae was positive for Amazonia (5.7%), and was higher in eastern Amazonia (19.5%) and the Guiana Shield (12.5%). It was negative in southwestern Amazonia (-0.3%), and lower but positive in central (3.7%), northwestern (3.4%) and southern Amazonia (1.4%) (Appendix S4.3; Fig. S4.4 B).

**Figure 4.4.** Increment in mean environmental suitability and increment in mean species richness during the mid-late Holocene (% , between current and middle Holocene, last 6,000 yr Bp. a, Increment in mean environmental suitability during late Holocene. b, Increment in mean species richness. Gray line, Amazonian rainforest and Amazonian sub-regions (TER STEEGE et al., 2013). Maps created with custom R script. Base map source (country.shp, rivers.shp): ESRI.



Fonte: ESRI (2016); R Core Team (2018).

The mean predicted species richness for 0.5-degree grid cells strongly increased throughout Amazonia during the late Holocene (110%). Mean predicted species richness was lower in eastern Amazonia (Fig. 4.1 B), but this region showed the highest increment in mean predicted species richness during the late Holocene (345%) (Appendix S4.3; 4.3 B). Northwestern Amazonia showed the highest predicted species richness, but a lower increment during the late Holocene (17%). The mean predicted species richness showed the lowest values in southern, southwestern and eastern Amazonia. For Moraceae, the mean increment in predicted species richness was higher in a large area in the Guiana Shield, central and eastern Amazonia (Appendix S4.3; Fig S4.5 A).

Urticaceae followed a similar predicted species richness pattern in comparison with Moraceae but also showed some peaks in northwestern and southwestern Amazonia (Appendix S4.3; Fig S4.5 B). Furthermore, we found that the mean increment in pollen assemblage in the paleoecological sites diagrams was higher in southern Amazonia, followed by southwestern, northwestern Amazonia, Guiana Shield and central Amazonia, but it was negative in eastern Amazonia though (Appendix S4.4).

#### **4.5 Discussion**

The mid to late Holocene was a time of strong climate change in Amazonia. This change of climate clearly affected the habitat suitability of many rainforest species, as exemplified by Moraceae and Urticaceae here. Moraceae not only has widely distributed species in southern Amazonia, but also species which extend beyond Amazonia into the Brazilian Cerrado and Atlantic forest biomes (CARDOSO et al., 2017; TER STEEGE et al., 2016). Moraceae species grow, not only within *terra firme* rainforest, but also seasonally-inundated rainforest, semi-deciduous dry forests and savannas (KILLEN, 1998). *Brosimum gaudichaudii* Trécul is a Moraceae species that does not even grow in rainforest, but is an indicator species for open woodland and Cerrado savanna communities (EITEN, 1972; MARCHANT et al., 2002).

One of the aims of our study was to determine whether the abundance of Moraceae/Urticaceae in modern pollen records serves as a good proxy for their relative abundance of these families in the parent vegetation. At an Amazon basin-wide scale we found that surface-sediment pollen assemblages of Moraceae/Urticaceae were well correlated with the relative abundance of both families lumped together. The pollen assemblages from Laguna Bella Vista and Laguna Chaplin were a good signature of the rainforest surrounding these lakes in eastern Bolivia (GOSLING et al., 2009; MAYLE; BURBRIDGE; KILLEEN, 2000).

We also found Moraceae/Urticaceae pollen registered in modern assemblages of all Amazonian regions being more abundant in southwestern, northwestern and southern Amazonia (ABSY et al., 1991; BEHLING et al., 2001b; BEHLING; DA COSTA, 2000; BEHLING; HOOGHMSTRA, 2000; BERRÍO et al., 2002; BUSH et al., 2000, 2004, 2007; BUSH; COLINVAUX, 1988; BUSH SILMAN, M. R., 2007; COLINVAUX et al., 1988, 1996, 1997; DA SILVA MENESES; DA COSTA; BEHLING, 2013; FROST, 1988; HERMANOWSKI et al., 2012; IRION et al., 2006; LEDRU, 2001; LIU; COLINVAUX, 1988; MAYLE; BURBRIDGE; KILLEEN, 2000; ROUCOUX et al., 2013; URREGO et al., 2013; WENG; BUSH; SILMAN, 2004).

Burn et al. (2010) showed that pollen rain from artificial pollen traps are a good representation of the surface sediment pollen assemblage of lakes from both moist forests of the Madeira-Tapajós ecoregion and the savanna of the Beni ecoregion, where these ecosystems could be differentiated not only floristically, but also palynologically. Gosling et al. (2009) compared modern pollen rain obtained from artificial pollen traps within plots with floristic inventories in northeast Bolivia and their results showed that no taxon could be used as an indicator of tropical rainforest or Cerrado savannas. Their results did confirm that high abundances of Moraceae (over 40%) could serve as an indicator for *terra firme* rainforest. We conclude that the increases and decreases of pollen in the cores can be interpreted as increases and decreases of the abundances of trees of these families in the forest.

In our analyses, pollen of Moraceae/Urticaceae was present in assemblages of sediment cores corresponding to mid Holocene in all Amazonia regions. The pollen concentration of Moraceae/Urticaceae increased in the sediment cores between mid and late Holocene, especially for the cores in the ecotonal southern and northern parts of Amazonia: Loma Linda in eastern Colombia (BEHLING; HOOGHMSTRA, 2000), middle Caquetá river basin (Colombia) (BEHLING; CARLOS BERRIO; HOOGHMSTRA, 1999), Fazenda Cigana and Terra indígena Aningal (Roraima, northern Brazil) (DA SILVA MENESES; DA COSTA; BEHLING, 2013), and lakes Marcio and Tapera in Amapá (northern Brazil) (DE TOLEDO; BUSH, 2007), and further increase in forest close to Pantanal (WHITNEY et al., 2011) and increase of Moraceae/Urticaceae pollen in Lago do Saci (FONTES et al., 2017).

Nevertheless, mid Holocene assemblages of Moraceae/Urticaceae pollen were registered in sediment cores in all Amazonian regions, consistent with the fact that Moraceae species were modelled to be present in those areas, throughout the period. Sites where continuous forest cover was suggested by pollen of forest trees included eastern Amazonia (BARBERI; SALGADO-LABOURIAU; SUGUIO, 2000), forests near the mouth of the Amazon river (BEHLING, 1996), French Guiana, Equador (LIU; COLINVAUX, 1988), central around Morro de 6 Lagos (BUSH et al., 2004). Moraceae/Urticaceae pollen was present in all these cores with high abundances in western Amazonia and much lower, but constant, abundances in the Guyana Shield sites, consistent with the low current abundances of these families in the forest at present (LEDRU, 2001). Eastern Amazonian sites showed increase of savannas (DE TOLEDO; BUSH, 2007), consistent with mean pollen decrease during mid-late Holocene in the regions (BEHLING; DA COSTA, 2000; BUSH et al., 2000, 2007).

For the present analysis, the mean environmental suitability for Moraceae and Urticaceae and species richness of the two families was higher in northwestern and central Amazonia, and lower in southern regions. A similar pattern was observed by Gomes et al.'s (submitted) analysis of the distributions of all Amazonian tree species. Ter Steege et al (2003) mapped Amazonian average tree  $\alpha$ -diversity and also found a similar pattern, and hypothesized that the low diversity in Bolivian and Brazilian ecotonal rainforests reflected their recent expansion within the last 2-3 millennia, as shown by Mayle et al (2000) (within the last 2-3 millennia).

This could imply that these young rainforests are still undergoing succession and are still accumulating species (TER STEEGE et al., 2000), and that the high abundance of Moraceae and Urticaceae species in these ecotonal rainforests likely reflects their rapid dispersal and fast growth rates. In contrast, the higher biodiversity observed in western Amazonia may be result of the relatively stable climatic conditions in the region since the last glacial period Cheng et al. (2013). Both, predicted species richness and mean environmental suitability of Moraceae and Urticaceae contrasted strongly with their relative abundance in the forest. The relative abundance was highest in south-western Amazonia and lower in northwest and central Amazonia. For Moraceae this pattern was more pronounced.

Species distribution in the tropics is strongly associated with precipitation, and taxa with wide ranges, such as Moraceae and Urticaceae, are widespread across the precipitation gradient of the region, showing higher tolerance to water-stress (ESQUIVEL-MUELBERT et al., 2016). Environmental suitability was also higher in a narrow band in Guiana Shield, but neither species richness or abundance were high in that area. This may reflect the influence of other factors on species distribution, such as biotic interactions which may dissociate a species' observed distribution from its potential distribution as predicted by environmental suitability (ANDERSON; MARTÍNEZ-MEYER, 2004; ELITH et al., 2011). Ter Steege et al. (2003) suggested that the low diversity in the Guiana Shield may be linked to the small size of this area in comparison with the much larger tract of forest dominating the Amazon watershed. The Guianas also hold very poor soils, and low forest dynamics, which together may restrict possibilities for fast growing species, such as Moraceae and Urticaceae (GRAU et al., 2017; TER STEEGE; HAMMOND, 2001; VAN DER SANDE et al., 2018).

Modelling past climatic conditions of Amazonia may be problematic since Global Climate Models (GCMs) may diverge in modelling some part of the Amazonian basin (SMITH; SINGARAYER; MAYLE, 2018). We minimized such divergences by averaging several GCMs from CMIP5. The mean environmental suitability for Moraceae and Urticaceae increased in southwestern and southern Amazonia during the mid-late Holocene, especially in the ecotonal area near the margins of the rainforest. This increase in environmental suitability suggests that Amazonian species may have tracked climate change southward in the last two to three millennia as argued by Mayle et al. (2000).

## 4.6 Conclusion

We have shown that mean environmental suitability for Moraceae and Urticaceae increased during the mid-late Holocene in Amazonia, especially in the ecotonal boundary between the rainforest in the southern part of Amazonia and Cerrado savannas and in the northern part bordering the Llanos in Colombia (and probably Venezuela), supporting the assumption that long-term climate change favored the southern forest expansion, affecting species dynamics, and thus their distribution. Furthermore, the relative abundance of these two families was significantly correlated to their modern pollen assemblage in lake/bog surface sediment throughout Amazonia. We therefore conclude that the transition for a wetter climate during the late Holocene increased the mean environmental suitability for Amazonian tree families, which affected their distribution in its southern rainforest–savanna boundaries.

## **CAPÍTULO 5 AMAZONIAN TREE SPECIES THREATENED BY DEFORESTATION AND CLIMATE CHANGE<sup>4</sup>**

### **Abstract**

Deforestation is currently a major source of threat to Amazonian tree species. However, climate change may surpass deforestation in a few decades. Here, we quantify the impacts of deforestation and climate change of all known Amazonian tree species by overlaying species distribution models for current and future climate change scenarios with historical and projected deforestation. We show that deforestation alone may cause a 19-36% decline in species richness and climate change 31-37% by 2050. Their combination is expected to cause a decline up to 58%. Species may lose on average 66% of their original environmentally suitable area, and a total 53% may be threatened according to IUCN Red List criteria. Amazonian protected area networks may mitigate climate change and deforestation impacts, where the mean loss of estimated AOO inside these areas may vary between 8-28%, against 40-60% on the outside. We found mean species richness to be also higher inside these areas. Our analyses suggest that the Amazonian lowland rainforest may be cut in two blocks according to the worst-case scenario for 2050, one continuous block with 53% of the original area, and another severely fragmented block. This scenario assumes no significant changes in governance on deforestation and climate change rates. The vast potential degradation of Amazonia urges a reduction to zero deforestation, which would also reduce CO<sub>2</sub> emissions, mitigate climate change and foster biodiversity conservation.

**Keywords:** Amazonia, Climate change, Deforestation, Global change, Tree species.

---

<sup>4</sup>Artigo em revisão na revista Nature Climate Change, Qualis A1 na Área de Avaliação em Ciências Ambientais. Material suplementar (Appendices S5.1 - S5.5) disponível em <https://drive.google.com/file/d/1FZJqP0Kx1tHpQ1DkZcdcupkfineriNP/view?usp=sharing>.

## 5.1 Introduction

The Amazonian lowland rainforest is the single largest rainforest block on earth. With ~5.7 million km<sup>2</sup> it currently holds close to 13% of all trees (dbh > 10 cm) of the world and 49% of those in tropical moist forests (CROWTHER et al., 2015). Amazonia is arguably also the richest rainforest but the actual tree species richness is still under debate, ranging from ~7,000 (CARDOSO et al., 2017) to 16,000 (TER STEEGE et al., 2013). Amazonian diversity is not immune to deforestation and human driven climate change and their impacts are usually estimated separately because of the differences of time scales and patterns of biodiversity loss (HUNTINGFORD et al., 2008). A realistic scenario that will guide public policies, however, should take both processes into account.

The future of Amazonia facing global change has been debated (BETTS; MALHI; ROBERTS, 2008; TER STEEGE, 2010). Amazonia has lost ~11% of its area by 2013 (HANSEN et al., 2013; SOARES-FILHO et al., 2013). This is enough to qualify 27% of all Amazonian tree species as being globally threatened by IUCN categories and criteria at present, and projections show that deforestation may increase Amazonian forest loss to 9-28% by 2050, and the number of threatened species to 40-64% (TER STEEGE et al., 2015). Although habitat loss caused by deforestation is currently a major source of threat to Amazonian tree species diversity (HUBBELL et al., 2008; LOVEJOY; NOBRE, 2018), evidence suggests that human induced climate change may surpass the impact of deforestation in a few decades (BELLARD et al., 2012). Amazonian forest may already crossed a climate resiliency threshold (COWLING et al., 2004) due to climate change. The median spatial distance between current climate and their closest future climate analogues may increase by more than 300 km in 2050 considering only temperature, increasing by over 475 km when including precipitation, rising species vulnerability, especially when considering that deforestation creates migration barriers for slowly migrating species (FEELEY; REHM, 2012). As environmental tolerance is a driver of the geographic distribution of species, species must either tolerate new climates or track optimal environmental conditions (PECL et al., 2017).

During the late Holocene Amazonian tree communities have expanded their distribution southward beyond the forest boundaries driven by climate change, in a three millennia process, reaching a distance no further than 100 kilometers (MAYLE; BURBRIDGE; KILLEEN, 2000). Therefore, most tree species are likely unable to track future climate, facing extinction in areas where climatic conditions are no longer suitable (FEELEY; SILMAN, 2016).

Here, we quantify the combined impacts of deforestation and climate change of 10,070 Amazonian tree species. We model the original environmental suitability for species, which we call estimated area of occupancy (AOO), based on a species distribution model but constrained by the known extent of occurrence (EOO) (Fig. S5.1). Then, we quantify losses produced by historical deforestation, two deforestation scenarios for 2050, two climate change scenarios for 2050, and their interaction. We also ask to what extent the Amazonian protected area network may prevent habitat loss and the decline in species richness. Finally, we assess the species' threat status for each of the scenarios, based on the criteria of the IUCN Red List of Threatened Species.

## **5.2 Methods**

### **5.2.1 Species and collections**

We focused our analysis on the most recent checklist of lowland Amazonian trees that can reach 10 cm stem diameter at breast height (DBH) (TER STEEGE et al., [s.d.]). We downloaded species collections from Global Biodiversity Information Facility (GBIF, [www.gbif.org](http://www.gbif.org)) using the 'gbif' function from R package 'dismo' (August 2017). For each species we downloaded not only the Amazonian occurrences, but all occurrences in the Neotropics to avoid problems in species distribution models (SDMs) related to modelling with partial geographic ranges (RAES, 2012). We assigned all single collections at species level, ignoring intraspecific levels. We followed Gomes et al. (GOMES et al., 2018), using a new conservative pipeline to remove inconsistencies and outliers from collection data. Imprecise georeferences were also removed (BOYLE et al., 2013; MALDONADO et al., 2015; ZIZKA; ANTONELLI, 2015).

Since sample size is a relevant aspect of model accuracy, species with less than 6 records (here defined as locations, or single occurrence per 0.1 degree cell) were not used to produce SDMs (VAN PROOSDIJ et al., 2015). All the species with small number of collections (<6) were tested with a large plot dataset from Steege et al (TER STEEGE et al., 2015), to identify poor collected species. Species with a small number of collections and not present in the large plot dataset were listed as threatened according IUCN D2 criterion (IUCN, 2017).

### 5.2.2 Deforestation, protected areas and indigenous territories

Deforestation was based on historical deforestation up to 2013 (HANSEN et al., 2013; SOARES-FILHO et al., 2006, 2013), and projected deforestation for 2050 (historical deforestation plus the predicted deforestation) (SOARES-FILHO et al., 2006, 2013) at 10 by 10 km resolution, using an improved governance scenario (IGS) and a business-as-usual scenario (BAU) (Fig. S5.2 A, B, C). We gathered the spatial data of Amazonian protected areas and indigenous territories from the World Database of Protected Areas (Fig. S5.3) (April 2018, <https://www.protectedplanet.net>) (UNEP-WCMC; IUCN; PLANET, 2018), and updated with data from Red Amazónica de Información Socioambiental Georreferenciada - RAISG (January 2019, <http://raisg.socioambiental.org/>) (RAISG, 2017).

### 5.2.3 Amazonian base map

To produce an Amazonian lowland forest base map we followed ter Steege et al. (2015), eliminating cells with more than 50% water, areas originally without forest and areas above 500 m of elevation at 10 by 10 km resolution. The base map consists of 47,038 0.1-degree cells, or 5.7 million km<sup>2</sup> (Fig. S5.4). We followed ter Steege et al. (2013) and divided the area into six regions, Guiana Shield (GS), north-western Amazonia (WAN), southwestern Amazonia (WAS), southern Amazonia (SA), eastern Amazonia (EA) and central Amazonia (CA).

#### 5.2.4 Species area of occupancy

We estimated area of occupancy based on environmental suitability (GOMES et al., 2018; IUCN, 2012). For that, we assessed environmental suitability by constructing species distribution models using MaxEnt version 3.3.3k (PHILLIPS; ANDERSON; SCHAPIRE, 2006; PHILLIPS; DUDÍK; SCHAPIRE, 2004). We downloaded 19 environmental variables data from WorldClim (HIJMANS et al., 2005) at 0.16 degree resolution, produced by means of average monthly interpolated climate data. We resampled all variables to 0.1 degree (approximately 10 km<sup>2</sup>) spatial resolution, using the function 'resample' from R package 'raster' (HIJMANS; VAN ETTEN, 2016). The original environmental suitability for species was based on average climate data for 1950-2000 (HIJMANS et al., 2005).

Species future environmental suitability for 2050 (averages for 2041-2060) was based on two representative concentration pathways (RCPs), RCP 2.6 and RCP 8.5 (RIAHI; GRÜBLER; NAKICENOVIC, 2007; VAN VUUREN et al., 2006, 2007), using seven global climate model (GCM) projections (HIJMANS et al., 2005), from the Intergovernmental Panel on Climate Change (IPCC) Fifth Assessment Report (AR5), BCC-CSM (XIAO-GE; TONG-WEN; JIE, 2013), CCSM4 (YEAGER et al., 2012), HadGEM2-ES (JONES et al., 2011), IPSL-CM5A-LR (SWINGEDOUW et al., 2013), MIROC-ESM (WATANABE et al., 2011), MPI-ESM-LR (GIORGETTA et al., 2013) and MRI-CGCM3 (TATEBE et al., 2012). These RCPs represent increasing projections of global warming from 0.4 to 2.6°C by 2050, with mean range of 1°C (RCP 2.6) and 2°C (RCP 8.5), and radiative forcing of 2.6 and 8.5 W/m<sup>2</sup>, corresponding to atmosphere CO<sub>2</sub> concentration of 450 to 750 ppm/CO<sub>2</sub>eq (CLARKE et al., 2014; EDENHOFER et al., 2014; VAN VUUREN et al., 2011). They reflect trends of CO<sub>2</sub> emissions based on improvements of governance (RCP 2.6) and absence of climate change polices (RCP 8.5).

We based the selection of the variables on their biological relevance and on their scores using a Spearman's rank correlation coefficient threshold of  $|\rho| > 0.7$  (DORMANN et al., 2013). Precipitation variables based on temperature, and temperature variables based on precipitation were also removed. We selected isothermality, temperature seasonality, and maximum temperature of warmest month for temperature; and annual precipitation, wettest month precipitation and driest month precipitation for precipitation. Finally we cropped the environmental variables to the extent of the Neotropics (RAES, 2012).

We corrected the SDMs for geographical sampling bias by employing a target-group background method, producing a background file, based on a bias file according the efforts of collection of Amazonian tree species (GOMES et al., 2018; PHILLIPS; DUDÍK, 2008; TER STEEGE et al., [s.d.]). We used only product, threshold and hinge features of MaxEnt (BOUCHER-LALONDE; MORIN; CURRIE, 2012; MEROW; SMITH; SILANDER, 2013). MaxEnt's logistic output was transformed into binary maps with a 10% training presence threshold, and a convex hull was used around the species records to estimate their EOO.

We then estimated the AOO of the species by restricting the environmental suitability as modelled by MaxEnt to the EOO plus a buffer of 300 km (GOMES et al., 2018; IUCN, 2012; SYFERT et al., 2014). We produced SDM maps for all species, considering all three climate scenarios: "original forest", "2050 RCP 2.6" and "2050 RCP 8.5". For the 2050 scenarios (RCP 2.6 and RCP 8.5) we considered only grid cells predicted by all seven IPCC AR5 GCMs. We then produced three S-SDMs maps by stacking all SDMs maps for each one of the three climate scenario, in order to assess species richness by summing the predicted species in each one of the grid cell (ALGAR et al., 2009; DISTLER et al., 2015).

### 5.2.5 Data analysis

To estimate the impacts of deforestation and climate change on Amazonian tree species we produced ten different scenarios. First, we modelled the species' original environmental suitability. We tested which models were significantly different from random expectation using bias corrected null-models (GOMES et al., 2018; RAES; TER STEEGE, 2007b). Models not significantly different were excluded from further analysis. We then estimated species original AOO for forested grid cells  $F$  and the losses of all deforestation and climate change scenarios over species original estimated AOO, producing ten maps for each of these species (Fig 5.1), starting with the historical deforestation for 2013 (Fig 5.1 B) and two projected deforestation scenarios for 2050 (IGS and BAU) (Fig 5.1 C, D). Then, we estimated the impacts of climate change by 2050 (RCP 2.6 and RCP 8.5) (Fig. 5.1 E, H). Furthermore, we calculated the impacts of four combined scenarios of deforestation and climate change on species original area of occupancy for 2050, one best-case scenario (RCP 2.6 and IGS), two intermediates scenarios (RCP 2.6 and BAU, RCP 8.5 and IGS) and a worst-case scenario (RCP 8.5 and BAU) (Fig. 5.1 F, G, I, J). We also tested if the estimated loss of AOO by deforestation was correlated with population loss as estimated by ter Steege et al. (2015). We then assigned categories of threat for all species according to IUCN A2, A4, B1 and D2 criteria, and three categories: Critically Endangered (CR), Endangered (EN) and Vulnerable (VU), based on geographic range losses, in the form of the estimated AOO, and restricted number of locations. Finally, we analysed the extent of estimated loss of AOO and the decrease in species richness inside and outside of the Amazonian protected area network using the S-SDM maps. All calculations and analyses were performed with R version 3.4.3 (R CORE TEAM, 2018), including the R packages 'raster' version 2.6-7 (HIJMANS, 2017a), 'dismo' version 1.1-4 (HIJMANS et al., 2017b), 'gstat' version 1.1-6 (PEBESMA; HEUVELINK, 2016), 'maptools' version 0.9-2 (BIVAND; LEWIN-KOH, 2017), 'rgdal' version 1.2-16 (BIVAND; KEITT; ROWLINGSON, 2017), 'rgeos' version 0.3-26 (BIVAND; RUNDEL, 2017), 'rJava' version 0.9-9 (URBANEK, 2017) and 'speciesgeocodeR' version 1.0-4 (ZIZKA, 2015).

### 5.2.6 Data availability

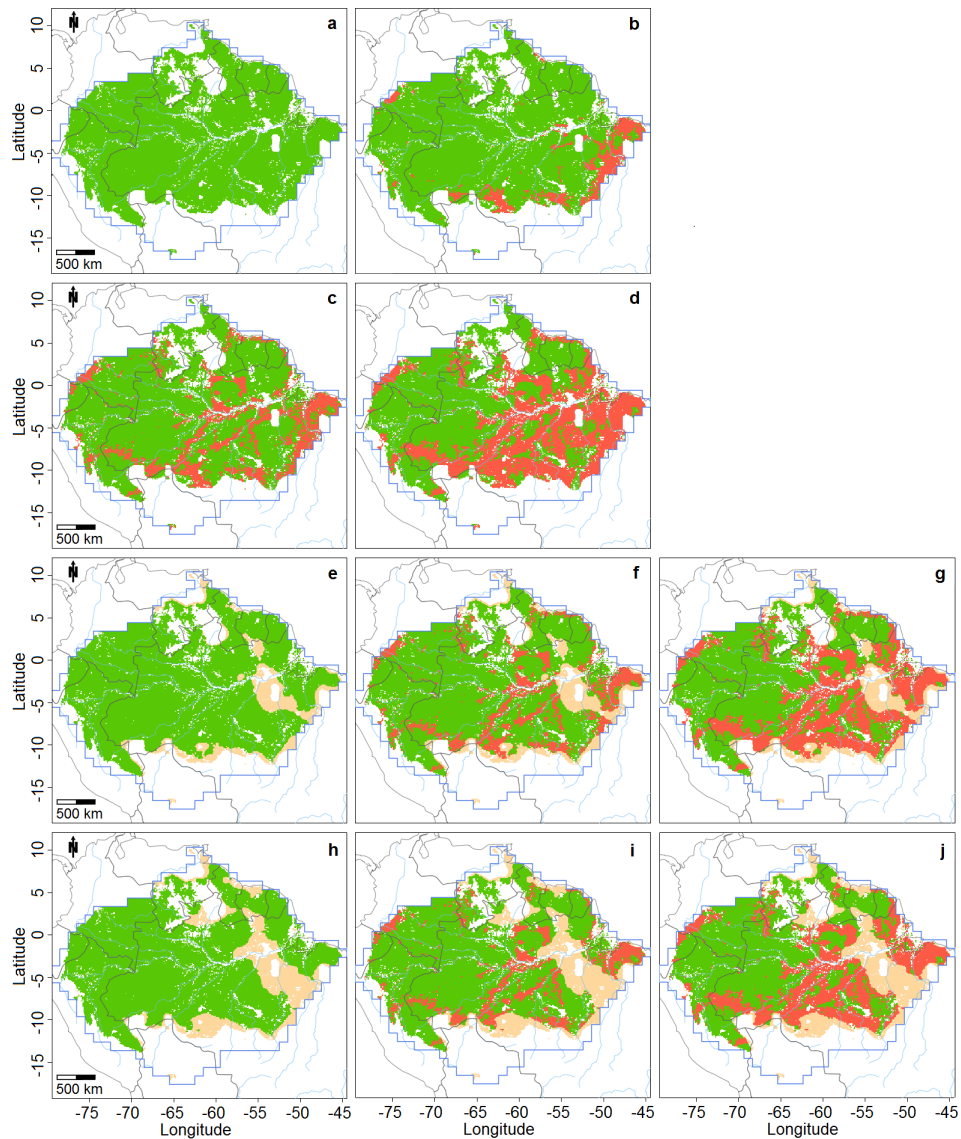
All data used can be freely downloaded from GBIF (<http://www.gbif.org>) and WorldClim (<http://www.worldclim.org>) and are also available from the corresponding author upon request. A full list of species used can be found in Appendix S5.1.

## 5.3 Results

### 5.3.1 Original area of occupancy

Our analysis was conducted for 6,394 Amazonian tree species (62% of the 10,070 species) with available records, after we removed inconsistencies from collection data. Furthermore, species with available records below the minimum (<6), an environmental suitability model non-significantly different from a bias corrected null model, and no estimated AOO within Amazonia were removed (Appendix S5.1). A total of 406 species with restricted EOO (325) and AOO (81) were qualified as threatened according IUCN B1 and D2 criteria (Table 5.1; Appendix S5.1). Further analyses were conducted for 4,935 species (49% of the 10,070, Appendix S5.2), as in the example of *Eschweilera coriacea* (D.C.) S.A. Mori, the most common tree species of Amazonia (TER STEEGE et al., 2013) (Fig. 5.1).

**Figure 5.1.** Loss by global change for *Eschweiler coriacea* (D.C.) S.A. Mori, the most common species in Amazonia15. Beige, Loss in AOO (area of occupancy). a, Original AOO. b, Original AOO and deforestation by 2013. c, Original AOO and 2050 IGS (improved governance deforestation scenario). d, Original AOO and 2050 BAU (business as usual deforestation scenario) (SOARES-FILHO et al., 2006, 2013). e, 2050 RCP 2.6 AOO. f, 2050 RCP 2.6 AOO and 2050 IGS (improved governance deforestation scenario). (G) 2050 RCP 2.6 AOO and 2050 BAU deforestation. h, 2050 RCP 8.5 AOO. i, 2050 RCP 8.5 AOO and 2050 IGS deforestation. j, 2050 RCP 8.5 AOO and 2050 BAU deforestation. Maps created with custom R script. Base map source (country.shp, rivers.shp): ESRI.



Fonte: ESRI (2016); R Core Team (2018).

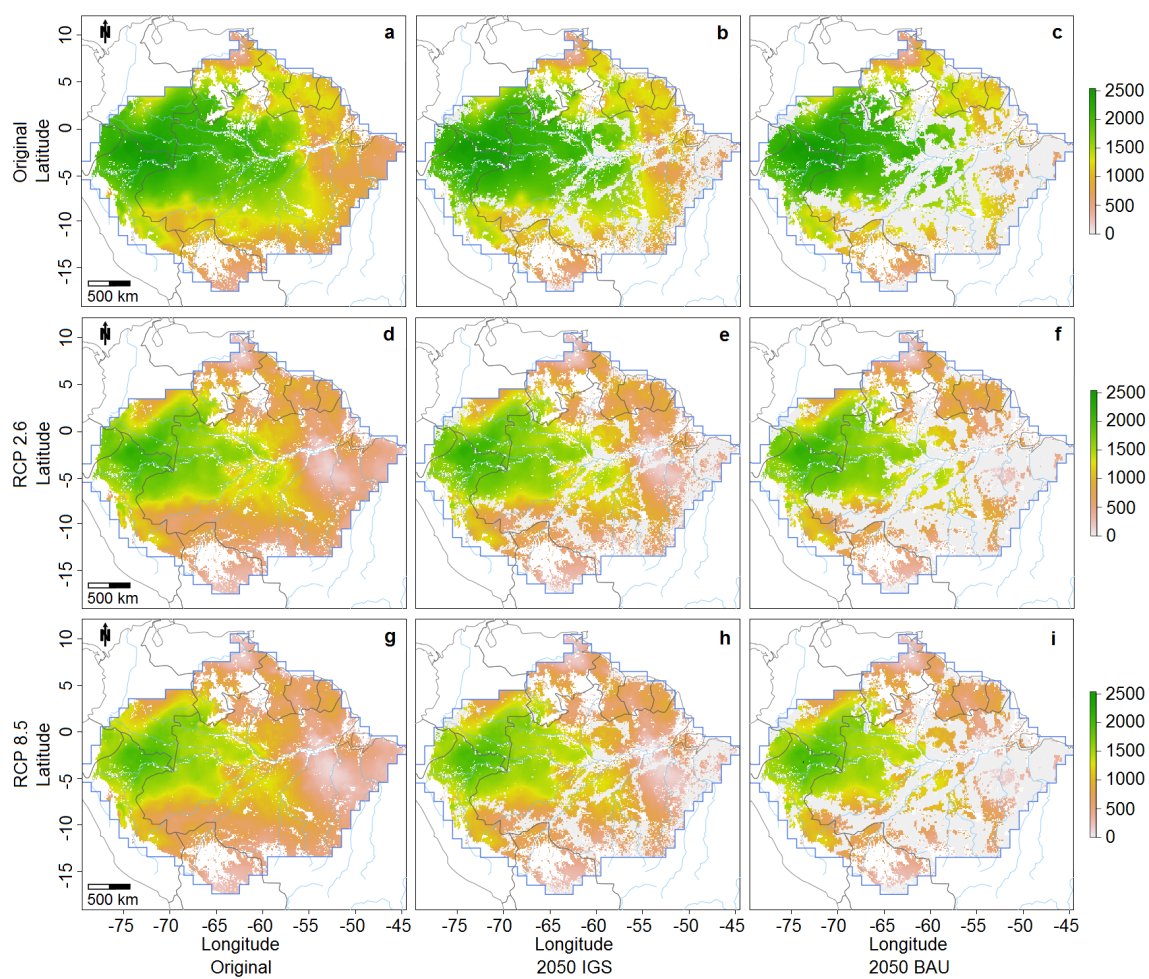
### 5.3.2 Impact of historical forest loss

The historical forest loss of 11% (Fig. S5.2 A) impacted mainly species in southern and eastern Amazonia (Appendix S5.3, S5.4). The forest loss by 2013 was responsible for a mean decline of 7% in the estimated AOO of Amazonian tree species (median = 3%) (Appendix S5.2). A total of 423 (4.2%) species lost a sufficiently large proportion of their original AOO, to be qualified as threatened according to IUCN A2 criterion (Appendix S5.2). Adding the 406 species already listed in the IUCN B1 and D2 criteria a total of 829 (8.2%) can be considered threatened (Table 5.1). Only 133 (1.3%) species had no losses of their original AOO in 2013. Most of the species with no losses were predicted on the Guiana Shield (58%) or in north-western Amazonia (25%), and only 3% of these species were predicted in eastern and southern Amazonia, where species were already greatly impacted by historical deforestation (Appendix S5.2; S5.4). The correlation between the estimated loss of AOO by deforestation with population loss as estimated by ter Steege et al. (2015), throughout Amazonia, was moderate for historical deforestation by 2013 ( $\rho = 0.48$ ) (Fig. S5.5 A; Appendix S5.5).

### 5.3.3 Impact of projected forest loss

The projected deforestation scenarios for 2050, with forest loss of 22% (IGS) and 42% (BAU), resulted in an average loss of AOO of 19% for the IGS scenario and 33% for the BAU scenario (Fig. 5.2 B, C; Appendix S5.2). As the projected deforestation is concentrated in southern and eastern Amazonia, the species were predicted to suffer higher impacts in these regions, with an average loss of estimated AOO of 58% (IGS) and 87% (BAU) (Appendix S5.3). *Tetragastris altissima* (Aubl.) Swart is an example of southern/eastern hyperdominant species which may be greatly impacted by deforestation, with losses reaching up to 50% of its estimated AOO by 2050 (BAU) (Fig. S5.6; Appendix S5.2). By 2050 between 1,802 (18%) to 3,512 (35%) species would lose enough AOO to be threatened according to the IUCN A4 criterion, considering IGS and BAU scenarios, respectively (Table 5.1; Appendix S5.2). A total 22-39% may be considered threatened when adding the IUCN B1 and D2 criteria (Appendix S5.1). The correlation between the estimated loss of AOO by deforestation and the population loss as estimated by ter Steege et al. (2015) was moderate for both the IGS projected deforestation scenario ( $\rho = 0.46$ ) and the BAU projected deforestation ( $\rho = 0.54$ ) (Fig. S5.5 B, C; Appendix S5.5).

**Figure 5.2.** Amazonian species richness (number of species per grid cell) impacted by global change and deforestation. a, Original AOO only. b, Original AOO and 2050 IGS (improved governance deforestation scenario). c, Original AOO and 2050 BAU (business as usual deforestation scenario). d, 2050 RCP 2.6 AOO only. e, 2050 RCP 2.6 AOO combined with 2050 IGS deforestation. f, 2050 RCP 2.6 AOO combined with 2050 BAU deforestation. g, 2050 RCP 8.5 AOO only. h, 2050 RCP 8.5 AOO combined with 2050 IGS deforestation. i, 2050 RCP 8.5 AOO combined with 2050 BAU deforestation. Maps created with custom R script(R CORE TEAM, 2018). Base map source (country.shp, rivers.shp): ESRI.



Fonte: ESRI (2016); R Core Team (2018).

### 5.3.4 Impacts of climate change

The predicted losses caused by climate change were even higher. Climate change will impact Amazonian lowland forest as a whole, increasing the rate of environmental suitability loss and, thus, decreasing species richness throughout all of its extent (Fig. S5.7 D, G; Appendix S5.2, S5.3). For the RCP 2.6 scenario the average loss of AOO by 2050 was 47% and for RCP 8.5 scenario this number was 53% (Appendix S5.2). Northern/central Amazonian species, such as the hyperdominant *Eperua falcata* Aubl. (Fig. S5.6), although far from the “Arc of Deforestation”, may be greatly impacted by climate change in RCP 2.6 and RCP 8.5 scenarios (56-63%). The number of threatened species according to the IUCN A4 criterion was 4,320 (43%) for RCP 2.6 scenario and 4,588 (46%) for RCP 8.5 scenario (Appendix S5.2). Adding the IUCN B1 and D2 criteria (Appendix S5.1), the total species threatened may rise to 4,726 (47%) and 4,994 (50%).

### 5.3.5 Impacts of combined projected deforestation and climate change

The best-case scenario for 2050 (RCP 2.6 and IGS) resulted in an average loss of estimated AOO of 53%, followed by the intermediate scenarios RCP 8.5 and IGS (59%) and RCP 2.6 and BAU (60%), and the worst-case scenario (RCP 8.5 and BAU) with 65% (Table 5.1; Appendix S5.2). Species with a western distribution, such as *Iriartea deltoidea* Ruiz & Pav. (16-22% of AOO loss by 2050), may be less impacted by this interaction (Fig. S5.6; Appendix S5.2; S5.4). The total number of threatened species according to IUCN A4, B1 and D2 criteria (Appendix S5.1) in the best-case scenario was 5,188 (51.5%), followed by RCP 8.5 and IGS with 5,325 (52.2%), RCP 2.6 and BAU with 5,308 (52.4%), and the worst-case scenario with 5,362 (52.8%) (Table 5.1; Appendix S5.2).

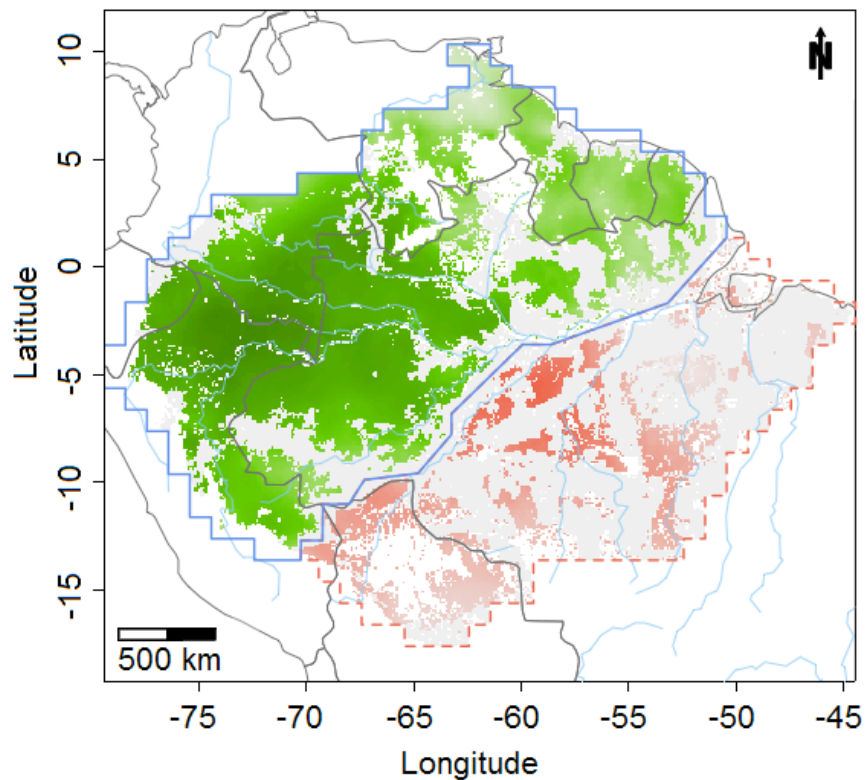
Furthermore, some species may lose their entire estimated AOO, facing a high probability of extinction in Amazonia by 2050 (Appendix S5.2). The number of species with 100% loss of AOO was higher in the combined scenarios which included the BAU deforestation scenario, with 140 (1.4%) species in RCP 2.6 and BAU, and 156 (1.5%) species in RCP 8.5 and BAU. The two other scenarios, including the IGS scenario, resulted in a total number of 113 (1.12%) species for RCP 2.6 and IGS and 130 (1.3%) species for RCP 8.5 and IGS. By 2050 the AOO of all species will be impacted by deforestation and climate change (Appendix S5.2).

### 5.3.6 Impacts on species richness

The mean original species richness (defined as the number of species per grid cell, based on their original estimated AOO) was 1,458, with a median of 1,394 (Fig. 5.2 A; Table 5.1; Appendix S5.3;). The highest species richness values were found in North-western Amazonia (with a total of 3,784 species, and average of 1,896 per grid cell), the Guiana Shield (3,865 total, 1,406 average), and central Amazonia (3,840 total, 1,813 average) (Appendix S5.3, S5.4). Mean original species richness across Amazonia (by grid cell) is expected to decrease between 19% in the IGS scenario to 36% in the BAU scenario, and 30% in RCP 2.6 to 37% in RCP 8.5 (Fig. 5.2 D, G; Appendix S5.3). It also dropped 43%-58% (from best to worst-case scenarios) in the combined scenarios (Table 5.1; Appendix S5.3; Fig. 5.2 E, F, H, I).

The worst-case scenario for 2050 (RCP 8.5 and BAU) showed that Amazonia may be severally impacted, which may divide the original forest into two blocks, one smaller continuous block, with 53% of the original area, and another severely fragmented one (Fig. 5.3). A major part of the continuous block is located in north-western and central Amazonia, and in the Guiana Shield. A smaller part of the continuous block is located in southwestern Amazonia. The other, fragmented block, is located in eastern, southern and a major part of southwestern Amazonia.

**Figure 5.3.** Only half of the Amazonian forest may remain in 2050 (2050 RCP 8.5 AOO combined with 2050 BAU deforestation). Green, a relatively intact Amazonian forest block, composed of north-western and central Amazonia, the Guiana Shield and smaller part of southwestern Amazonia (max number of species per grid cell of 1393, with mean 578). Red, a largely degraded Amazonian forest block composed of eastern, southern and a major part of southwestern Amazonia (max number of species per grid cell of 898, with mean 142). Light grey, forest loss. Map created with custom R script. Base map source (country.shp, rivers.shp): ESRI.



Fonte: ESRI (2016); R Core Team (2018).

### 5.3.7 Protected areas and indigenous territories

The Amazonian network of protected areas and indigenous territories (PAs) had close to 0.9% loss of area of occupancy due to historical forest loss by 2013, covering 54.8% of the remaining forest. In the forest outside the network the loss was 23% (Fig. S5.8 A; Fig. S5.9 A). Mean species richness (by 0.1 grid cells) by 2013 was 1,535 inside, and 1,133 outside the PAs (Table 5.1; Appendix S5.6, S5.7). By 2050 the loss of estimated AOO may vary between 8-28% inside, and 40-60% outside the PAs. Mean species richness (by grid cell) may vary between 639-995 species inside and 438-756 outside the PAs (Fig. S5.8 B, C) in 2050. The forest may have 1.0-1.6 million km<sup>2</sup> of its remaining area outside the network (Fig. S5.9 B, C), including areas with species richness reaching up to 1,986-2,188 species.

**Table 5.1.** Results for all ten scenarios, estimating the losses of AOO, mean species richness, number of species listed in IUCN A2, A4, B1 and D2 criteria, total number of threatened species and percentage of threatened species.

Scenarios	Average loss of AOO (%)	Mean species richness	No. of species listed in IUCN A2/A4 criteria	No. of species listed in IUCN B1/D2 criteria	Total no. of threatened species	% of threatened species	Mean species richness within PA's	Mean species richness outside PA's
<b>Original</b>	0,0	1.458	0	406	406	4,0	1.544	1.353
<b>Original and 2013</b>	7,3	1,353	406		829	8,2	1.535	1.113
<b>Original and IGS</b>	18,7	1.183	1.802		2.208	21.9	1.417	898
<b>Original and BAU</b>	33,2	929	3.512		3.918	38.9	1,158	650
<b>RCP 2.6</b>	46,5	1.013	4.320		4.726	46.9	1.082	929
<b>RCP 8.5</b>	53,4	919	4.588		4.994	49.5	980	844
<b>RCP 2.6 and IGS</b>	52,7	834	4.782		5.188	51.5	995	639
<b>RCP 2.6 and BAU</b>	60,3	672	4.871		5.277	52.4	831	478
<b>RCP 8.5 and IGS</b>	58,8	757	4.854		5.260	52.2	901	583
<b>RCP 8.5 and BAU</b>	65,4	612	4.908		5.314	52.8	756	438

## 5.4 Discussion

The combined losses by deforestation and climate change, suggest that Amazonian tree species may lose 53-65% of their estimated AOO by 2050. This would be enough to qualify 48-49% of all known Amazonian tree species as threatened according IUCN A4 criterion, including almost all (96%) of the hyperdominant species (TER STEEGE et al., 2013). Adding the 425 species with small number of already qualified as threatened under IUCN Criteria B1 and D2, the total proportion increases to 51-53% (Appendix S5.2). There is still a data void in the tropics (FEELEY; SILMAN, 2010) and the number of new species of flowering plants is still expected to increase by 10-50% in Brazilian Amazonia alone (PIMM et al., 2010). Considering the limitation of our analyses for rare and as yet unknown species the estimates of the number of species qualified as threatened are likely higher than we report here.

Our analyses were based on 49% of all known Amazonian tree species. However, this should not affect species richness patterns. We omitted only those species that were either too rare or did not have enough available records to produce significant models. Major ecological patterns are likely to be maintained, since the most common species generally define large-scale patterns, and rare species are often too restricted to affect it (POS et al., 2014). Furthermore, rare species and species with low prevalence are likely to be over-predicted, compromising model accuracy and the reliability of the stacked SDMs (S-SDMs) (VAN PROOSDIJ et al., 2015).

We used S-SDMs to estimate species richness, which tends to over-predicted by such models, since they model environmental suitability, rather than the species' real range (CALABRESE et al., 2014). We believe that over-prediction effects were reduced by our SDMs, based on a conservative estimate of an environmental suitability model (area slightly larger than species EOO, compatible with e.g. the IUCN red list assessments, Fig. S5.1). S-SDMs may also reduce species richness accuracy affected by elevation (POUTEAU et al., 2015). As we only modelled Amazonian lowland forest, and areas above 500 m of elevation were removed, this will not have greatly affected our results.

These high elevation areas could represent an alternative for species tracking colder temperatures in a global warming future (COLWELL; LEES, 2000), but they probably could not establish viable population in time, since it takes a few thousand years for species to move hundreds of kilometres (MAYLE; BURBRIDGE; KILLEEN, 2000), and on top of that deforestation has created migration barriers and will create others (FEELEY; REHM, 2012).

Deforestation is also expected to reduce populations of Amazonian tree species in the future (TER STEEGE et al., 2015). We found deforestation to be responsible for a decline of 7% of the estimated AOO of the Amazonian tree species, considering the historical deforestation until 2013, and this may potentially reach 19-33% by 2050, considering our projected deforestation analyses. We compared our results of the estimated loss of AOO against estimated population loss as estimated by ter Steege et al. (2015). The correlations for historical deforestation by 2013 and IGS projected deforestation scenario by 2050 were moderate. For 2050 projections of the BAU scenario, the correlation was slightly higher. Although the correlations are mostly moderate, both estimates may be realistic. Area changes will occur first in the edges of the range, where the population densities are likely lowest, decoupling the two measures to some extent.

Despite that, the losses produced by climate change are expected to be even higher. According to our climate change mitigation scenario (RCP 2.6) mean species richness may be reduced by almost one-third (30%) and estimated AOO may drop almost by half (47%) by 2050. This scenario limits global warming below 2° C (STOCKER, 2014). Our business-as-usual climate change scenario (RCP 8.5) scenario shows higher emissions trends, close to those observed since 2000 (PETERS et al., 2012), and will drive the forest in more extreme climate conditions (DIFFENBAUGH; FIELD, 2013), which is expected to raise tree mortalities by drought and severe heat (ESQUIVEL-MUELBERT et al., 2016; NEPSTAD et al., 2007). According this scenario estimated AOO loss may increase to 53% and mean species richness losses may reach 37%.

The interaction between deforestation and climate change may be the greatest threat to Amazonian biodiversity (NEPSTAD et al., 2008), especially for trees (BRODIE; POST; LAURANCE, 2012). Southwestern, southern, and eastern Amazonia are the regions likely to be most affected by the synergetic impacts of deforestation and climate change. Eastern Amazonia alone may suffer up to 95% of forest loss by 2050, followed by southwestern (81%). and southern Amazonia (78%) (Appendix S5.4).

Adding the influence of fire to the synergy of deforestation and climate change, a 20-25% deforestation is already expected to be the tipping point for these regions to no longer support rain forest ecosystems (LOVEJOY; NOBRE, 2018), especially in eastern and southern Amazonia. By 2007 and 2010 southern/eastern Amazonia lost already 12% and 5% of its forests by regional fire during severe drought events (BRANDO et al., 2014). Furthermore, deforestation has also influenced regional climate in Amazonia (SILVÉRIO et al., 2015) by affecting the balance and water cycle in southern/eastern Amazonia due to land uses that follows deforestation, such as, agricultural expansion.

The interaction between deforestation and climate change, for the best-case combined scenario for 2050 (RCP 2.6 and IGS) shows only a small reduction in the total number of threatened species. It makes a difference in the level of threat, however, as the number of species listed as “critically endangered” (CR) drops from 22% in our worst-case combined scenario (RCP 8.5 and BAU) to 11% in the best-case combined scenario. The worst-case combined scenario for 2050 (RCP 8.5 and BAU) shows what may called “a half Amazonia” by 2050. (Fig. 5.3). The severe fragmentation outside this block will add to species loss (TAUBERT et al., 2018), and will provoke alterations in tree-community composition (LAURANCE et al., 2006). Big tree species, for instance, are largely impacted by fragmentation due to influences of wind turbulence, desiccation and infestation by lianas, common effects observed near forest edges (LAURANCE et al., 2000). Those species strongly influence forest structure, composition, hydrology, contributing also importantly to carbon storage (CLARK; CLARK, 1996; FELDPAUSCH et al., 2005; LINDENMAYER; LAURANCE; FRANKLIN, 2012).

Our analyses show that big hyperdominant tree species, such as *Bertholletia excelsa* Bonpl. and *Mezilaurus itauba* (Meisn.) Taub. ex Mez will be threatened in 2050 according to the worst-case scenario. Small forest fragments will also lose species and biomass quickly due to overhunting, decreasing populations of large bodied animals (BICKNELL; PERES, 2010), further reducing species richness for trees depending on these species for their dispersal (BELLO et al., 2015). High intensity events, such as droughts, will impact Amazonia in the future, with fires reaching deeper into the drier forests (DAVIDSON et al., 2012; LONGO et al., 2018).

Although the impacts in some Amazonian countries such as Guyana (MACDICKEN et al., 2016), may be lower and deforestation rates have declined compared to projected deforestation scenarios (STEEGE et al., 2015), the worst case scenario cannot be discarded given the recent rising deforestation trends in Brazil (FEARNSIDE, 2017). Brazil joined the Paris agreement in 2015, and pledges to cut its greenhouse gas emissions by 37%, reach zero deforestation, and reforest 12 million ha by 2030 (TOLLEFSON, 2015b). However, the country still suffers with high deforestation rates (MOUTINHO; GUERRA; AZEVEDO-RAMOS, 2016), and a future reduction of this trend remains uncertain (TOLLEFSON, 2015a). Deforestation has increased during the past five years at a rate of ~7,000 km<sup>2</sup> per year (INPE, 2018). Furthermore, international negotiations on limiting global warming have failed (CHRISTOPHER, 2017) and recent Brazilian law changes may severely limit scientific research, including the monitoring of forest and biodiversity loss (BOCKMANN et al., 2018).

Other Amazonian countries, such as Colombia, showed a recent increase of fires in protected areas after demobilization of the guerrilla (ARMENTERAS; SCHNEIDER; DÁVALOS, 2018). Studies have pointed out positive correlations between and coca cultivation(DÁVALOS, 2018) and guerrilla activities within protected areas (HANAUER; CANAVIRE BACARREZA, 2018) and reductions in deforestation in Colombia and Peru. Protected areas have protected tree populations from deforestation all over Amazonia till now (TER STEEGE et al., 2015).

The protected areas network shows an important inhibitory effect on the deforestation of Amazonian forest in Brazil (SOARES-FILHO et al., 2010). Protected areas are also effective in preventing deforestation fires - fewer of these fires occur within protected areas compared to areas on the outside (ADENEY; CHRISTENSEN; PIMM, 2009). Those areas are not immune to the impacts of climate change, however, and the absence of protected corridors may isolate species from suitable areas under different future climate conditions (FEELEY; SILMAN, 2016).

We found that inside the PA network mean species richness may drop to 639 species per grid cell and total habitat loss may reach 28%. Even though, protected areas may provide benefits for biodiversity (GRAY et al., 2016), especially when they focus on governance quality and planning methods (WATSON et al., 2014). We found even worse results for the areas outside the network, with mean species richness dropping down to 438 species per grid cell and total habitat loss reaching up to 60%. Amazonia may have around 50% of its forest outside the network, mostly in central and north-western Amazonia. This unprotected half of the remaining forest has grid cells with a high predicted number of species, with great relevance for biodiversity conservation and establishment of new PAs.

## **5.5 Conclusion**

Tropical forests have a major environmental roles by stabilizing atmospheric CO<sub>2</sub> (HOUGHTON; BYERS; NASSIKAS, 2015), regulating climate (BONAN, 2008) and maintenance of biodiversity (GIBSON et al., 2011). Tropical forests also provide benefits to the society (ecosystems services), and their losses generally are not compensated by the development of other sectors, such as, manufacturing and services, leading to unsustainable development pathways (CARRASCO et al., 2017). The true losses behind their degradation may be immeasurable. Biologists have warned for more than one century about the possible demise of the Atlantic forest (DEAN, 1997), and yet, only 12% of its original cover remains (RIBEIRO et al., 2009). We must try to avoid that Amazonia will suffer the same fate.

## CAPÍTULO 6 SÍNTESE

Esta tese aborda um dos maiores desafios ambientais atuais: os impactos das globais sobre a biodiversidade amazônica. Entender como estas mudanças afetam as florestas tropicais significa investigar como a diversidade tropical foi influenciada a partir de sua interação com tais mudanças ao longo do tempo. Esta tese objetivou investigar os impactos das mudanças climáticas e do desflorestamento sobre as espécies arbóreas amazônicas em condições passadas, presentes e futuros. Em condições passadas, foram investigadas mudanças ocorridas entre condições climáticas passadas (mais secas) e presentes (mais úmidas) durante o Holoceno médio e o Holoceno tardio (último 6.000 anos), quando, uma evidenciada expansão ocorreu ao sul da floresta amazônica. Foram também investigados os impactos do desflorestamento histórico sobre a floresta amazônica (até o ano de 2013). Em condições presentes, foram testados métodos de estimação de riqueza e distribuição de espécies arbóreas amazônicas, para definição de boas práticas em uma área tão grande e biodiversa quanto a Amazônia. Além disso foram investigados os padrões de riqueza e distribuição das espécies arbóreas amazônicas hiperdominantes no presente, onde foi também investigada a relação entre as coleções de história natural das espécies com suas abundâncias relativas. Em condições futuras, utilizando projeções para o ano de 2050, foram investigados os impactos das mudanças climáticas e do desflorestamento sobre todas as espécies arbóreas conhecidas da Amazônia. Este capítulo apresenta as principais conclusões da investigação, e uma discussão geral sobre a pesquisa proposta por esta tese. O capítulo conclui destacando a perspectiva para futuros esforços sobre a investigação da conservação da biodiversidade amazônica.

## 6.1 Principais conclusões

- Estimadores de riqueza de espécies não-paramétricos não são adequados para florestas tropicais. Estes métodos de estimativa subestimam a riqueza de espécies em tais áreas. Florestas tropicais, incluindo a floresta amazônica, são paisagens heterogêneas, onde a intensidade amostral é usualmente baixa e a riqueza de espécies é alta. As premissas destes métodos (amostragem com reposição e esforço amostral relativamente alto) não são encontradas nos esforços de coleta utilizados pela maioria dos estudos. A série logarítmica, apesar de também necessitar de um esforço amostral significativo, é muito mais eficiente na estimativa da riqueza de espécies em florestas tropicais que os estimadores não-paramétricos mais comumente utilizados, suas premissas têm melhor adequação à forma como os dados de campo são coletados.
- Os registros de ocorrências de espécies em coleções de história natural (*natural history collections* – NHCs) utilizadas pelos modelos de distribuição de espécies (*species distribution models* – SDMs) que usam dados de presença, tal como o MaxEnt, foram apenas pouco correlacionadas com a abundância relativa da maioria das espécies arbóreas hiperdominantes amazônicas, tal como estimada pela ponderação da distância inversa (*inverse distance weighting* – IDW). Para um terço das espécies a correlação foi negativa ou inexistente, e para dois terços a correlação foi positiva, mas muito fraca, o que viola a principal premissa do MaxEnt, na qual os locais de coleta são independentemente compostos pela probabilidade de distribuição das espécies, que deve ser desconhecida. Isto implica que uma maior abundância local aumenta de maneira muito baixa a chance das espécies hiperdominantes em serem coletadas, e para alguma destas a abundância não apresenta relação com a chance das espécies serem coletadas. Apesar disso, MaxEnt e IDW foram igualmente efetivos em prever a presença de espécies tal como definida um pelo outro, e consequentemente, a sensibilidade de ambos os métodos foi alta (aproximadamente 90% para ambos). Além disso, um processo de limpeza proposto demonstrou que metade de todas os registros de ocorrência das NHCs obtidas por meio de bases de dados *on-line* são provavelmente inconsistências, com informações geográficas ausentes, tais como latitude, longitude e localidade.

- Mudanças climáticas de longa duração influenciaram a Amazônia durante os Holocenos médio e tardio (6000 anos atrás), por meio do aumento da precipitação. Esta influência é apoiada por registros fósseis de pólen obtidos em núcleos de sedimentos retirados de lagos amazônicos. A aptidão ambiental aumentou para espécies arbóreas das famílias Moraceae e Urticaceae durante este período, e a riqueza de espécies modelada destas famílias apresentou um incremento médio, em uma escala espacial de 0,5 grau, de 132%. O incremento na aptidão ambiental foi mais alto na porção sul da Amazônia, corroborando com a sugerida expansão da floresta durante o período. A abundância total das famílias Moraceae e Urticaceae se correlacionou de forma significativa com os registros de pólen ( $R^2 = 0,54$ ), sugerindo que estes registros são relativamente bons representantes para a abundância das árvores, e que a abundância destas famílias também foi incrementada durante os Holocenos médio e tardio em algumas áreas. Mudanças no clima mais seco do médio Holoceno contribuíram para o aumento da aptidão ambiental de provavelmente várias famílias de árvores na Amazônia, e conseqüentemente, para mudanças em suas distribuições, o que pode ter contribuído também para a expansão da floresta durante os Holocenos médio e tardio.
- A Amazônia já perdeu cerca de 12% de sua cobertura florestal pelo impacto do desflorestamento. O desflorestamento tem sido e continuará sendo uma grande fonte de impacto sobre o tamanho das populações de espécies arbóreas na Amazônia, mas as mudanças climáticas podem superá-lo no futuro. O desflorestamento pode causar entre 19% e 36% de declínio na riqueza de espécies até o ano de 2050, enquanto que as mudanças climáticas podem causar um declínio entre 31% e 37%. Seus impactos combinados podem causar um declínio de até 58%. As espécies podem perder uma média de 66% das áreas para as quais estão adaptadas, e um total de 53% das espécies podem estar ameaçadas de extinção segundo os critérios da lista vermelha da União Internacional para Conservação da Natureza (do inglês, *International Union for Conservation of Nature – IUCN*). A rede de áreas protegidas da Amazônia pode mitigar os impactos das mudanças globais, apesar de aproximadamente 50% da floresta se encontrar fora da rede. No pior cenário projetado, a floresta amazônica pode ser dividida pela metade até 2050, em um bloco contínuo formado pelas porções central e oeste do bioma, e um outro bloco severamente fragmentado formado pelas porções ao leste e ao sul.

## 6.2 Discussão geral

### 6.2.1 Estimativa da distribuição e da riqueza de espécies arbóreas na Amazônia

A estimativa da riqueza de espécies é uma das análises mais utilizadas para investigar a diversidade de espécies. Nesta tese, a estimativa de riqueza de espécies foi investigada por meio da comparação de métodos baseados em dados de abundância, utilizando estimadores não-paramétricos e paramétricos. Um dos achados mais importantes desta investigação foi que, apesar do fato de estimadores não-paramétricos serem os métodos mais comumente utilizados para prever a riqueza de espécies (CHAO et al., 2009; CHIARUCCI et al., 2003), eles subestimam a riqueza severamente na Amazônia, pois estes métodos requerem alta intensidade amostral (WANG; LINDSAY, 2005), um requisito que não pode ser encontrado em uma área tão grande, heterogênea, rica em espécies, e que também é subamostrada. Estimadores paramétricos foram muito eficientes em estimar a riqueza de espécies. A estrutura dos dados de campo de árvores tropicais conformam-se à série logarítmica (FISHER; CORBET; WILLIAMS, 1943), um estimador paramétrico, que se ajusta à distribuição de abundância (IZSÁK; PAVOINE, 2012; XU et al., 2012), como apresentado por vários estudos (BALDRIDGE et al., 2016; BRANCO; FIGUEIRAS; CERMEÑO, 2018; HUBBELL, 2001).

Os dados de abundância podem também ser utilizados para modelar a distribuição de espécies (TER STEEGE et al., 2013), e nesta tese foi comparada a distribuição de espécies baseada em abundância, por meio do inverso da potência das distâncias (*inverse distance weighting* – IDW) com a distribuição de espécies baseada em aptidão ambiental (MaxEnt). Foi observado que as coleções de história natural (*natural history collections* – NHCs) utilizadas pelo MaxEnt não apresentaram fortes relações com a abundância local das espécies arbóreas amazônicas hiperdominantes, que representam metade dos indivíduos de árvores nas florestas tropicais da Amazônia, mas compreendem apenas 1,4% de sua diversidade de árvores. Isto pode limitar a validade dos modelos que utilizam apenas dados de presença em prever a probabilidade de ocorrência das espécies.

NHCs superestimam as espécies raras enquanto subestimam as espécies comuns, pois os coletores de espécies são eficientes em coletar o maior número possível de espécies (TER STEEGE et al., 2010). Os coletores tendem a focar em espécies raras, e negligenciam espécies comuns, e assim, NHCs falham em representar bem a abundância local. Além disso, as coleções de espécies podem ser enviesadas contra ou a favor de grupos taxonômicos específicos. Este foi o caso para a excessiva representação de espécies de palmeiras nas NHCs obtidas do grande número de registros da base de dados de transecções de palmeiras da Universidade Aarhus no oeste da Amazônia, o que enviesou a distribuição de palmeiras modeladas pelo MaxEnt à Amazônia Ocidental.

Em contraste à forma que as NHCs são coletadas, os dados de parcelas utilizados pela interpolação da IDW, são uma representação da amostragem total das espécies dentro das parcelas, onde os esforços de coleta cobrem todos os indivíduos, independentemente de sua raridade. Assim, os dados de parcelas podem ser vistos e utilizados como uma representação da densidade de distribuição de espécies. No entanto, os dados de parcela também têm limitações, e esse foi, por exemplo, o caso de espécies de matas ciliares, tais como, *Macrolobium acaciifolium* (Benth.) Benth. Esta espécie hiperdominante está subrepresentada dentro das parcelas, porque as parcelas são, em sua maioria, implantadas longe das margens dos rios, e a distribuição das espécies, tal como predita pelo modelo da IDW, falhou em prover uma boa representação da distribuição desta espécie.

Um outro importante achado relacionado às NHCs veio do processo de limpeza conduzido em nossos dados. Existem muitas inconsistências na considerável quantidade de informações de espécies disponíveis em plataformas on-line por conta da falta de processo de limpeza (MALDONADO et al., 2015), que podem criar divergências na aptidão ambiental, tal como estimada pelo MaxEnt. O procedimento de limpeza desenvolvido surpreendentemente removeu metade de todos os registros NHCs, considerando-os como inconsistências. Estas inconsistências são, em sua maioria, geográficas, incluindo informações ausentes das coordenadas, tais como, latitude, longitude, localidade ou valores duplicados, além de coordenadas baseadas em centroides de cidade, estados ou países (ZIZKA; ANTONELLI, 2015).

Além disso, foram também removidos *outliers* espaciais, por meio de uma estimativa de densidade de *kernel*, omitindo coordenadas muito afastadas da porção central da distribuição das espécies, assumindo que estas coordenadas são prováveis erros de identificação. Além disso, o procedimento restringiu a distribuição das espécies modelada pelo MaxEnt à área de ocupação das espécies (*area of occupancy* – AOO), que é definida como a distribuição potencial da espécie, restringida à sua extensão de ocorrência (*extent of occupancy* – EOO), mais uma faixa de área de 300 km. Esta abordagem também lidou com uma desvantagem bem conhecida do MaxEnt, na qual a distribuição das espécies é superestimada para além da EOO conhecida (FITZPATRICK; GOTELLI; ELLISON, 2013).

A AOO estimada pelo procedimento de limpeza apresentou uma alta “sensibilidade” (proporção de presenças conhecidas corretamente preditas pela distribuição modelada) aos dados das parcelas, saindo-se muito bem em prever a distribuição das espécies em áreas com presença dados de presença em parcelas de inventários florestais (PEARSON, 2010). A distribuição das espécies tal como predito pela IDW também apresentou alta “sensibilidade” em prever as NHCs. Portanto, apesar da violação da principal premissa do MaxEnt, na qual as coleções constituídas aleatoriamente da distribuição da densidade hipotética de uma espécie, o procedimento de limpeza conservador, utilizando o MaxEnt, apresentou boa performance na modelagem de distribuições das espécies.

#### 6.2.2 A influência do clima sobre a riqueza e a distribuição de espécies durante o Holoceno

A floresta Amazônica abriga potencialmente 16.000 espécies de árvores (TER STEEGE et al., 2013), e toda essa diversidade foi moldada por processos geológicos e climáticos ao longo de sua história (HOORN et al., 2010). Nos últimos três milênios, a floresta expandiu-se para o sul pelo aumento da precipitação entre um Holoceno médio mais seco e um Holoceno tardio mais úmido, evento evidenciado por registros fósseis de pólen de árvores amazônicas (BURBRIDGE; MAYLE; KILLEEN, 2004; MAYLE; BURBRIDGE; KILLEEN, 2000).

No Capítulo 4, foi modelada a aptidão ambiental de espécies arbóreas de Moraceae e Urticaceae durante o Holoceno (cerca de 6 mil anos atrás) em toda a Amazônia para testar a influência das mudanças climáticas de longo prazo sobre a aptidão ambiental das espécies da floresta tropical. Observou-se que durante o Holoceno médio e tardio, a aptidão ambiental média para Moraceae e Urticaceae aumentou na Amazônia. Esse aumento foi especialmente alto no limite de ecótono entre a floresta ao sul da Amazônia e as savanas do Cerrado. Um achado importante foi que os registros de pólen de Moraceae e Urticaceae são uma boa representação para sua abundância relativa destas famílias em toda a Amazônia. A riqueza de espécies locais também aumentou durante o período. Foi encontrado um aumento médio de 132% na riqueza de espécies predita em toda a Amazônia. A riqueza atual de espécies para estas duas famílias é maior na Amazônia ocidental e central, regiões conhecidas pela alta diversidade de espécies de árvores (STEEGE et al., 2003).

Na análise da riqueza de espécies, incluindo todas as espécies de árvores amazônicas desenvolvida no capítulo 5, também foi observada maior diversidade na Amazônia ocidental e central. Os padrões de diversidade mais elevados observados nessa área têm sido atribuídos às condições climáticas relativamente estáveis desde o último máximo glacial (CHENG et al., 2013). Esta área apresentou baixa variação na riqueza de espécies e aptidão ambiental durante o Holoceno médio e tardio, o que contrastou com as variações observadas na parte sul da Amazônia. As variações observadas na parte sul da Amazônia foram maiores, e possivelmente causadas pelo aumento da aptidão ambiental (LATRUBESSE; RAMONELL, 1994; MARTIN et al., 1997).

A baixa diversidade de Moraceae e Urticaceae encontrada na parte sul da Amazônia, especialmente nas florestas tropicais nos ecótonos na Bolívia e no Brasil, pode indicar que essas áreas ainda estão em processo de sucessão, acumulando espécies de rápida dispersão e altas taxas de crescimento, como Moraceae e Urticaceae, também corroborando com a expansão florestal sugerida nos últimos milênios.

O estabelecimento de conexões sobre como as condições climáticas influenciaram a expansão florestal nos últimos milênios, afetando a diversidade e distribuição de espécies de árvores, inspirou o questionamento das possíveis influências das mudanças globais atuais e futuras sobre a floresta amazônica, particularmente considerando possíveis condições mais secas no futuro.

### 6.2.3 Os impactos das mudanças globais sobre a floresta Amazônica

Atualmente, a Amazônia está enfrentando ameaças de mudanças globais. O maior bloco de floresta tropical do planeta sofre com o aumento das mudanças climáticas e do desflorestamento, chegando perto de um ponto de onde pode não haver retorno (LOVEJOY; NOBRE, 2018). As mudanças globais podem afetar diretamente a biodiversidade, uma vez que afeta o habitat natural das espécies, que é consistentemente relacionado com a distribuição de espécies (ELITH; LEATHWICK, 2009). Mudanças no habitat das espécies podem promover mudanças nos padrões de distribuição das espécies se elas forem capazes de se dispersar.

Avaliar os impactos das mudanças globais é um desafio, porque a Amazônia ainda é pouco conhecida. Embora a modelagem seja possível para muitas espécies, ainda se tem poucos dados para a maioria das espécies amazônicas, mesmo para as mais comuns. O “grande vazio de dados” referido por Feeley e Silman (2010) está longe de ser resolvido. Mesmo na Amazônia, não existem mais que 10 coletas/100Km<sup>2</sup> (TER STEEGE et al., 2016). Além disso, espécies coletadas e depositadas em NHCs em todo o mundo sofrem com erros de identificação, que dificultam a compilação de novas listas de espécies (GOODWIN et al., 2015). As listas mais recentes de espécies arbóreas da Amazônia discordam em relação ao número total de espécies amazônicas já descritas, variando entre 6.727 e 11.676 (CARDOSO et al., 2017; TER STEEGE et al., 2016).

Com base na lista de espécies mais recente (TER STEEGE et al., submetido) foram avaliados os impactos das mudanças globais sobre a floresta amazônica, quantificando os impactos das mudanças climáticas e do desflorestamento, separados e combinados, sobre todas as espécies de árvores amazônicas compiladas. Esta análise sugeriu que a perda histórica de áreas florestadas reduziu em média 7% da AOO estimada das espécies arbóreas da Amazônia até 2013.

Foi encontrado que 425 espécies perderam uma proporção tão grande de sua AOO original, que podem ser qualificadas como ameaçadas de extinção de acordo com os critérios A2 e B2 da IUCN (Capítulo 5). O desflorestamento é considerado uma das principais fontes de ameaça para as espécies arbóreas da Amazônia no presente. No entanto, as mudanças climáticas podem ser potencialmente mais ameaçadoras. Com dois cenários diferentes (“governança”, otimista; e “condições usuais”, pessimista), as espécies arbóreas da Amazônia podem ter uma perda média de AOO entre 19-33% até 2050, enquanto a análise das mudanças climáticas, baseada em duas “vias representativas” (*representative pathways* – RCP) de mudanças climáticas (RCP 2.6 - otimista; e RCP 8.5 - pessimista) mostrou uma perda média de AOO entre 47-54%. Segundo os critérios da IUCN, isto representa uma ameaça para 22-39% das espécies de árvores, quando considerados os impactos do desflorestamento, e entre 47-50%, quando considerados os impactos das mudanças climáticas. Quando ambas as fontes de ameaça são combinadas, a perda total de AOO é projetada para atingir valores entre 53-65%, enquanto a riqueza de espécies pode diminuir em média entre 43-58%.

Estes cenários combinados mostraram que um total entre 56-58% das espécies de árvores amazônicas podem enfrentar ameaças de extinção até 2050, com base nos critérios da IUCN. Este resultado é bastante alarmante, mostrando que com base nos cenários combinados, mais da metade da flora arbórea da Amazônia pode enfrentar ameaças de extinção em aproximadamente trinta anos. Mesmo considerando o cenário “melhor caso” (*best-case*), a Amazônia ainda pode estar sofrendo perdas severas de riqueza e distribuição. No cenário “pior caso” (“*worst-case*”), a floresta Amazônica pode ser reduzida a cerca de 50% de sua área original, ou “metade da Amazônia”. Este cenário segue a linha de base “condições usuais” para o desflorestamento e a ausência de mitigação das mudanças climáticas, assumindo que não haverá melhoria na governança até 2050 (MARKANDYA; HALSNAES, 2000; SOARES-FILHO et al., 2006).

Apesar do fato de que, na verdade, as pressões das mudanças globais podem ter sido reduzidas, mesmo em comparação ao cenário de melhoria de governança (TER STEEGE et al., 2015), um cenário “pior caso” não pode ser descartado, dado o recente aumento das tendências de desflorestamento no Brasil (que detém o maior pedaço da floresta amazônica), que seguiu os fracassos das agendas internacionais em relação à limitação do aquecimento global, o enfraquecimento da capacidade de governança nos trópicos (BARLOW et al., 2018; CHRISTOPHER, 2017; FEARNSIDE, 2017). Este eventos adicionam incertezas à conquista de um cenário de melhoria da governança no futuro (TOLLEFSON, 2018). Além disso, a possibilidade de redução das áreas de reservas legal para proteção da natureza na Amazônia brasileira, está na mesa para o debate, o que pode potencialmente aumentar o desflorestamento legal na região (FREITAS et al., 2018).

Essas expectativas sobre a governança futura na Amazônia não são muito encorajadoras para a conservação de sua biodiversidade. O potencial de degradação da Amazônia é enorme, e a redução do desflorestamento é urgente, o que pode contribuir positivamente para a redução de emissões de CO<sub>2</sub> e para a mitigação das mudanças climáticas. Esta tese mostrou que as mudanças globais moldaram a floresta Amazônica em processos de longa duração no passado, e também mostrou que as mudanças projetadas para o futuro da floresta Amazônica podem moldá-la de maneira bastante diferente, afetando a riqueza e a distribuição de mais da metade de todas as espécies de árvores.

### 6.3 Perspectiva futura

Nesta seção será destacada a perspectiva para futuros esforços sobre a investigação da conservação da biodiversidade amazônica. Ao abordar os impactos das mudanças globais nas espécies arbóreas da Amazônia em diferentes escalas temporais, esta tese contribuiu para uma melhor compreensão dos padrões que vêm moldando a floresta tropical amazônica ao longo do tempo. No entanto, o futuro da floresta depende da governança implementada a forma como a agenda política será construída no futuro é bastante imprevisível. Ainda assim, as projeções climáticas futuras utilizadas nesta tese avaliam mudanças globais para o ano de 2050 (meados do século 21). Estratégias de conservação baseadas em uma perspectiva política tão longa (cerca de trinta anos) podem ser impactadas pelas renovações políticas promovidas pela eleição de novas lideranças em todo o mundo, especialmente nos países Amazônicos, onde as agendas de conservação ambiental e apoio à ciência podem sofrer impactos diretos (BARBUY, 2018; ESCOBAR, 2018; FEARNSIDE, 2016; KEMP, 2017; REARDON, 2018). Aprofundar o entendimento sobre os impactos das mudanças globais na Amazônia com base em termos mais curtos pode fornecer metas mais tangíveis, e ser mais adequado aos modelos de governança atual.

## REFERÊNCIAS

- ABSY, M. L. *et al.* Mise en évidence de quatre phases d'ouverture de la forêt dense dans le Sud-Est de l'Amazonie au cours des 60 000 dernières années: première comparaison avec d'autres régions tropicales. **Comptes rendus de l'académie des sciences. Série 2: Mécanique**, v. 312, n. 6, p. 673–678, 1991.
- ADENEY, J. M.; CHRISTENSEN, N. L.; PIMM, S. L. Reserves protect against deforestation fires in the Amazon. **PLoS ONE**, v. 4, n. 4, p. e5014, 2009.
- AGUIRRE-GUTIÉRREZ, J. *et al.* Fit-for-purpose: species distribution model performance depends on evaluation criteria – Dutch hoverflies as a case study. **PLoS ONE**, v. 8, n. 5, p. e63708, 14 maio 2013.
- ALGAR, A. C. *et al.* Predicting the future of species diversity: macroecological theory, climate change, and direct tests of alternative forecasting methods. **Ecography**, v. 32, n. 1, p. 22–33, 2009.
- ANDERSON, R. P.; MARTÍNEZ-MEYER, E. Modeling species' geographic distributions for preliminary conservation assessments: an implementation with the spiny pocket mice (*Heteromys*) of Ecuador. **Biological Conservation**, v. 116, n. 2, p. 167–179, 2004.
- ARAÚJO, M. B.; NEW, M. Ensemble forecasting of species distributions. **Trends in Ecology and Evolution**, v. 22, n. 1, p. 42–47, 2007.
- ARAÚJO, M. B.; PETERSON, A. T. Uses and misuses of bioclimatic envelope modeling. **Ecology**, v. 93, n. 7, p. 1527–1539, jul. 2012.
- ARMENTERAS, D.; SCHNEIDER, L.; DÁVALOS, L. M. Fires in protected areas reveal unforeseen costs of Colombian peace. **Nature ecology & evolution**, p. 1, 2018.
- ASPINALL, R. J.; LEES, B. G. Sampling and analysis of spatial environmental data. **Advances in GIS Research. Taylor and Francis, Southampton**, p. 1086–1098, 1994.
- BADDELEY, A.; RUBAK, E.; TURNER, R. **Spatial point patterns: methodology and applications with R**. [s.l.] CRC Press, 2015.
- BALDRIDGE, E. *et al.* An extensive comparison of species-abundance distribution models. **PeerJ**, v. 4, p. e2823–e2823, 22 dez. 2016.
- BARBERI, M.; SALGADO-LABOURIAU, M. L.; SUGUIO, K. Paleovegetation and paleoclimate of “vereda de águas emendadas”, central Brazil. **Journal of South American Earth Sciences**, v. 13, n. 3, p. 241–254, 2000.
- BARLOW, J. *et al.* The future of hyperdiverse tropical ecosystems. **Nature**, v. 559, n. 7715, p. 517, 2018.
- BARNES, M. D. *et al.* Prevent perverse outcomes from global protected area policy. **Nature Ecology & Evolution**, v. 2, n. 5, p. 759, 2018.

- BECK, J. *et al.* Spatial bias in the GBIF database and its effect on modeling species' geographic distributions. **Ecological Informatics**, v. 19, p. 10–15, jan. 2014.
- BEERLING, D. J.; MAYLE, F. E. Contrasting effects of climate and CO<sub>2</sub> on Amazonian ecosystems since the last glacial maximum. **Global Change Biology**, v. 12, n. 10, p. 1977–1984, 2006.
- BEHLING, H. First report on new evidence for the occurrence of *Podocarpus* and possible human presence at the mouth of the Amazon during the Late-glacial. **Vegetation History and Archaeobotany**, v. 5, n. 3, p. 241–246, 1996.
- BEHLING, H. Late Quaternary vegetational and climatic changes in Brazil. **Review of Palaeobotany and Palynology**, v. 99, n. 2, p. 143–156, 1998.
- BEHLING, H. Late Quaternary environmental changes in the Lagoa da Curuca region (eastern Amazonia, Brazil) and evidence of *Podocarpus* in the Amazon lowland. **Vegetation History and Archaeobotany**, v. 10, p. 175–183, 2001.
- BEHLING, H. *et al.* Holocene environmental changes in the Central Amazon Basin inferred from Lago Calado (Brazil). **Palaeogeography, Palaeoclimatology, Palaeoecology**, v. 173, n. 1–2, p. 87–101, 2001a.
- BEHLING, H. *et al.* Holocene environmental changes in the Central Amazon Basin inferred from Lago Calado (Brazil). **Palaeogeography, Palaeoclimatology, Palaeoecology**, v. 173, p. 87–101, 2001b.
- BEHLING, H.; CARLOS BERRIO, J.; HOOGHIEMSTRA, H. Late Quaternary pollen records from the middle Caquetá river basin in central Colombian Amazon. **Palaeogeography, Palaeoclimatology, Palaeoecology**, v. 145, n. 1, p. 193–213, 1999.
- BEHLING, H.; DA COSTA, M. L. da. Holocene Environmental Changes from the Rio Curuá Record in the Caxiuana Region, Eastern Amazon Basin. **Quaternary Research**, v. 53, n. 3, p. 369–377, 2000.
- BEHLING, H.; HOOGHIEMSTRA, H. Environmental history of the Colombian savannas of the Llanos Orientales since the last glacial maximum from lake records El Pinal and Carimagua. **Journal of Paleolimnology**, v. 21, n. 4, p. 461–476, 1999.
- BEHLING, H.; HOOGHIEMSTRA, H. Holocene Amazon rainforest-savanna dynamics and climatic implications: high-resolution pollen record from Laguna Loma Linda in eastern Colombia. **Journal of Quaternary Science**, v. 15, n. 7, p. 687–695, 2000.
- BELLARD, C. *et al.* Impacts of climate change on the future of biodiversity. **Ecology Letters**, v. 15, n. 4, p. 365–377, 2012.
- BELLO, C. *et al.* Defaunation affects carbon storage in tropical forests. **Science Advances**, v. 1, n. 11, p. e1501105–e1501105, 2015.
- BERRÍO, J. C. *et al.* Late-glacial and Holocene history of the dry forest area in the south. **Journal of Quaternary Science**, v. 17, n. 7, p. 667–682, 2002.

BETTS, R. A.; MALHI, Y.; ROBERTS, J. T. The future of the Amazon: new perspectives from climate, ecosystem and social sciences. **Philosophical transactions of the Royal Society of London. Series B, Biological sciences**, v. 363, n. 1498, p. 1729–35, 2008.

BICKNELL, J.; PERES, C. A. Vertebrate population responses to reduced-impact logging in a neotropical forest. **Forest Ecology and Management**, v. 259, n. 12, p. 2267–2275, 2010.

BIVAND, R.; KEITT, T.; ROWLINGSON, B. **Rgdal**: bindings for the “geospatial” Data Abstraction Library, 2017. Disponível em: <<https://cran.r-project.org/package=rgdal>>. Acesso em: 03.09.2017.

BIVAND, R.; LEWIN-KOH, N. **Maptools**: tools for reading and handling spatial objects, 2017. Disponível em: <<https://cran.r-project.org/package=maptools>>. Acesso em: 15.09.2017.

BIVAND, R.; RUNDEL, C. **Rgeos**: interface to geometry engine - open source (“GEOS”), 2017. Disponível em: <<https://cran.r-project.org/package=rgeos>>. Acesso em: 20.09.2017.

BOCKMANN, F. A. *et al.* Brazil’s government attacks biodiversity. **Science**, v. 360, n. 6391, p. 865.1-865, 2018.

BONAN, G. B. Forests and climate change: forcings, feedbacks, and the climate benefits of forests. **Science**, v. 320, n. 5882, p. 1444–1449, 2008.

BOUCHER-LALONDE, V.; MORIN, A.; CURRIE, D. J. How are tree species distributed in climatic space? A simple and general pattern. **Global Ecology and Biogeography**, v. 21, n. 12, p. 1157–1166, 2012.

BOYLE, B. *et al.* The taxonomic name resolution service: an online tool for automated standardization of plant names. **BMC Bioinformatics**, v. 13, n. 1, p. 14–16, 2013.

BRANCO, M.; FIGUEIRAS, F. G.; CERMEÑO, P. Assessing the efficiency of non-parametric estimators of species richness for marine microplankton. **Journal of Plankton Research**, v. 40, n. 3, p. 230–243, 1 maio 2018.

BRANDO, P. M. *et al.* Abrupt increases in Amazonian tree mortality due to drought-fire interactions. **Proceedings of the National Academy of Sciences of the United States of America**, v. 111, n. 17, p. 6347–52, 2014.

BRODIE, J.; POST, E.; LAURANCE, W. F. Climate change and tropical biodiversity: a new focus. **Trends in Ecology and Evolution**, v. 27, n. 3, p. 145–150, 2012.

BROOKS, T. M. *et al.* Habitat loss and extinction in the hotspots of biodiversity. **Conservation Biology**, v. 16, n. 4, p. 909–923, 2 ago. 2002.

BROSE, U.; MARTINEZ, N. D.; WILLIAMS, R. J. Estimating species richness: sensitivity to sample coverage and insensitivity to spatial patterns. **Ecology**, v. 84, n. 9, p. 2364–2377, 2003.

BUNGE, J. *et al.* Estimating population diversity with CatchAll. **Bioinformatics**, v. 28, n. 7, p. 1045–1047, 2012.

BUNGE, J.; BARGER, K. Parametric models for estimating the number of classes. **Biometrical Journal: Journal of Mathematical Methods in Biosciences**, v. 50, n. 6, p. 971–982, 2008.

BURBRIDGE, R. E.; MAYLE, F. E.; KILLEEN, T. J. Fifty-thousand-year vegetation and climate history of Noel Kempff Mercado National Park, Bolivian Amazon. **Quaternary Research**, v. 61, n. 2, p. 215–230, 2004.

BURN, M. J.; MAYLE, F. E. Palynological differentiation between genera of the Moraceae family and implications for Amazonian palaeoecology. **Review of Palaeobotany and Palynology**, v. 149, n. 3–4, p. 187–201, 2008.

BURN, M. J.; MAYLE, F. E.; KILLEEN, T. J. Pollen-based differentiation of Amazonian rainforest communities and implications for lowland palaeoecology in tropical South America. **Palaeogeography, Palaeoclimatology, Palaeoecology**, v. 295, n. 1–2, p. 1–18, 2010.

BURNHAM, R.; GRAHAM, A. The history of neotropical vegetation: new developments and status. **Annals of the Missouri Botanical Garden**, v. 86, N, n. 2, p. 546–589, 1999.

BUSH, M. B. *et al.* Two histories of environmental change and human disturbance in eastern lowland Amazonia. **The Holocene**, v. 10, n. 5, p. 543–553, 2000.

BUSH, M. B. *et al.* Amazonian paleoecological histories: One Hill, three watersheds. **Palaeogeography, Palaeoclimatology, Palaeoecology**, v. 214, n. 4, p. 359–393, 2004.

BUSH, M. B. *et al.* Holocene fire and occupation in Amazonia: records from two lake districts. **Philosophical transactions of the Royal Society of London. Series B, Biological sciences**, v. 362, n. 1478, p. 209–18, 2007.

BUSH, M. B.; COLINVAUX, P. A. A 7000-year pollen record from the Amazon lowlands, Ecuador. **Vegetatio**, v. 76, n. 3, p. 141–154, 1988.

BUSH, M. B.; SILMAN, M. R. Observations on late Pleistocene cooling and precipitation in the lowland Neotropics. **Journal of Quaternary Science**, v. 19, n. 7, p. 677–684, 2004.

BUSH, M. B.; SILMAN, M. R. Amazonian exploitation revisited: ecological asymmetry and the policy pendulum. **Cushman, S. A., Mckelvey K. S., Flather, K.**, v. 5, n. 9, p. 457–465, 2007.

CALABRESE, J. M. *et al.* Stacking species distribution models and adjusting bias by linking them to macroecological models. **Global Ecology and Biogeography**, v. 23, n. 1, p. 99–112, 2014.

CÁMARA-LERET, R. *et al.* Modelling responses of western Amazonian palms to soil nutrients. **Journal of Ecology**, p. 1–15, 2016.

CARDOSO, D. *et al.* Amazon plant diversity revealed by a taxonomically verified species list. **Proceedings of the National Academy of Sciences**, p. 201706756, 2017.

CARRASCO, L. R. *et al.* Unsustainable development pathways caused by tropical deforestation. **Science Advances**, v. 3, n. 7, p. 1–10, 2017.

CASTILHO, C. V. DE. **Variação espacial e temporal da biomassa arbórea viva em 64 km<sup>2</sup> de floresta de terra firme na Amazônia central**. Instituto Nacional de Pesquisas da Amazônia, Universidade Federal do Amazonas, Manaus, 2004.

CHAO, A. Estimating population size for sparse data in capture-recapture experiments. **Biometrics**, p. 427–438, 1989.

CHAO, A. *et al.* Sufficient sampling for asymptotic minimum species richness estimators. **Ecology**, v. 90, n. 4, p. 1125–1133, 2009.

CHAO, A.; BUNGE, J. Estimating the number of species in a stochastic abundance model. **Biometrics**, v. 58, n. 3, p. 531–539, 2002.

CHAO, A.; LEE, S.-M. Estimating the number of classes via sample coverage. **Journal of the American statistical Association**, v. 87, n. 417, p. 210–217, 1992.

CHAVE, J. *et al.* Improved allometric models to estimate the aboveground biomass of tropical trees. **Global Change Biology**, v. 20, n. 10, p. 3177–3190, 2014.

CHENG, H. *et al.* Climate change patterns in Amazonia and biodiversity. **Nature communications**, v. 4, p. 1411, 2013.

CHIARUCCI, A. *et al.* Performance of nonparametric species richness estimators in a high diversity plant community. **Diversity and distributions**, v. 9, n. 4, p. 283–295, 2003.

CHIARUCCI, A. Estimating species richness: still a long way off! **Journal of Vegetation Science**, v. 23, n. 6, p. 1003–1005, 2012.

CHISHOLM, R. A.; LICHSTEIN, J. W. Linking dispersal, immigration and scale in the neutral theory of biodiversity. **Ecology Letters**, v. 12, n. 12, p. 1385–1393, 2009.

CHRISTOPHER, J. US withdrawal from the COP21 Paris climate change agreement, and its possible implications. **Science Progress**, v. 100, n. 4, p. 411, 2017.

CLARK, D. B.; CLARK, D. A. Abundance, growth and mortality of very large trees in neotropical lowland rain forest. **Forest Ecology and Management**, v. 80, n. 1–3, p. 235–244, 1996.

CLARKE, L. E. *et al.* Assessing transformation pathways. **Climate change 2014: mitigation of climate change**. Contribution of working group III to the fifth assessment report of the intergovernmental panel on climate change, 2014. p. 413–510,

COHEN, M. C. L. *et al.* Holocene palaeoenvironmental history of the Amazonian mangrove belt. **Quaternary Science Reviews**, v. 55, n. NOVEMBER, p. 50–58, 2012.

COLINVAUX, P. A. *et al.* Three pollen diagrams of forest disturbance in the western amazon basin. **Review of Palaeobotany and Palynology**, v. 55, n. 1, p. 73–81, 1988.

COLINVAUX, P. A. *et al.* A Long pollen record from lowland Amazonia: forest and cooling in glacial times. **Science**, v. 274, p. 85–88, Nov. 1996.

COLINVAUX, P. A. *et al.* Glacial and postglacial pollen records from the ecuadorian Andes and Amazon. **Quaternary Research**, v. 48, n. 48, p. 69–78, 1997.

COLINVAUX, P. A.; OLIVEIRA, P. E. de. Amazon plant diversity and climate through the Cenozoic. **Palaeogeography, Palaeoclimatology, Palaeoecology**, v. 166, n. 1–2, p. 51–63, 2001.

COLWELL, Robert K. Biodiversity: concepts, patterns, and measurement. **The Princeton guide to ecology**, p. 257-263, 2009.

COLWELL, R. K.; LEES, D. C. The mid-domain effect: geometric constraints on the geography of species richness. **Trends in Ecology and Evolution**, v. 15, n. 2, p. 70–76, 2000.

CONDIT, R. *et al.* Beta-diversity in tropical forest trees. **Science**, v. 295, n. 5555, p. 666–669, 2002.

COWLING, S. A. *et al.* Contrasting simulated past and future responses of the Amazonian forest to atmospheric change. **Philosophical transactions of the Royal Society of London. Series B, Biological sciences**, v. 359, n. 1443, p. 539–47, 2004.

CRIA. Specieslink - simple search. available from. Centro de Referência e Informação Ambiental, 2011. Disponível em: <http://www.splink.org.br/index> . Acesso em: 22 October 2018.

CROWTHER, T. W. *et al.* Mapping tree density at a global scale. **Nature**, v. 525, n. 7568, p. 201–205, 2015.

DA SILVA MENESES, M. E. N.; DA COSTA, M. L.; BEHLING, H. Late Holocene vegetation and fire dynamics from a savanna-forest ecotone in Roraima state, northern Brazilian Amazon. **Journal of South American Earth Sciences**, v. 42, p. 17–26, 2013.

DÁVALOS, Liliana M. The ghosts of development past: deforestation and coca in western Amazonia. In: **The Origins of Cocaine**. Routledge, 2018. p. 31-64.

DAVIDSON, E. A. *et al.* The Amazon basin in transition. **Nature**, v. 481, n. 7381, p. 321–328, 2012.

DEAN, W. **With broadax and firebrand**: the destruction of the Brazilian Atlantic forest. [California]: Univ of California Press, 1997.

DIFFENBAUGH, N. S.; FIELD, C. B. Changes in ecologically critical terrestrial climate conditions. **Science**, v. 341, n. 6145, p. 486–492, 2013.

DIGGLE, P. J. A Kernel Method for Smoothing Point Process Data. **Journal of the Royal Statistical Society. Series C (Applied Statistics)**, v. 34, n. 2, p. 138–147, 1985.

DISTLER, T. *et al.* Stacked species distribution models and macroecological models provide congruent projections of avian species richness under climate change. **Journal of Biogeography**, v. 42, n. 5, p. 976–988, 2015.

DORMANN, C. F. *et al.* Collinearity: a review of methods to deal with it and a simulation study evaluating their performance. **Ecography**, v. 36, n. 1, p. 27–46, 2013.

DUAN, R.-Y. *et al.* The potential effects of climate change on amphibian distribution, range fragmentation and turnover in China. **PeerJ**, v. 4, p. e2185, 2016.

EDENHOFER, O. *et al.* Climate change 2014: mitigation of climate change. In: AFRICAN CLIMATE POLICY CENTRE (ACPC). **Contribution of working group III to the fifth assessment report of the intergovernmental panel on climate change**, v. 5, 2014. Disponível em: <https://repository.uneca.org/pdfpreview/bitstream/handle/10855/22514/b10825526.pdf?sequence=1>. Acesso em: 03.05.2017.

EITEN, G. The cerrado vegetation of Brazil. **The Botanical Review**, v. 38, n. 2, p. 201–341, 1972.

ELITH, J. *et al.* Novel methods improve prediction of species' distributions from occurrence data. **Ecography**, v. 29, n. 2, p. 129–151, 2006.

ELITH, J. *et al.* A statistical explanation of MaxEnt for ecologists. **Diversity and Distributions**, v. 17, n. 1, p. 43–57, 2011.

ELITH, J.; LEATHWICK, J. R. Species distribution models: ecological explanation and prediction across space and time. **Annual Review of Ecology, Evolution, and Systematics**, v. 40, p. 677–697, 2009.

ESRI. DeLorme Publishing Company. **Countries and rivers WGS84**. Disponível em: <http://www.esri.com/data/basemaps>, © Esri, DeLorme Publishing Company. Acesso em: 17.06.2016.

ESQUIVEL-MUELBERT, A. *et al.* Seasonal drought limits tree species across the Neotropics. **Ecography**, v. 40, n. 5, p. 618–629, 2017.

FEARNSIDE, P. M. **A floresta amazônica nas mudanças globais**. Manaus: INPA, 2003.

FEARNSIDE, P. M. Desmatamento na Amazônia: dinâmica, impactos e controle. **Acta Amazônica**, v. 36, n. 3, p. 395 - 400, 2006.

FEARNSIDE, P. M. Business as usual: a resurgence of deforestation in the Brazilian Amazon. **Yale Environ** **360**, v. 16, April, 2017. Disponível em: <https://e360.yale.edu/features/business-as-usual-a-resurgence-of-deforestation-in-the-brazilian-amazon>. Acesso em: 07.06.2018.

FEELEY, K. J.; REHM, E. M. Amazon's vulnerability to climate change heightened by deforestation and man-made dispersal barriers. **Global Change Biology**, v. 18, n. 12, p. 3606–3614, 2012.

FEELEY, K. J.; SILMAN, M. R. Extinction risks of Amazonian plant species. **Proceedings of the National Academy of Sciences**, v. 106, n. 30, p. 12382–12387, 2009.

FEELEY, K. J.; SILMAN, M. R. The data void in modeling current and future distributions of tropical species. **Global Change Biology**, v. 17, n. 1, p. 626–630, Dez. 2010.

FEELEY, K. J.; SILMAN, M. R. Disappearing climates will limit the efficacy of Amazonian protected areas. **Diversity and Distributions**, v. 22, n. 11, p. 1081–1084, 2016.

FELDPAUSCH, T. R. *et al.* When big trees fall: damage and carbon export by reduced impact logging in southern Amazonia. **Forest ecology and management**, v. 219, n. 2–3, p. 199–215, 2005.

FERREIRA, L. V.; VENTICINQUE, E.; ALMEIDA, S. O desmatamento na Amazônia e a importância das áreas protegidas. **Estudos avançados**, v. 19, n. 53, p. 157–166, 2005.

FINE, P. V. A. An evaluation of the geographic area hypothesis using the latitudinal gradient in North American tree diversity. **Evolutionary Ecology Research**, v. 3, n. 4, p. 413–428, 2001.

FISHER, R. A.; CORBET, A. S.; WILLIAMS, C. B. The relation between the number of species and the number of individuals in a random sample of an animal population. **The Journal of Animal Ecology**, p. 42–58, 1943.

FITZPATRICK, M. C.; GOTELLI, N. J.; ELLISON, A. M. MaxEnt versus MaxLike: empirical comparisons with ant species distributions. **Ecosphere**, v. 4, n. 5, p. art55, 2013.

FONTES, D. *et al.* Paleoenvironmental dynamics in South Amazonia, Brazil, during the last 35,000 years inferred from pollen and geochemical records of Lago do Saci. **Quaternary Science Reviews**, v. 173, p. 161–180, 2017.

FOURCADE, Y. *et al.* Mapping species distributions with MaxEnt using a geographically biased sample of presence data: a performance assessment of methods for correcting sampling bias. **PLoS ONE**, v. 9, n. 5, p. e97122, 12 maio 2014.

FREITAS, F. L. M. *et al.* Potential increase of legal deforestation in Brazilian Amazon after Forest Act revision. **Nature Sustainability**, v. 1, n. 11, p. 665–670, 2018.

FROST, I. A Holocene sedimentary record from Anaguncocha in the Ecuadorian Amazon. **Ecology**, v. 69, n. 1, p. 66–73, 1988.

GASTON, K. J. Geographic range limits: achieving synthesis. **Proceedings of the Royal Society B**, v. 276, n. 1661, p. 1395–1406, 2009.

GASTON, Kevin J.; SPICER, John I. **Biodiversity: an introduction**. John Wiley & Sons, 2013.

GBIF. **The global biodiversity information facility (year) what is GBIF? Available from** <https://www.gbif.org/what-is-gbif> [22 October 2018], 2018.

GENTRY, A. H. Tree species richness of upper Amazonian forests. **Ecology**, v. 85, n. January, p. 156–159, 1988a.

GENTRY, A. H. Changes in plant community diversity and floristic composition on environmental and geographical gradients. **Annals of the Missouri Botanical Garden**, p. 1–34, 1988b.

GIBSON, L. *et al.* Primary forests are irreplaceable for sustaining tropical biodiversity. **Nature**, v. 478, n. 7369, p. 378–381, 2011.

GIORGETTA, M. A. *et al.* Climate and carbon cycle changes from 1850 to 2100 in MPI-ESM simulations for the Coupled Model Intercomparison Project phase 5. **Journal of Advances in Modeling Earth Systems**, v. 5, n. 3, p. 572–597, 2013.

GIOVANELLI, J. G. R. R. *et al.* Modeling a spatially restricted distribution in the Neotropics: How the size of calibration area affects the performance of five presence-only methods. **Ecological Modelling**, v. 221, n. 2, p. 215–224, jan. 2010.

GOMES, V. H. F. *et al.* Amazonian tree species threatened by deforestation and climate change. **Nature Climate Change**, submetido.

GOMES, V. H. F. *et al.* Species distribution modelling: contrasting presence-only models with plot abundance data. **Scientific Reports**, v. 8, n. 1, p. 1003, 2018.

GOODWIN, Z. A. *et al.* Widespread mistaken identity in tropical plant collections. **Current Biology**, v. 25, n. 22, p. R1066–R1067, 2015.

GOSLING, W. D. *et al.* Differentiation between Neotropical rainforest, dry forest, and savannah ecosystems by their modern pollen spectra and implications for the fossil pollen record. **Review of Palaeobotany and Palynology**, v. 153, n. 1–2, p. 70–85, 2009.

GOTELLI, N. J.; COLWELL, R. K. Quantifying biodiversity: procedures and pitfalls in the measurement and comparison of species richness. **Ecology Letters**, v. 4, n. 4, p. 379–391, 2001.

GRAHAM, C. . H. *et al.* The influence of spatial errors in species occurrence data used in distribution models. **Journal of Applied Ecology**, v. 45, n. 1, p. 239–247, 2008.

GRAHAM, C. H.; MORITZ, C.; WILLIAMS, S. E. Habitat history improves prediction of biodiversity in rainforest fauna. **Proceedings of the National Academy of Sciences of the United States of America**, v. 103, n. 3, p. 632–636, 2006.

GRAU, O. *et al.* Nutrient-cycling mechanisms other than the direct absorption from soil may control forest structure and dynamics in poor Amazonian soils. **Scientific Reports**, v. 7, n. March, p. 1–11, 2017.

GRAY, C. L. *et al.* Local biodiversity is higher inside than outside terrestrial protected areas worldwide. **Nature Communications**, v. 7, p. 12306, 28 jul. 2016.

GRENYER, R. *et al.* Global distribution and conservation of rare and threatened vertebrates. **Nature**, v. 458, n. 7235, p. 238–238, 2006.

GUILLERA-ARROITA, G. *et al.* Is my species distribution model fit for purpose? Matching data and models to applications. **Global Ecology and Biogeography**, v. 24, n. 3, p. 276–292, 2015.

GUISAN, A.; ZIMMERMANN, N. E. Predictive habitat distribution models in ecology. **Ecological Modelling**, n. 135, p. 147–186, 2000.

HANAUER, Merlin; CANAVIRE BACARREZA, Gustavo. **Civil Conflict Reduced the Impact of Colombia's Protected Areas**. Inter-American Development Bank, 2018.

HANSEN, M. C. C. *et al.* High-resolution global maps of 21st-century forest cover change. **Science**, v. 342, n. November, p. 850–854, 2013.

HARIPERSAUD, Padmattie Persaud. **Collecting biodiversity**. 2009. Tese de Doutorado. Utrecht University.

HARTE, J. *et al.* Maximum entropy and the state-variable approach to macroecology. **Ecology**, v. 89, n. 10, p. 2700–2711, 2008.

HARTE, J. Maximum entropy and ecology: a theory of abundance, distribution, and energetics. **Oikos**, p. 257, 2011.

HARTE, J.; KITZES, J. Inferring regional-scale species diversity from small-plot censuses. **PLoS one**, v. 10, n. 2, p. e0117527, 2015.

HE, F.; GASTON, K. J. Occupancy-abundance relationships and sampling scales. **Ecography**, v. 23, n. 4, p. 503–511, 2000.

HERMANOWSKI, B. *et al.* Palaeoenvironmental dynamics and underlying climatic changes in southeast Amazonia (Serra Sul dos Carajás, Brazil) during the late Pleistocene and Holocene. **Palaeogeography, Palaeoclimatology, Palaeoecology**, v. 365–366, p. 227–246, 2012.

HIJMANS, R. J. *et al.* Very high resolution interpolated climate surfaces for global land areas. **International Journal of Climatology**, v. 25, n. 15, p. 1965–1978, 2005.

HIJMANS, R. J. **Raster**: geographic data analysis and modeling, 2017a. Disponível em: <<https://cran.r-project.org/package=raster>>. Acesso em: 15.06.2017.

HIJMANS, R. J. *et al.* **Dismo**: species distribution modeling, 2017b. Disponível em: <<https://cran.r-project.org/package=dismo>>. Acesso em: 21.06.2017.

HIJMANS, R. J.; VAN ETTEN, J. **Raster**: geographic data analysis and modelingR package version 2.5-8, 2016.

HIRZEL, A. H. *et al.* Ecological-niche factor analysis: How to compute habitat-suitability maps without absence data? **Ecology**, v. 83, n. 7, p. 2027–2036, 2002.

HOORN, C. *et al.* Amazonia through time: andean. **Science**, v. 330, n. November, p. 927–931, 2010.

HORTAL, J.; BORGES, P. A. V.; GASPAR, C. Evaluating the performance of species richness estimators: sensitivity to sample grain size. **Journal of Animal Ecology**, v. 75, n. 1, p. 274–287, 2006. HOUGHTON, R. A.; BYERS, B.; NASSIKAS, A. A. A role for tropical forests in stabilizing atmospheric CO<sub>2</sub>. **Nature Climate Change**, v. 5, n. 12, p. 1022–1023, 2015.

HUBBELL, S. P. **The unified neutral theory of biodiversity and biogeography**. Princeton, New Jersey, USA: Princeton Monographs in Population Biology. Princeton University Press, 2001.

HUBBELL, S. P. *et al.* How many tree species are there in the Amazon and how many of them will go extinct? **Proceedings of the National Academy of Sciences**, v. 105, n. Supplement 1, p. 11498–11504, 2008.

HUBBELL, S. P.; FOSTER, R. B. Diversity of canopy trees in a neotropical forest and implications for conservation. **Tropical rain forest: ecology and Management**, p. 25–41, 1983.

HUNTINGFORD, C. *et al.* Towards quantifying uncertainty in predictions of Amazon “dieback”. **Philosophical Transactions of the Royal Society B: Biological Sciences**, v. 363, n. 1498, p. 1857–1864, 2008.

HUTCHINSON, G. E. Cold spring harbor symposium on quantitative biology. **Concluding remarks**, v. 22, p. 415–427, 1957.

IKNAYAN, K. J. *et al.* Detecting diversity: emerging methods to estimate species diversity. **Trends in Ecology and Evolution**, v. 29, n. 2, p. 97–106, 2014.

INPE, I. N. DE P. E. **Mapeamento do desmatamento da Amazônia com imagens de satélite**. São José dos Campos. Instituto Nacional de Pesquisas Espaciais, 2018. Disponível em: <http://www.obt.inpe.br/OBT/assuntos/programas/amazonia/prodes>. Acesso em: 08.10.2018.

IRION, G. *et al.* A multiproxy palaeoecological record of Holocene lake sediments from the Rio Tapajós, eastern Amazonia. **Palaeogeography, Palaeoclimatology, Palaeoecology**, v. 240, n. 3–4, p. 523–535, 2006.

IUCN. IUCN Red List Categories and criteria: version 3.1. **Gland, Switzerland**: and Cambridge, UK: IUCN, p. iv + 32pp, 2012.

IUCN, S. AND P. S. Guidelines for using the IUCN red list categories and criteria. Version 13. **Prepared by the Standards and Petitions Subcommittee.**, 2017.

IZSÁK, J.; PAVOINE, S. Links between the species abundance distribution and the shape of the corresponding rank abundance curve. **Ecological indicators**, v. 14, n. 1, p. 1–6, 2012.

JARAMILLO, C. *et al.* The origin of the modern Amazon rainforest: implications of the palynological and paleobotanical record. **Amazonia, Landscape and Species Evolution: A Look into the Past**, p. 317–334, 2010.

JONES, C. D. *et al.* The HadGEM2-ES implementation of CMIP5 centennial simulations. **Geoscientific Model Development**, v. 4, n. 3, p. 543–570, 2011.

KADMON, R.; FARBER, O.; DANIN, A. Effect of roadside bias on the accuracy of predictive maps produced by bioclimatic models. **Ecological Applications**, v. 14, n. 2, p. 401–413, abr. 2004.

KILLEEN, T. J.; SOLÓRZANO, L. A. Conservation strategies to mitigate impacts from climate change in Amazonia. **Philosophical transactions of the Royal Society of London. Series B, Biological sciences**, v. 363, n. 1498, p. 1881–1888, 2008.

KILLEN, T. J. Vegetation and flora of Parque Nacional Noel Kempff Mercado. In: KILLEEN, T. J., SCHULENBERG, T. S. (eds.). **A biological assessment of Parque Nacional Noel Kempff Mercado, Bolivia**. Washington, DC (EUA): Conservation International, Dept. of Conservation Biology, 1998.

KIMURA, M. **The neutral theory of molecular evolution**. Cambridge University Press, 1983.

KOCHERGINSKY, M.; HE, X. M.; MU, Y. M. Practical confidence intervals for regression quantiles. **Journal of Computational and Graphical Statistics**, v. 14, n. 1, p. 41–55, 2005.

KOENKER, R. **Quantreg**: quantile regression R package version 5.05, 2013.

KRISHNAMANI, R.; KUMAR, A.; HARTE, J. Estimating species richness at large spatial scales using data from small discrete plots. **Ecography**, v. 27, n. 5, p. 637–642, 2004.

KRITICOS, D. J. *et al.* CliMond: global high-resolution historical and future scenario climate surfaces for bioclimatic modelling. **Methods in Ecology and Evolution**, v. 3, n. 1, p. 53–64, 2012.

LAHOZ-MONFORT, J. J.; GUILLERA-ARROITA, G.; WINTLE, B. A. Imperfect detection impacts the performance of species distribution models. **Global Ecology and Biogeography**, v. 23, n. 4, p. 504–515, 2014.

LATRUBESSE, E. M.; RAMONELL, C. G. A climatic model for southwestern Amazonia in Last Glacial times. **Quaternary International**, v. 21, p. 163–169, 1994.

LAURANCE, W. F. *et al.* Rainforest fragmentation kills big trees. **Nature**, v. 404, n. 6780, p. 836, 2000.

LAURANCE, W. F. *et al.* Environment. The future of the Brazilian Amazon. **Science (New York, N.Y.)**, v. 291, n. 5503, p. 438–439, 2001.

LAURANCE, W. F. *et al.* Rapid decay of tree-community composition in Amazonian forest fragments. **Proceedings Of The National Academy Of Sciences Of The United States Of America**, v. 103, n. 50, p. 19010–19014, 2006.

LAWSON, C. R. *et al.* Prevalence, thresholds and the performance of presence–absence models. **Methods in Ecology and Evolution**, v. 5, n. 1, p. 54–64, 2014.

LEDRU, M. P. *et al.* Palynological reconstruction of the rain forest in French Guiana during the past 3000 years. **Comptes Rendus de l'Academie des Sciences Serie 2, Sciences de la Terre et des Planetes**, n. 6-t324, p. 469–476, 1997.

LEDRU, M. P. Late holocene rainforest disturbance in French Guiana. **Review of Palaeobotany and Palynology**, v. 115, n. 3–4, p. 161–176, 2001.

LINDENMAYER, D. B.; LAURANCE, W. F.; FRANKLIN, J. F. Global decline in large old trees. **Science**, v. 338, n. 6112, p. 1305–1306, 2012.

LIU, C.; WHITE, M.; NEWELL, G. Selecting thresholds for the prediction of species occurrence with presence-only data. **Journal of Biogeography**, v. 40, n. 4, p. 778–789, 2013.

LIU, K.-B.; COLINVAUX, P. A. A 5200-Year History of Amazon Rain Forest. **Journal of Biogeography**, v. 15, n. 2, p. 231–248, 1988.

LOISELLE, B. A. *et al.* Predicting species distributions from herbarium collections: does climate bias in collection sampling influence model outcomes? **Journal of Biogeography**, v. 35, n. 1, p. 105–116, 6 set. 2008.

LONGO, M. *et al.* Ecosystem heterogeneity and diversity mitigate Amazon forest resilience to frequent extreme droughts. 2018.

LOVEJOY, T. E.; NOBRE, C. Amazon tipping point. **Science Advances**, v. 4, n. 2, p. 2340, 2018.

MACARTHUR, R. H.; WILSON, E. O. **The theory of island biogeography**. Princeton, NJ, 1967.

MACDICKEN, K. *et al.* **Global forest resources assessment 2015**: how are the world's forests changing? 2016.

MAGURRAN, Anne E. **Measuring biological diversity**. John Wiley & Sons, 2013.

MAGURRAN, A. E.; HENDERSON, P. A. Explaining the excess of rare species in natural species abundance distributions. **Nature**, v. 422, n. 6933, p. 714–716, 2003.

MAHER, S. P. *et al.* Pattern-recognition ecological niche models fit to presence-only and presence-absence data. **Methods in Ecology and Evolution**, v. 5, n. 8, p. 761–770, 2014.

MALDONADO, C. *et al.* Estimating species diversity and distribution in the era of Big Data: To what extent can we trust public databases? **Global Ecology and Biogeography**, v. 24, n. 8, p. 973–984, 2015.

MALHI, Y. *et al.* Exploring the likelihood and mechanism of a climate-change-induced dieback of the Amazon rainforest. **Proceedings of the National Academy of Sciences**, v. 106, n. 49, p. 20610–20615, 2009.

MALHI, Y.; WRIGHT, J. Spatial patterns and recent trends in the climate of tropical rainforest regions. **Philosophical Transactions of the Royal Society of London B: Biological Sciences**, v. 359, n. 1443, p. 311–329, 2004.

MARCHANT, R. *et al.* Distribution and ecology of parent taxa of pollen lodged within the Latin American Pollen Database. **Review of Palaeobotany and Palynology**, v. 121, n. 1, p. 1–75, 2002.

MARKANDYA, A.; HALSNAES, K. Costing methodologies. **Guidance papers on the cross cutting issues of the third assessment report of the IPCC**, 2000. p. 15–31.

MARTIN, L. *et al.* Astronomical forcing of contrasting rainfall changes in tropical South America between 12,400 and 8800 cal yr BP. **Quaternary Research**, v. 47, n. 1, p. 117–122, 1997.

MATEO, R. G. *et al.* Do stacked species distribution models reflect altitudinal diversity patterns? **PLoS ONE**, v. 7, n. 3, 2012.

MAYLE, F. E. *et al.* Responses of Amazonian ecosystems to climatic and atmospheric carbon dioxide changes since the last glacial maximum. **Philosophical transactions of the Royal Society of London. Series B, Biological sciences**, v. 359, n. 1443, p. 499–514, 2004.

MAYLE, F. E.; BURBRIDGE, R.; KILLEEN, T. J. Millennial-scale dynamics of southern Amazonian rain forests. **Science**, v. 290, n. 5500, p. 2291–2294, 2000.

MAYLE, F. E.; POWER, M. J. Impact of a drier early–mid-Holocene climate upon Amazonian forests. **Philosophical Transactions of the Royal Society B: Biological Sciences**, v. 363, n. 1498, p. 1829–1838, 2008.

MCGILL, B. J. *et al.* Species abundance distributions: moving beyond single prediction theories to integration within an ecological framework. **Ecology Letters**, v. 10, n. 10, p. 995–1015, 2007.

MERCKX, B. *et al.* Null models reveal preferential sampling, spatial autocorrelation and overfitting in habitat suitability modelling. **Ecological Modelling**, v. 222, n. 3, p. 588–597, fev. 2011.

MEROW, C.; SMITH, M. J.; SILANDER, J. A. A practical guide to MaxEnt for modeling species' distributions: What it does, and why inputs and settings matter. **Ecography**, v. 36, n. 10, p. 1058–1069, 2013.

MILLER, J. Species distribution modeling. **Geography Compass**, v. 4, n. 6, p. 490–509, 4 jun. 2010.

MITTERMEIER, R. A. *et al.* Wilderness and biodiversity conservation. **Proceedings of the National Academy of Sciences of the United States of America**, v. 100, n. 18, p. 10309–13, 2003.

MORRONE, J. J. Biogeographical regionalisation of the Neotropical region. **Zootaxa**, v. 3782, n. 1, p. 1–110, 2014.

MOUTINHO, P.; GUERRA, R.; AZEVEDO-RAMOS, C. Achieving zero deforestation in the Brazilian Amazon: what is missing? **Elementa: Science of the Anthropocene**, v. 4, p. 125, 2016.

NAUGHTON-TREVES, L.; HOLLAND, M. B.; BRANDON, K. The role of protected areas in conserving biodiversity and sustaining local livelihoods. **Annual Review of Environment and Resources**, v. 30, n. 1, p. 219–252, 2005.

NEPSTAD, D. C. *et al.* Mortality of large trees and lianas following experimental drought in an Amazon forest. **Ecology**, v. 88, n. 9, p. 2259–2269, 2007.

NEPSTAD, D. C. *et al.* Interactions among Amazon land use, forests and climate: prospects for a near-term forest tipping point. **Philosophical transactions of the Royal Society of London. Series B, Biological sciences**, v. 363, n. 1498, p. 1737–46, 2008.

NEWBOLD, T. Applications and limitations of museum data for conservation and ecology, with particular attention to species distribution models. **Progress in physical geography**, v. 34, n. 1, p. 3–22, 2010.

OKSANEN, A. J. *et al.* **Community ecology package**: vegan version 2.3-0, 2015.

OKSANEN, J. Vegan: an introduction to ordination. **Management**, v. 1, p. 1–10, 2008.

ORTEGA-HUERTA, M. A.; PETERSON, A. T. Modeling ecological niches and predicting geographic distributions: a test of six presence-only methods. **Revista mexicana de Biodiversidad**, v. 79, n. 1, p. 205–216, 2008.

PEARSON, R. G. Species' distribution modeling for conservation educators and practitioners. **Lessons in Conservation**, v. 3, n. 3, p. 54–89, 2010.

PEBESMA, E.; GRAELER, B. **Gstat**: spatial and spatio-temporal geostatistical modelling, prediction and simulation R package version 1.0-19, 2014.

PEBESMA, E.; HEUVELINK, G. Spatio-temporal interpolation using gstat. **RFID Journal**, v. 8, n. 1, p. 204–218, 2016.

PEBESMA, E. J.; BIVAND, R. **Sp**: classes and methods for spatial data in R package version 1.0-15, 2014.

PECL, G. T. *et al.* Biodiversity redistribution under climate change: Impacts on ecosystems and human well-being. **Science**, v. 355, n. 6332, 2017.

PEREIRA, H. M.; NAVARRO, L. M.; MARTINS, I. S. Global biodiversity change: the bad, the good, and the unknown. **Annual Review of Environment and Resources**, v. 37, 2012.

PERES, C. A. *et al.* Biodiversity conservation in human-modified Amazonian forest landscapes. **Biological Conservation**, v. 143, n. 10, p. 2314–2327, 2010.

PETERS, G. P. *et al.* The challenge to keep global warming below 2°C. **Nature Climate Change**, v. 3, p. 4, 2 dez. 2012.

PETERSON, A. T. *et al.* **Ecological niches and geographic distributions**. Princeton University Press, 2011.

PHILLIPS, S. J. *et al.* Sample selection bias and presence-only distribution models: implications for background and pseudo-absence data. **Ecological Applications**, v. 19, n. 1, p. 181–197, jan. 2009.

PHILLIPS, S. J.; ANDERSON, R. P.; SCHAPIRE, R. E. Maximum entropy modeling of species geographic distributions. **Ecological Modelling**, v. 190, n. 3–4, p. 231–259, jan. 2006.

PHILLIPS, S. J.; DUDÍK, M. Modeling of species distributions with MaxEnt: New extensions and a comprehensive evaluation. **Ecography**, v. 31, n. 2, p. 161–175, 2008.

PHILLIPS, S. J.; DUDÍK, M.; SCHAPIRE, R. E. A maximum entropy approach to species distribution modeling. **Proceedings of the Twenty-First International Conference on Machine Learning**, v. 83, 2004.

PIMM, S. L. *et al.* How many endangered species remain to be discovered in Brazil? **Natureza a Conservacao**, v. 8, n. 1, p. 71–77, 2010.

PINEDA, E.; LOBO, J. Assessing the accuracy of species distribution models to predict amphibian species richness patterns. **Journal of Animal Ecology**, v. 78, n. i, p. 182–190, 2009.

PLOTKIN, J. B. *et al.* Predicting species diversity in tropical forests. **Proceedings of the National Academy of Sciences**, v. 97, n. 20, p. 10850–10854, 2000.

POS, E. *et al.* Estimating and interpreting migration of Amazonian forests using spatially implicit and semi-explicit neutral models. **Ecology and Evolution**, v. 7, n. 12, p. 4254–4265, 2017.

POS, E. T. *et al.* Are all species necessary to reveal ecologically important patterns? **Ecology and Evolution**, v. 4, n. 24, p. 4626–4636, 2014.

POUTEAU, R. *et al.* Accounting for the indirect area effect in stacked species distribution models to map species richness in a montane biodiversity hotspot. **Diversity and Distributions**, v. 21, n. 11, p. 1329–1338, 2015.

PRESTON, F. W. The commonness, and rarity, of species. **Ecology**, v. 29, n. 3, p. 254–283, 1948.

R CORE TEAM. **R**: a language and environment for statistical computing. Vienna, Austria: R Foundation for Statistical Computing, 2011. 2011.

R CORE TEAM. **R**: a language and environment for statistical computing. Vienna, Austria: R Foundation for Statistical Computing, 2016.

R CORE TEAM. **R**: a language and environment for statistical computing. Vienna, Austria: R Foundation for Statistical Computing, 2018.

RAES, N. Partial versus full species distribution models. **Natureza a Conservacao**, v. 10, n. 2, p. 127–138, 2012.

RAES, N.; TER STEEGE, H. A null-model for significance testing of presence-only species distribution models. **Ecography**, v. 30, n. 5, p. 727–736, 2007a.

RAES, N.; TER STEEGE, H. A null-model for significance testing of presence-only species distribution models. **Ecography**, v. 30, n. 5, p. 727–736, 2007b.

RAISG, R. A. DE I. S. G. **Amazonia 2017** – protected areas and indigenous territories. Red mazónica de Información Socioambiental Georreferenciada, 2017. Disponível em: <https://www.amazoniasocioambiental.org/es/mapas/#!/descargas>. Acesso em: 07.01.2019.

REIS, L. S. *et al.* Environmental and vegetation changes in southeastern Amazonia during the late Pleistocene and Holocene. **Quaternary International**, v. 449, p. 83–105, 2017.

RENNER, I. W.; WARTON, D. I. Equivalence of MaxEnt and poisson point process models for species distribution modeling in ecology. **Biometrics**, v. 69, n. 1, p. 274–281, mar. 2013.

RIAHI, K.; GRÜBLER, A.; NAKICENOVIC, N. Scenarios of long-term socio-economic and environmental development under climate stabilization. **Technological Forecasting and Social Change**, v. 74, n. 7, p. 887–935, 2007.

RIBEIRO, J. E. L. DA S. *et al.* **Flora da Reserva Ducke**: guia de identificação das plantas vasculares de uma floresta de terra-firme na Amazonia Central. Manaus: INPA/DFID, 1999.

RIBEIRO, M. C. *et al.* The Brazilian Atlantic forest: how much is left, and how is the remaining forest distributed? Implications for conservation. **Biological Conservation**, v. 142, n. 6, p. 1141–1153, 2009.

ROCCHETTI, I.; BUNGE, J.; BÖHNING, D. Population size estimation based upon ratios of recapture probabilities. **The Annals of Applied Statistics**, v. 5, n. 2B, p. 1512–1533, 2011.

RODRIGUES, A. S. L. *et al.* The value of the IUCN red list for conservation. **Trends in ecology & evolution**, v. 21, n. 2, p. 71–76, 2006.

RODRÍGUEZ-ZORRO, P. A. *et al.* Forest stability during the early and late Holocene in the igapó floodplains of the Rio Negro, northwestern Brazil. **Quaternary Research (United States)**, v. 89, n. 1, p. 75–89, 2018.

ROSENZWEIG, M. L. **Species diversity in space and time**. Cambridge University Press, 1995.

ROUCOUX, K. H. *et al.* Vegetation development in an Amazonian peatland. **Palaeogeography, Palaeoclimatology, Palaeoecology**, v. 374, p. 242–255, 2013.

SABATIER, D. *et al.* The influence of soil cover organization on the floristic and structural heterogeneity of a Guianan rain forest. **Plant ecology**, v. 131, n. 1, p. 81–108, 1997.

SALOMÃO, R. DE P. **Restauração florestal de precisão**: dinâmica e espécies estruturantes. KG, Saarbrücken, Germany: OmniScriptum GmbH & Co., 2015.

SHUKLA, J.; NOBRE, C.; SELLERS, P. Amazon deforestation and climate change. **Science**, Washington, v. 247, n. 4948, p. 1322–1325, 1990.

SILVÉRIO, D. V *et al.* Agricultural expansion dominates climate changes in southeastern Amazonia: the overlooked non-GHG forcing. **Environmental Research Letters**, v. 10, n. 10, p. 104015, 2015.

SKOV, F.; SVENNING, J. Potential impact of climatic change on the distribution of forest herbs in Europe. **Ecography**, v. 27, n. 3, p. 366–380, 2004.

SLIK, J. W. F. *et al.* Environmental correlates for tropical tree diversity and distribution patterns in Borneo. **Diversity and Distributions**, v. 15, n. 3, p. 523–532, 2009.

SMITH, R. J.; MAYLE, F. E. Impact of mid- to late Holocene precipitation changes on vegetation across lowland tropical South America: a paleo-data synthesis. **Quaternary Research**, p. 1–22, 2017.

SMITH, R.; SINGARAYER, J.; MAYLE, F. **How well do vegetation models simulate mid-Holocene Amazonia?** EGU General Assembly Conference Abstracts. **Anais...2018**

SOARES-FILHO, B. *et al.* Role of Brazilian Amazon protected areas in climate change mitigation. **Proceedings of the National Academy of Sciences of the United States of America**, v. 107, n. 24, p. 10821–6, 15 jun. 2010.

SOARES-FILHO, B. S. *et al.* Modelling conservation in the Amazon basin. **Nature**, v. 440, n. 7083, p. 520–3, 2006.

SOARES-FILHO, B. S. *et al.* **LBA-ECO LC-14 modeled deforestation scenarios, Amazon basin**: 2002-2050 Oak Ridge, TN, Oak Ridge National Laboratory Distributed Active Archive Center, 2013.

SOARES-FILHO, B. S.; ASSUNÇÃO, R. M.; PANTUZZO, A. E. Modeling the spatial transition probabilities of landscape dynamics in an Amazonian colonization frontier: Transition probability maps indicate where changes may occur in the landscape, thus enabling better evaluation of the ecological consequences of lan. **AIBS Bulletin**, v. 51, n. 12, p. 1059–1067, 2001.

STOCKER, T. F. *et al.* Climate change 2013: The physical science basis. **Intergovernmental Panel on Climate Change, Working Group I Contribution to the IPCC Fifth Assessment Report (AR5) (Cambridge Univ Press, New York)**, v. 25, 2013.

STRAND, J. *et al.* Spatially explicit valuation of the Brazilian Amazon forest's ecosystem services. **Nature Sustainability**, v. 1, n. 11, p. 657, 2018.

SWINGEDOUW, D. *et al.* Initialisation and predictability of the AMOC over the last 50 years in a climate model. **Climate Dynamics**, v. 40, p. 2381–2399, 2013.

SYFERT, M. M. *et al.* The effects of sampling bias and model complexity on the predictive performance of MaxEnt species distribution models. **PLoS ONE**, v. 8, n. 2, p. e55158, 14 fev. 2013.

SYFERT, M. M. *et al.* Using species distribution models to inform IUCN red list assessments. **Biological Conservation**, v. 177, p. 174–184, 2014.

TABARELLI, M. *et al.* Challenges and opportunities for biodiversity conservation in the Brazilian Atlantic Forest. **Conservation Biology**, v. 19, n. 3, p. 695–700, 2005.

TATEBE, H. *et al.* The initialization of the MIROC climate models with hydrographic data assimilation for decadal prediction. **Journal of the Meteorological Society of Japan**, v. 90A, n. 0, p. 275–294, 2012.

TAUBERT, F. *et al.* Global patterns of tropical forest fragmentation. **Nature**, v. 554, p. 519, 14 fev. 2018.

TAYLOR, Z. P. *et al.* A multi-proxy palaeoecological record of late-Holocene forest expansion in lowland Bolivia. **Palaeogeography, Palaeoclimatology, Palaeoecology**, v. 293, n. 1–2, p. 98–107, 2010.

TER STEEGE, H. *et al.* Towards a dynamic list of Amazonian tree species. **Scientific Reports**. submetido.

TER STEEGE, H. *et al.* An analysis of the floristic composition and diversity of Amazonian forests including those of the Guiana Shield. **Journal of Tropical Ecology**, v. 16, n. 6, p. 801–828, 2000.

TER STEEGE, H.; HAMMOND, D. S. Character convergence, diversity, and disturbance in tropical rain forest in Guyana. **Ecology**, v. 82, n. 11, p. 3197–3212, 2001.

TER STEEGE, H. *et al.* A spatial model of tree  $\alpha$ -diversity and tree density for the Amazon. **Biodiversity and Conservation**, v. 12, n. 11, p. 2255–2277, 2003.

TER STEEGE, H. *et al.* Continental-scale patterns of canopy tree composition and function across Amazonia. **Nature**, v. 443, n. 7110, p. 0–2, 2006.

TER STEEGE, H. Will tropical biodiversity survive our approach to global change? **Biotropica**, v. 42, n. 5, p. 561–562, 2010.

TER STEEGE, H. *et al.* A model of botanical collectors' behavior in the field: never the same species twice. **American Journal of Botany**, v. 98, n. 1, p. 31–37, 2011.

TER STEEGE, H. *et al.* Hyperdominance in the Amazonian tree flora. **Science**, v. 342, n. 6156, p. 1243092, 17 out. 2013.

TER STEEGE, H. *et al.* Estimating the global conservation status of over 15,000 Amazonian tree species. **Science Advances**, 2015.

TER STEEGE, H. *et al.* The discovery of the Amazonian tree flora with an updated checklist of all known tree taxa. **Scientific Reports**, v. 6, p. 1–15, 2016.

- TER STEEGE, H. TER *et al.* <http://atdn.myspecies.info/>.
- THOMAS, C. D. *et al.* Protected areas facilitate species' range expansions. **Proceedings of the National Academy of Sciences of the United States of America**, v. 109, n. 35, p. 14063–8, 2012.
- TILMAN, D. *et al.* Habitat destruction and the extinction debt. **Nature**, v. 371, n. 6492, p. 65–66, 1994.
- TOBLER, M. *et al.* Implications of collection patterns of botanical specimens on their usefulness for conservation planning: an example of two neotropical plant families (Moraceae and Myristicaceae) in Peru. **Biodiversity and Conservation**, v. 16, n. 3, p. 659–677, 2007.
- TOLEDO, M. B. de; BUSH, M. B. A mid-Holocene environmental change in Amazonian savannas. **Journal of Biogeography**, v. 34, n. 8, p. 1313–1326, 2007.
- TOLLEFSON, J. Stopping deforestation: Battle for the amazon. **Nature**, v. 520, n. 7545, p. 20–23, 2015a.
- TOLLEFSON, J. Forests in spotlight at Paris climate talks. **Nature**, 1 dez. 2015b.
- TOLLEFSON, J. IPCC says limiting global warming to 1.5° C will require drastic action. **Nature News**, 2018. Disponível em: <https://www.nature.com/articles/d41586-018-06876-2>. Acesso em: 13.09.2018.
- TRAVIS, J. M. J. Climate change and habitat destruction: a deadly anthropogenic cocktail. **Proceedings of the Royal Society of London B: Biological Sciences**, v. 270, n. 1514, p. 467–473, 2003.
- TUCKER, C. M. *et al.* A guide to phylogenetic metrics for conservation, community ecology and macroecology. **Biological Reviews**, 2016.
- UNEP-WCMC; IUCN; PLANET, P. The world database on protected areas (WDPA)/The global database on protected areas management effectiveness (GD-PAME) [on-line], [04.04.2018]. **Cambridge, UK: UNEP-WCMC and IUCN**, 2018.
- URBANEK, M. S. **rJava**: low-level R to Java interface R package version 0.9-6, 2013.
- URBANEK, S. **rJava**: Low-Level R to Java Interface, 2017. Disponível em: <https://cran.r-project.org/package=rJava>. Acesso em: 30.10.2016.
- URREGO, D. H. *et al.* Holocene fires, forest stability and human occupation in south-western Amazonia. **Journal of Biogeography**, v. 40, n. 3, p. 521–533, 2013.
- VAN DER SANDE, M. T. *et al.* Soil fertility and species traits, but not diversity, drive productivity and biomass stocks in a Guyanese tropical rainforest. **Functional Ecology**, v. 32, n. 2, p. 461–474, 2018.
- VAN PROOSDIJ, A. S. J. *et al.* Minimum required number of specimen records to develop accurate species distribution models. **Ecography**, v. 39, n. 6, p. 542–552, 2015.

VAN VUUREN, D. P. *et al.* Long-term multi-gas scenarios to stabilise radiative forcing – exploring costs and benefits within an integrated assessment framework. **The Energy Journal**, v. 27, n. Multi-greenhouse gas mitigation and climate policy, p. 201–233, 2006.

VAN VUUREN, D. P. *et al.* Stabilizing greenhouse gas concentrations at low levels: An assessment of reduction strategies and costs. **Climatic Change**, v. 81, n. 2, p. 119–159, 2007.

VAN VUUREN, D. P. *et al.* The representative concentration pathways: an overview. **Climatic Change**, v. 109, n. 1, p. 5–31, 2011.

VANDERWAL, J. *et al.* Abundance and the environmental niche: environmental suitability estimated from niche models predicts the upper limit of local abundance. **American Naturalist**, v. 174, n. 2, p. 282–291, 2009.

VANDERWAL, J. *et al.* **SDMTools**: species distribution modelling tools: tools for processing data associated with species distribution modelling exercises R package version 1.1-20, 2014.

VARELA, S. *et al.* Environmental filters reduce the effects of sampling bias and improve predictions of ecological niche models. **Ecography**, v. 37, n. 11, p. 1084–1091, 2014.

WALKER, R. *et al.* Protecting the Amazon with protected areas. **Proceedings of the National Academy of Sciences of the United States of America**, v. 106, n. 26, p. 10582–6, 2009.

WALTHER, B. A.; MOORE, J. L. The concepts of bias, precision and accuracy, and their use in testing the performance of species richness estimators, with a literature review of estimator performance. **Ecography**, v. 28, n. 6, p. 815–829, 2005.

WANG, J.-P. Species: An R package for species richness estimation. **Journal of Statistical Software**, v. 40, n. 9, p. 1–15, 2011.

WANG, J.-P. Z.; LINDSAY, B. G. A penalized nonparametric maximum likelihood approach to species richness estimation. **Journal of the American Statistical Association**, v. 100, n. 471, p. 942–959, 2005.

WATANABE, S. *et al.* MIROC-ESM 2010: Model description and basic results of CMIP5-20c3m experiments. **Geoscientific Model Development**, v. 4, n. 4, p. 845–872, 2011.

WATSON, J. E. M. *et al.* The performance and potential of protected areas. **Nature**, v. 515, n. 7525, p. 67–73, 2014.

WENG, C.; BUSH, M. B.; ATHENS, J. S. Holocene climate change and hydrarch succession in lowland Amazonian Ecuador. **Review of Palaeobotany and Palynology**, v. 120, n. 1–2, p. 73–90, 2002.

WENG, C.; BUSH, M. B.; SILMAN, M. R. An analysis of modern pollen rain on an elevational gradient in southern Peru. **Journal of Tropical Ecology**, v. 20, n. 1, p. 113–124, 2004.

WHITNEY, B. S. *et al.* A 45kyr palaeoclimate record from the lowland interior of tropical South America. **Palaeogeography, Palaeoclimatology, Palaeoecology**, v. 307, n. 1, p. 177–192, 2011.

WISZ, M. S. *et al.* Effects of sample size on the performance of species distribution models. **Diversity and Distributions**, v. 14, n. 5, p. 763–773, set. 2008.

XIAO-GE, X.; TONG-WEN, W.; JIE, Z. Introduction of CMIP5 experiments carried out with the climate system models of beijing climate center. **Advances in climate Change Research**, v. 4, n. 1, p. 41–49, 2013.

XU, H. *et al.* Assessing non-parametric and area-based methods for estimating regional species richness. **Journal of Vegetation Science**, v. 23, n. 6, p. 1006–1012, 2012.

YEAGER, S. *et al.* A decadal prediction case study: late twentieth-century north Atlantic Ocean heat content. **Journal of Climate**, v. 25, n. 15, p. 5173–5189, 2012.

ZIZKA, A. **SpeciesgeocodeR**: prepare species distributions for the use in phylogenetic analyses, 2015. Disponível em: <https://cran.r-project.org/package=speciesgeocodeR>. Acesso em: 01.08.2017.

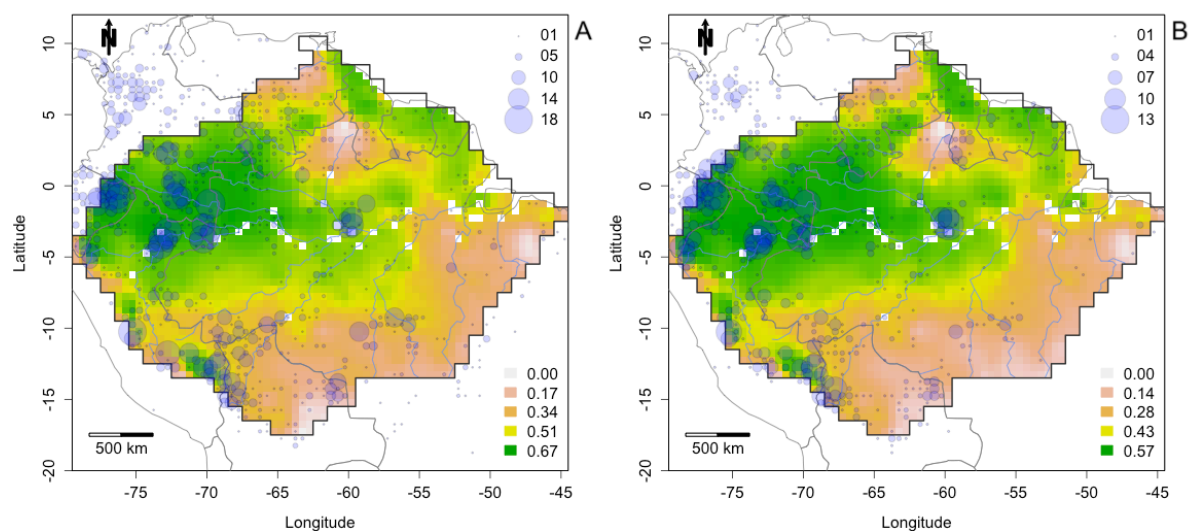
ZIZKA, A. *et al.* Finding needles in the haystack: where to look for rare species in the American tropics. **Ecography**, v. 41, n. 2, p. 321–330, 2018.

ZIZKA, A.; ANTONELLI, A. **SpeciesgeocodeR**: an R package for linking species occurrences, user-defined regions and phylogenetic trees for biogeography, ecology and evolution bioRxiv. 24 nov. 2015. Disponível em: <http://biorxiv.org/content/early/2015/11/24/032755.abstract>. Acesso em: 07.09.2017.

## APÊNDICES

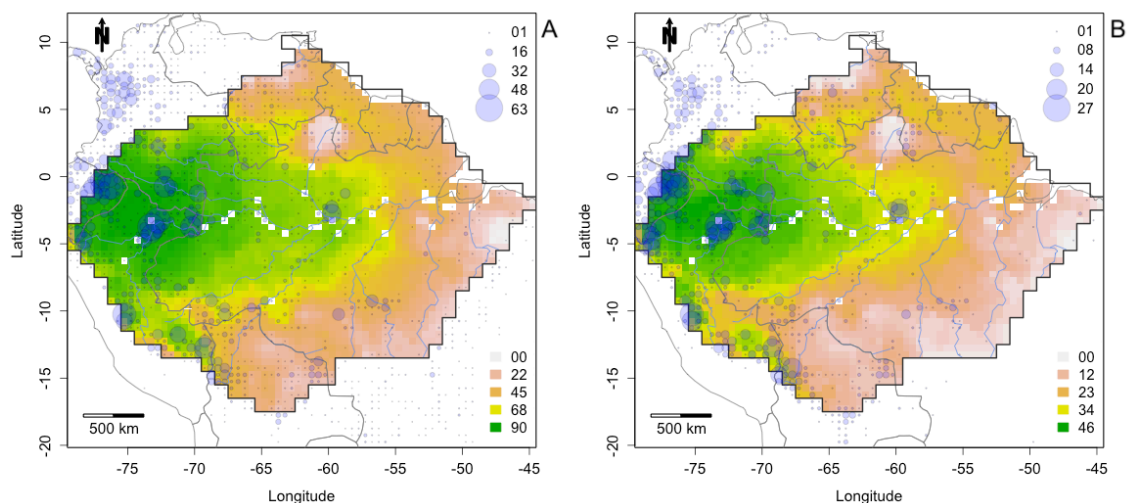
## APÊNDICE A

Figure S4.1- Current mean environmental suitability for the families Moraceae and Urticaceae (%). A, Moraceae. B, Urticaceae. Gray polygon, Amazonian rainforest. Circles in blue, Numbers of collections found in GBIF database, and checked for inconsistencies. Maps created with custom R script. Base map source (country.shp, rivers.shp): ESRI.



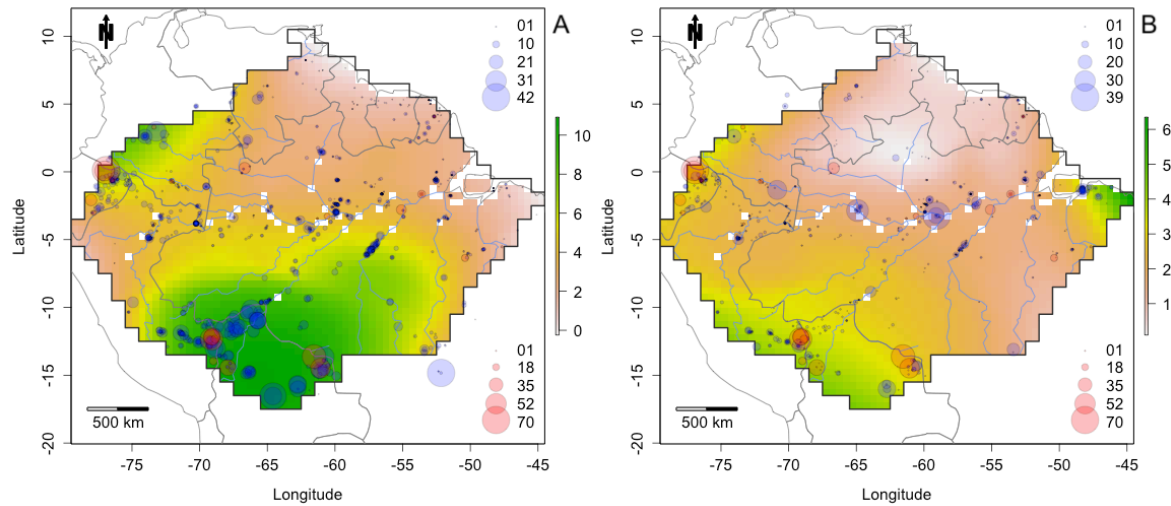
Fonte: ESRI (2016); R Core Team (2018).

Figure S4.2- Species richness. A, Modelled species richness for Moraceae. B, Modelled species richness for Urticaceae. Both maps are the result of stacking individual thresholded species distribution models. circles in blue, Numbers of species collected by 0.5 degree cell. Maps created with custom R script. Gray line, Amazonian rainforest. Circles in blue, Numbers of species collected by 0.5-degree cell. Base map source (country.shp, rivers.shp): ESRI.



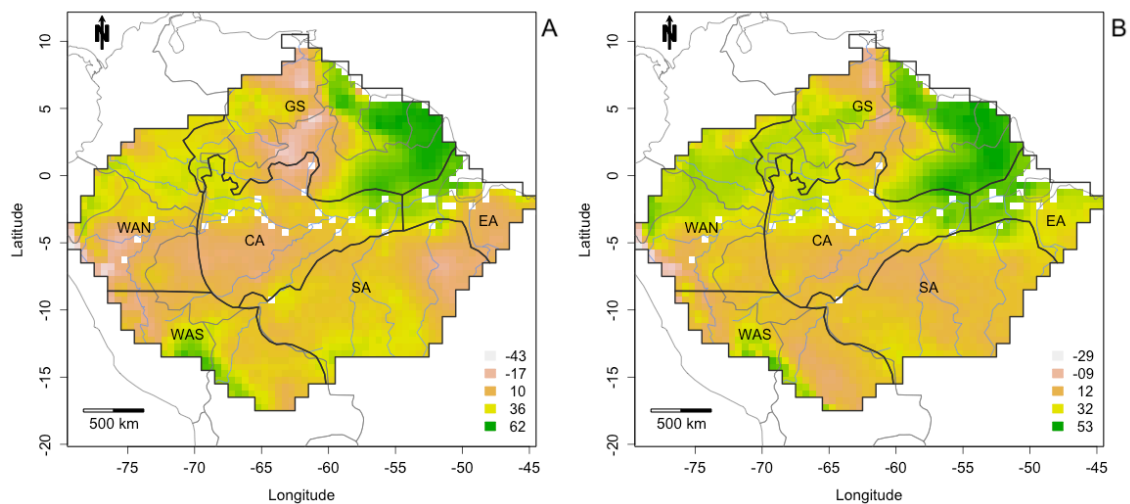
Fonte: ESRI (2016); R Core Team (2018).

Figure S4.3- Relative abundance for Moraceae and Urticaceae families. A, Relative abundance map for Moraceae based on tree inventory plot data. B, Relative abundance map for Urticaceae based on tree inventory plot data. circles in blue, number of plots with presence of the families. circles in pink, percentage of modern pollen assemblage of Moraceae/Urticaceae obtained from pollen diagrams of the paleoecological sites. Gray polygon, Amazonian rainforest. Maps created with custom R script. Base map source (country.shp, rivers.shp): ESRI.



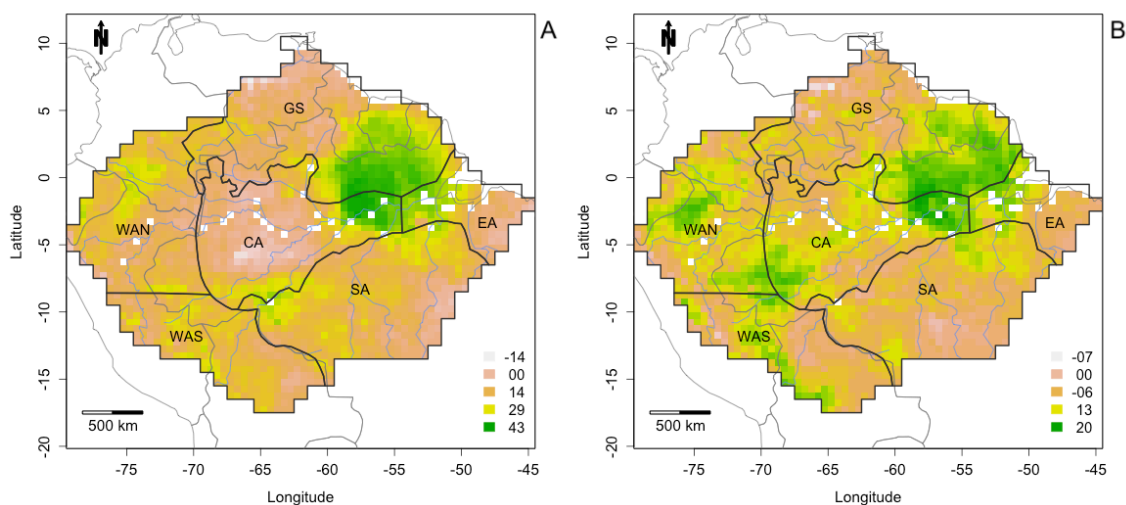
Fonte: ESRI (2016); R Core Team (2018).

Figure S4.4- Increment in environmental suitability between the middle and late Holocene (% between current and last 6 ka years). A, Increment for Moraceae family. B, Increment for Urticaceae family. Maps created with custom R script. Gray line, Amazonian rainforest and Amazonian sub-regions. Base map source (country.shp, rivers.shp): ESRI.



Fonte: ESRI (2016); R Core Team (2018).

Figure S4.5- Increment in species richness between the middle and late Holocene (% , between current and last 6 ka years). A, Increment for Moraceae family. B, Increment for Urticaceae family. Gray polygon, Amazonian rainforest and Amazonian sub-regions. Maps created with custom R script. Base map source (country.shp, rivers.shp): ESRI.



Fonte: ESRI (2016); R Core Team (2018).

Figure S4.6- Relationship between relative abundance. A, all Moraceae species, and B, all Urticaceae species in the vegetation and the percent abundance of their pollen in lake/bog surface sediment pollen assemblages.

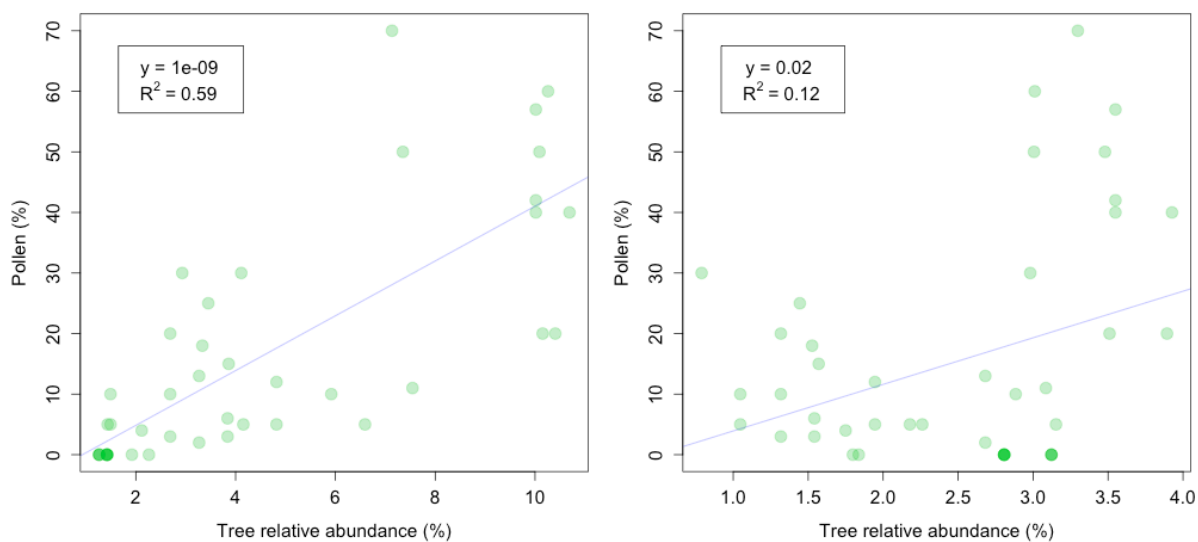
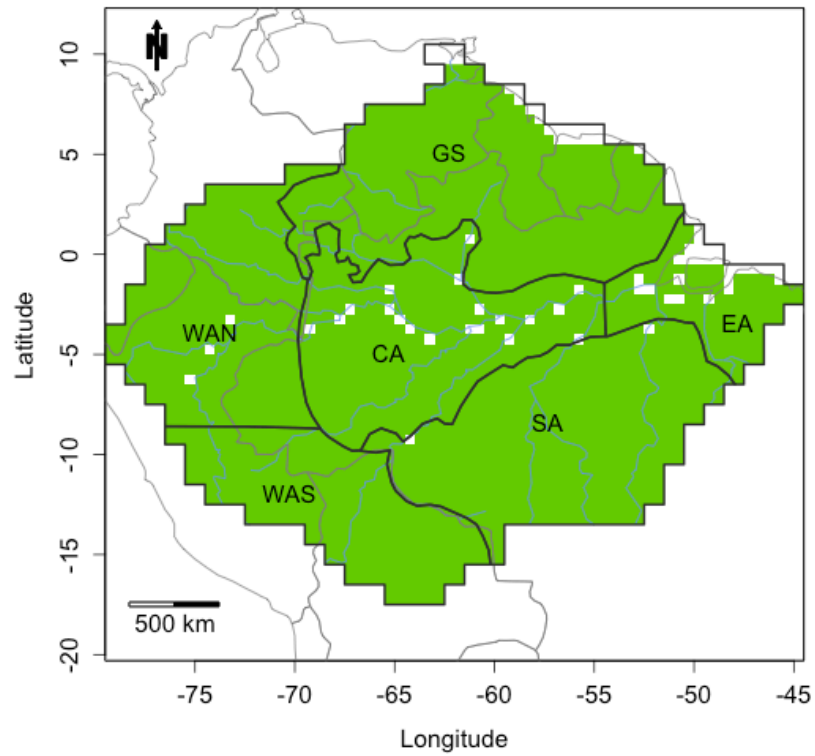
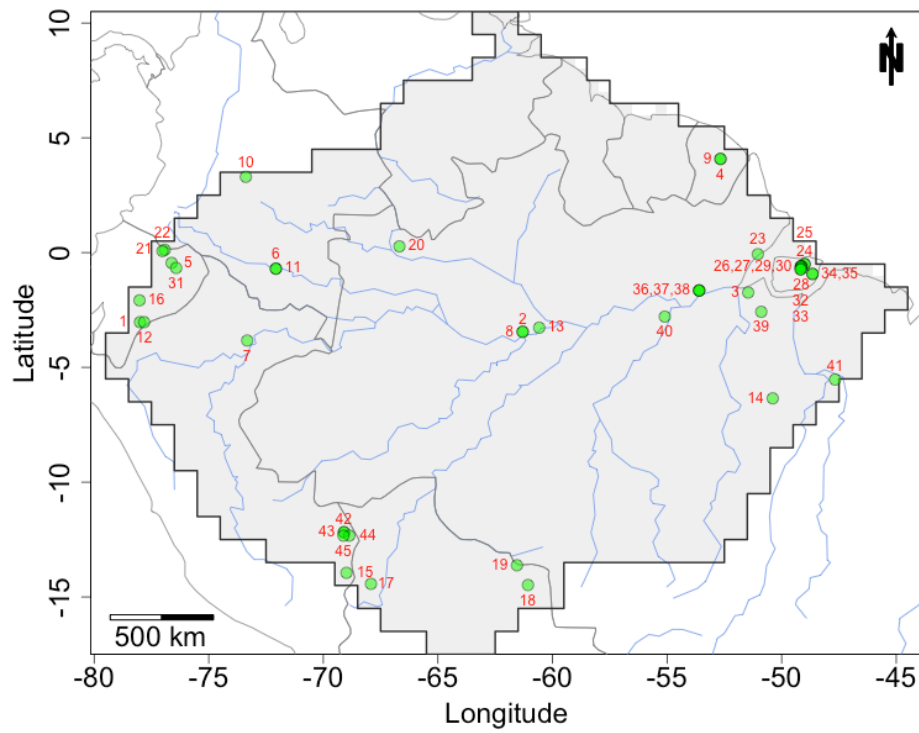


Figure S4.7- Map of original Amazonian lowland forest. The green area represents lowland forest area. Amazonia sub-regions: CA, central Amazonia; EA, eastern Amazonia; GS, Guiana Shield; SA, southern Amazonia; WAN, northwestern Amazonia; WAS, southwestern. Map created with custom R script. Base map source (country.shp, rivers.shp): ESRI.



Fonte: ESRI (2016); R Core Team (2018).

Figure S4.8- Locations for 45 paleoecological sites. Amazonian paleoecological sites locations in green and numeric ID in red corresponding to Appendix S4.4. Maps created with custom R script. Base map source (country.shp, rivers.shp): ESRI.



Fonte: ESRI (2016); R Core Team (2018).

Figure S5.1- Modelling the estimated area of occupancy (AOO). The representation of the area of occupancy (AOO) according to IUCN. a, Spatial distribution of all know collections of a species. b, Extent of occurrence (EOO) estimated as the boundary (convex hull) of all collections. c, Known area of occupancy (AOO), defined as the number of grid cells occupied by the species. d, Modelled AOO the result of modelling the suitable habitat for the species but constraining this by the known EOO plus a small buffer.

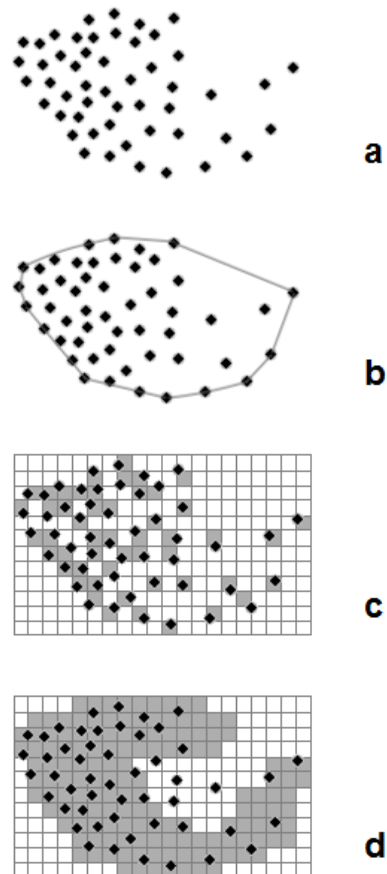
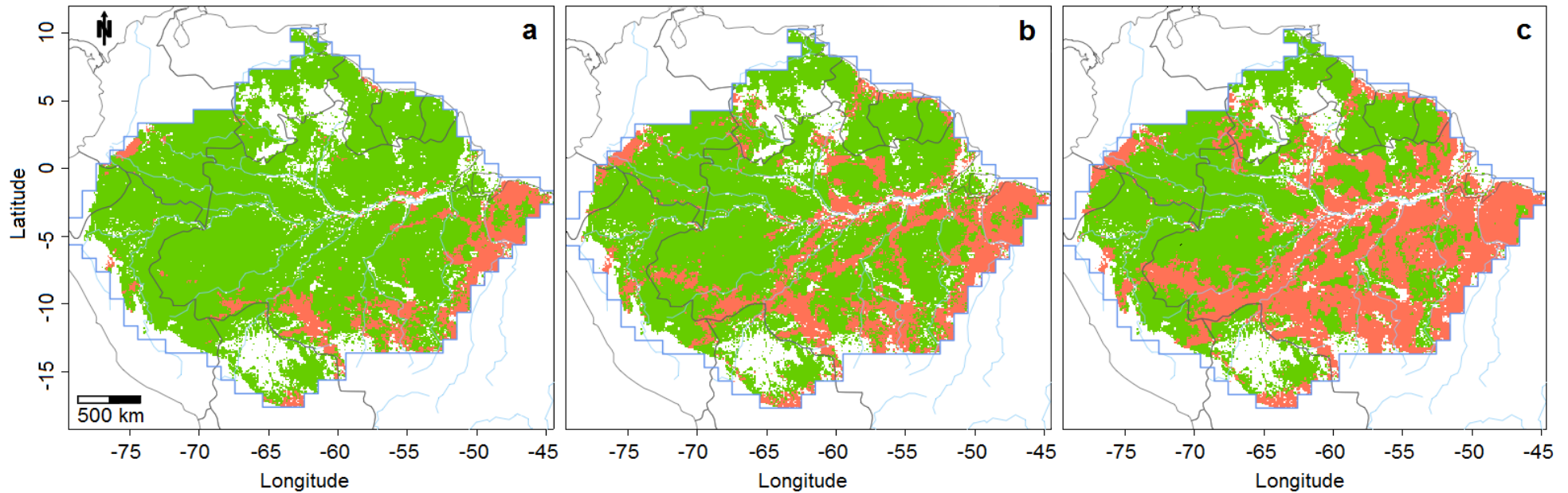
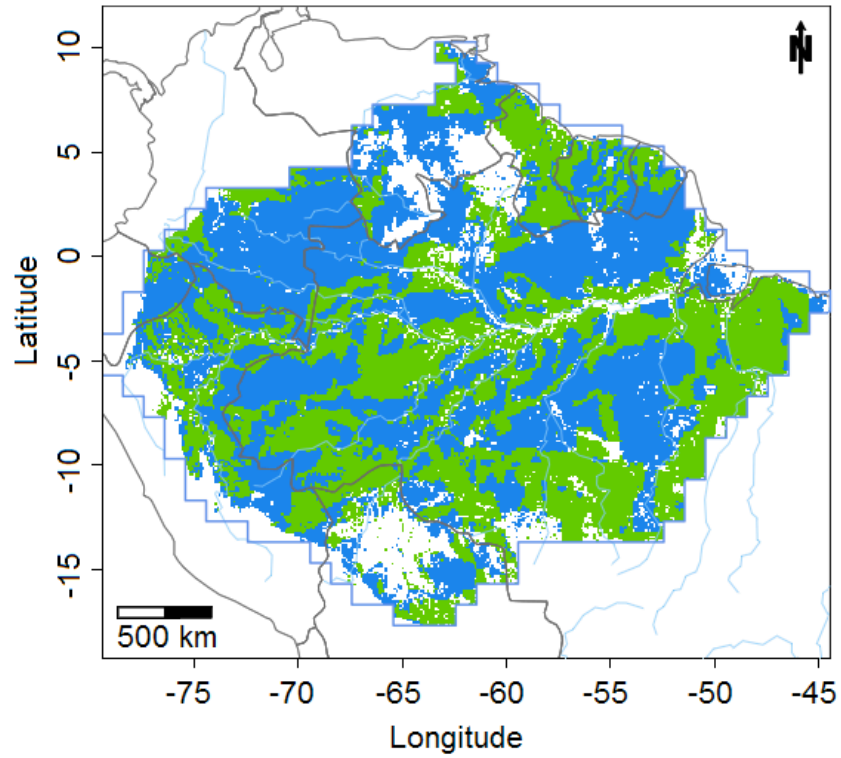


Figure S5.2- Deforestation scenarios by 2013 and projected forest loss by 2050. green, Forested area. red, Deforested area. a, Historical deforestation by 2013. b, Improved governance scenario (IGS) deforestation by 2050. c, Business as usual scenario (BAU) deforestation by 2050. Maps created with custom R script. Base map source (country.shp, rivers.shp): ESRI.



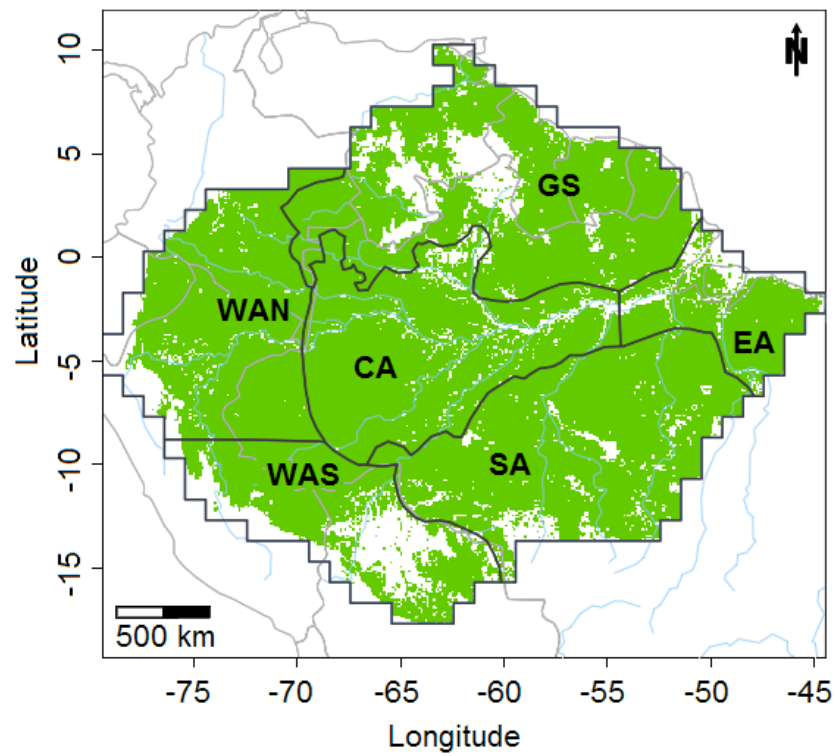
Fonte: ESRI (2016); R Core Team (2018).

Figure S5.3- Amazonian protected areas network. green, Original Amazonian lowland forest. Blue, Amazonian protected areas network. Maps created with custom R script. Base map source (country.shp, rivers.shp): ESRI.



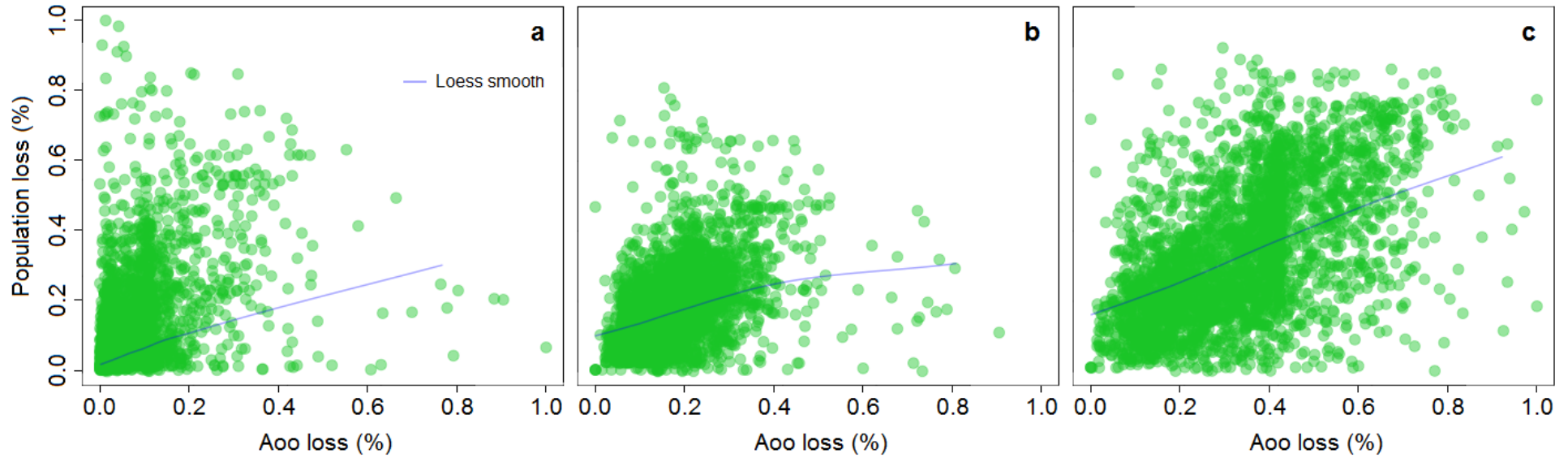
Fonte: ESRI (2016); R Core Team (2018).

1e S5.4. Map of original Amazonian lowland forest. The green area represents lowland forest area. Amazonia sub-regions: CA, central Amazonia; EA, eastern Amazonia; GS, Guiana Shield; SA, southern Amazonia; WAN, northwestern Amazonia; WAS, southwestern. Maps created with custom R script. Base map source (country.shp, rivers.shp): ESRI.

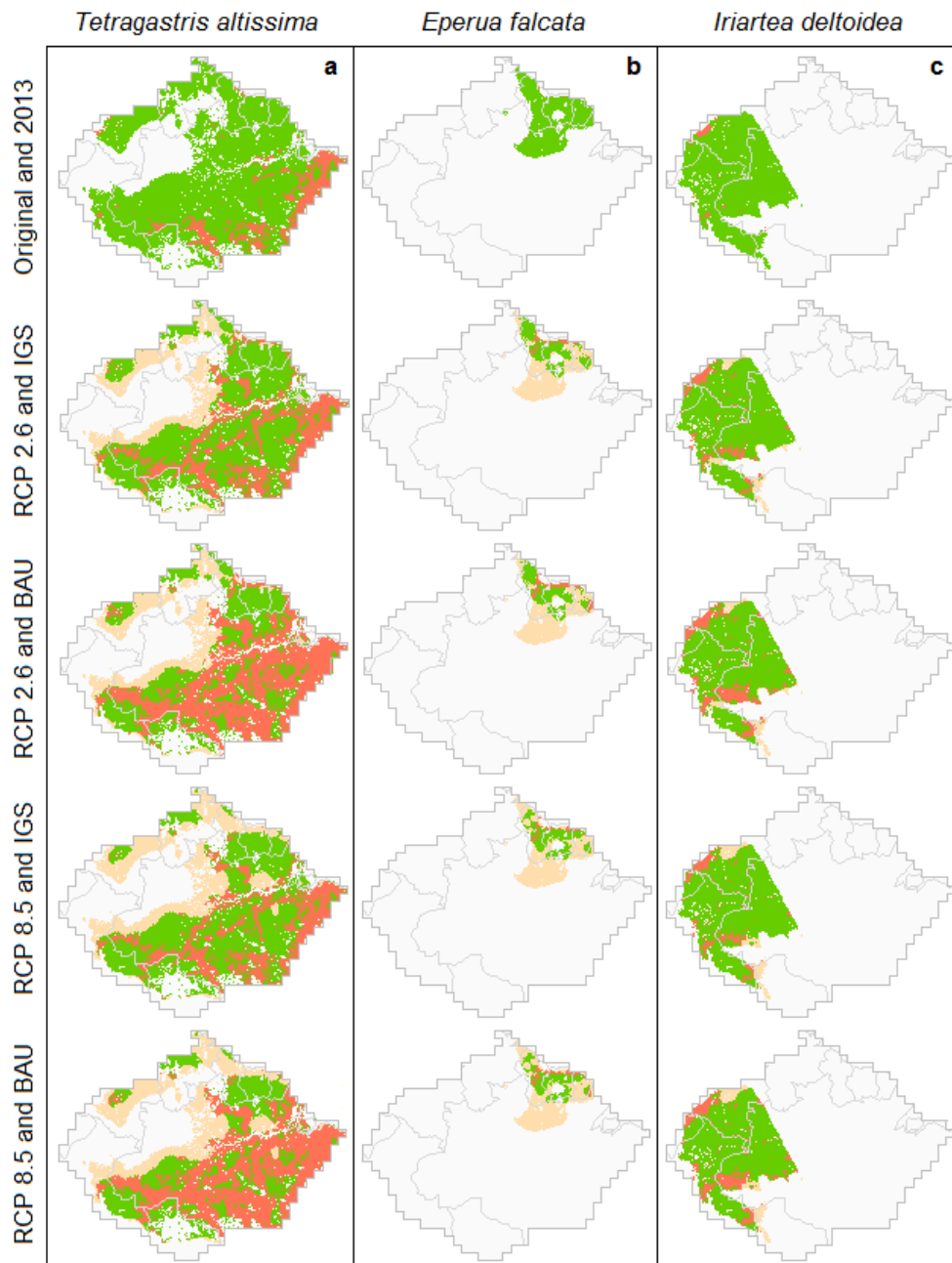


Fonte: ESRI (2016); R Core Team (2018).

Figure S5.5. Estimated AOO loss x population size loss. Loss in relative trees population size shows low but significant relationship with loss in trees AOO size in a, 2013 deforestation. b, 2050 IGS deforestation. c, 2050 BAU deforestation scenarios.

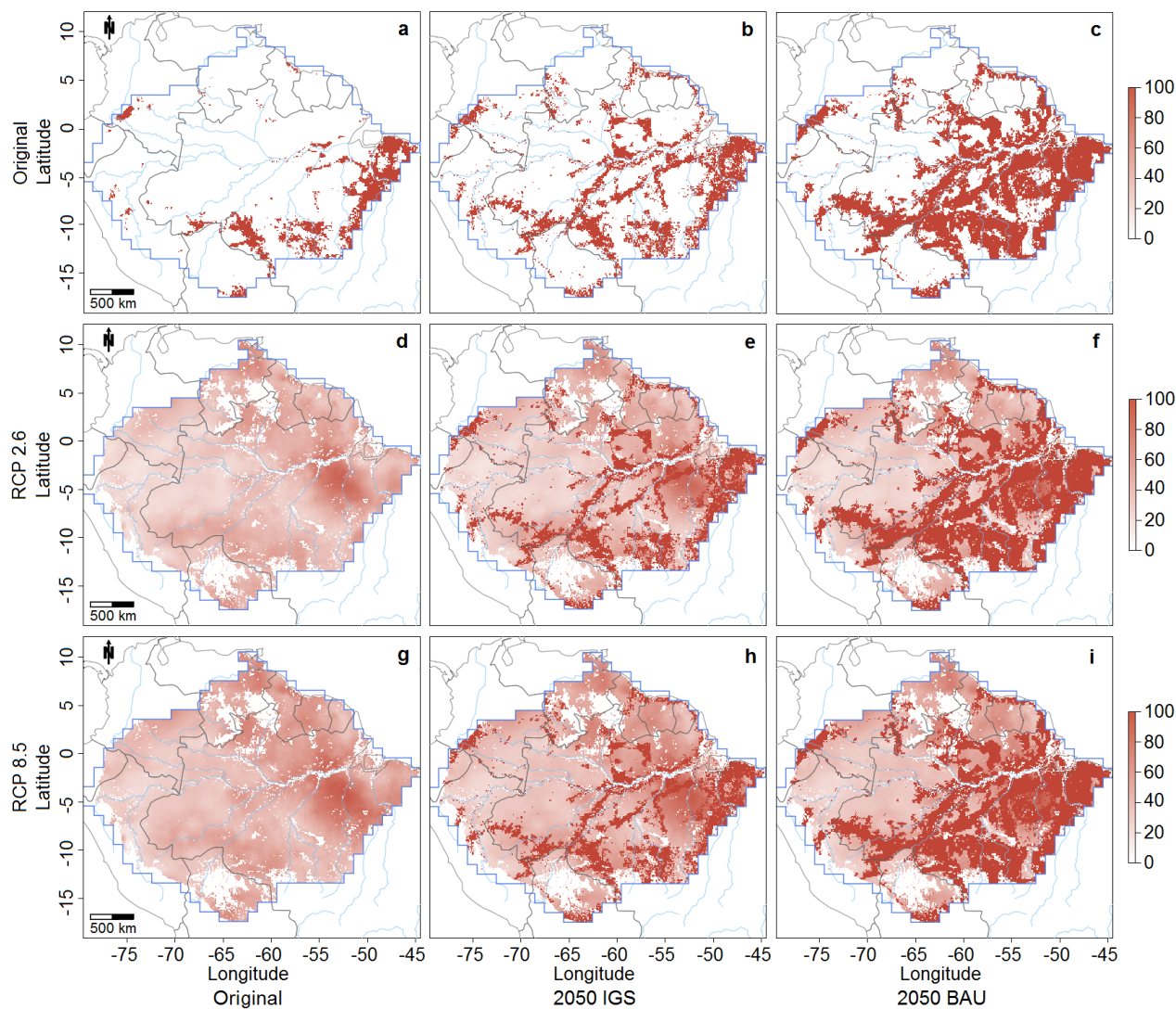


1e S5.6. Contrasting the estimated AOO loss for three hyperdominant Amazonian tree species. Green, Forested area. Red, Deforested area. Salmon, Loss in AOO. A, *Tetragastris altissima* (Aubl.) Swart, eastern/southern species. B, *Eperua falcata* Aubl., northern/central species. C, *Iriartea deltoidea* Ruiz & Pav., western species. Maps created with custom R script. Base map source (country.shp, rivers.shp): ESRI.



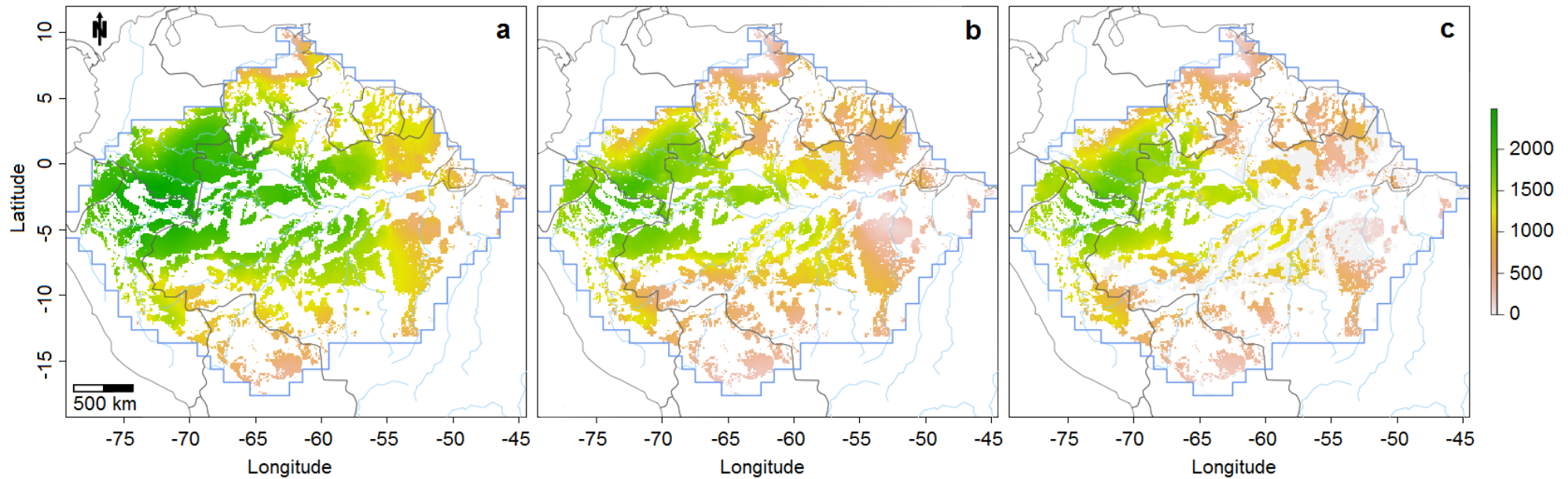
Fonte: ESRI (2016); R Core Team (2018).

Figure S5.7. Tree species richness loss (fraction) by grid cell. a, Original AOO only. b, Original AOO and 2050 IGS deforestation. c, Original AOO and 2050 BAU deforestation. d, 2050 RCP 2.6 AOO scenario only. e, 2050 RCP 2.6 AOO scenario combined with 2050 IGS deforestation. f, 2050 RCP 2.6 AOO scenario combined with 2050 BAU deforestation, g, 2050 RCP 8.5 AOO scenario only. h, 2050 RCP 8.5 AOO scenario combined with 2050 IGS deforestation. i, 2050 RCP 8.5 AOO scenario combined with 2050 BAU deforestation. Maps created with custom R script. Base map source (country.shp, rivers.shp): ESRI.



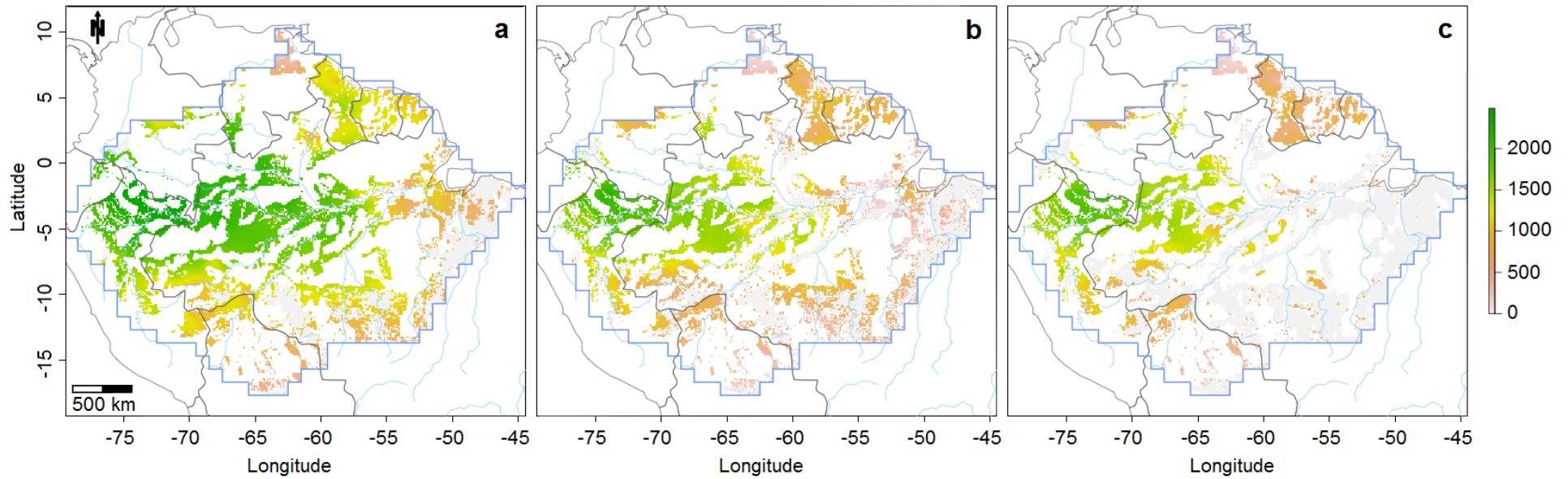
Fonte: ESRI (2016); R Core Team (2018).

Figure S5.8. Tree species richness of the forest fragments inside the protected area network. a, Species richness by 2013. b, Species richness by 2050 for the best-case scenario (RCP 2.6 AOO scenario and IGS deforestation). c, Species richness by 2050 for the worst-case scenario (RCP 8.5 AOO scenario and BAU deforestation). Maps created with custom R script. Base map source (country.shp, rivers.shp): ESRI.



Fonte: ESRI (2016); R Core Team (2018).

Figure S5.9. Tree species richness of the forest fragments outside Amazonian protected area network. a, Species richness by 2013. b, Species richness by 2050 for the best-case scenario (RCP 2.6 AOO scenario and IGS deforestation). c, Species richness by 2050 for the worst-case scenario (RCP 8.5 AOO scenario and BAU deforestation). Maps created with custom R script. Base map source (country.shp, rivers.shp): ESRI.



Fonte: ESRI (2016); R Core Team (2018).